

Vetiver grass as bank protection against vessel-induced loads

M. Sc. Thesis

D.J. Jaspers Focks
April 2006

Thesis committee:
Prof. dr. ir. M.J.F. Stive
Ir. H.J. Verhagen
Dr. ir. H.L. Fontijn
Drs. W.N.J. Ursem



TUDelft

Delft University of Technology

Faculty of Civil Engineering
and Geosciences
Section of Hydraulic Engineering

Acknowledgements

This report is the result of my M.Sc. thesis study, carried out at Delft University of Technology, Faculty of Civil Engineering and Geosciences, section Hydraulic Engineering. The study lasted from September 2005 until the end of April 2006.

First of all I would like to thank the members of my thesis committee for their contribution to this study, Professor M.J.F. Stive (TU Delft - CITG), Ir. H.J. Verhagen (TU Delft - CITG), Dr. ir. H.L. Fontijn (TU Delft - CITG) and Drs. W.N.J. Ursem (TU Delft - TNW, Botanical Garden).

Furthermore I would like to express my gratitude to all the people at the Botanical Garden as well as the people at the Laboratory of Fluid Mechanics - TU Delft, mr. de Visser from the Geomechanical Laboratory - TU Delft and mr. W. Verwaal and mr. A. Mulder from the faculty of Applied Earth Sciences for all the practical support they provided during this study.

Last but not least I would like to thank my wife, my parents (-in-law) and the rest of my family and friends for their support.

Dirk-Jan Jaspers Focks

Delft, April 2006

Summary

In many parts of the world, bank erosion in rivers, canals and other waterways is a major concern for engineering as well as environmental reasons. Hundreds of hectares of land on riverbanks have been lost annually and thousands of kilometers of dykes are threatened by wave erosion caused by motorized boats in for example the Mekong Delta, Vietnam. The problem of erosion tends to become even bigger due to lack of effective erosion controls and because of the increased usage of larger and more powerful vessels with higher sailing speeds. Therefore, banks that consist of easily erodible material may have to be protected or strengthened in order to reduce erosion. In countries like Vietnam traditional "hard" solutions, using wood, cement or rock, are often too costly to implement and are not always easily available. Bioengineering solutions on the other hand, are often low-cost and readily available, but labour intensive, which makes it highly suitable for countries like Vietnam where man power is relatively inexpensive.

In a number of tropical countries Vetiver grass (*Vetiveria zizanioides*) is a well-known bioengineering species for decennia now. Recently, it has also been tested as a bank protection. However, these tests did not derive data for basic understanding of the processes and properties, but were merely pilot projects. There is thus still a lack of both qualitative and quantitative knowledge on the protection of banks by Vetiver grass.

Vessel-related erosion, erosion of unprotected banks and the protection of banks by vegetation are still poorly understood phenomena at the current state-of-the-art. Therefore, more insight in the relevant physical processes is necessary. In this study a theoretical investigation of all possible influences of Vetiver grass on bank erosion was carried out. In total 14 possible adverse and/or beneficial effects were found. This investigation resulted in hypotheses related to mechanisms which were assumed to be dominant, and therefore had to be investigated into more detail by experiments.

Besides the investigation of the effects of Vetiver on erosion, it is also important to retrieve data on if and how Vetiver grass thrives on banks. For application of Vetiver grass the influence of phreatic level and soil type on its growth rate are for a large part still unknown but both may be very important. Therefore experiments were carried out in the Botanical Garden - Delft University of Technology. It was found that a cohesive soil reduced the growth rate of Vetiver grass by approx. 50% compared to a non-cohesive soil, which was a very significant result. Furthermore, a decrease in phreatic level of 0,17 m resulted in significant higher growth rates: differences were found in the order of 10-20%.

River banks consist predominantly of cohesive material and cohesive banks are assumed to be dominantly eroded by mass failure. Therefore, experiments with respect to erosion were focused on mass failure, which is in this study divided in small scale and large scale mass failure. Large scale refers to deep-seated failure planes, while small scale refers to shallow-seated failure planes and the so-called "pushing off" of material.

The direct influence of Vetiver grass on relevant soil parameters (undrained shear strength and saturated specific weight) related to large scale mass stability was investigated by execution of laboratory tests. An increase in the factor of safety of approximately 20% by the presence of Vetiver grass was found, mainly by an increase in undrained shear strength. These results, however, showed a large spread and were not significant. The direct influence of Vetiver grass on saturated specific weight was found to be not significant.

The influence of Vetiver grass on small scale mass failure was tested using a physical model test. The drawdown caused by passing ships was reproduced with the use of a wave flume

at the Laboratory of Fluid Mechanics - Delft University of Technology. Several series of successive drawdowns were carried out on a representation of a bank consisting of a cohesive or a non-cohesive soil type, both with or without Vetiver grass. The only variables in these tests were the soil type and the presence of the Vetiver grass. After a fixed number of cycles the bank profile was measured, from which the amount of erosion could be estimated. The erosion of the cohesive soil was, as predicted, observed to be dominantly caused by small scale mass failure. The amount of eroded material of a cohesive soil was approximately 8-10 times smaller using Vetiver grass. The erosion of a non-cohesive soil was observed to be not specifically related with small scale mass failure, but was reduced also drastically. Because the non-cohesive soil was unstable beforehand and because of the extremely high erosion rate no quantitative statements could be made. It was found that a combination of cohesive soil and Vetiver grass did have the lowest amount of erosion, even a full stop of erosion was recorded after approximately 800-1000 cycles.

Finally the results of the tests resulted in a couple of specific recommendations, in which attention is paid on the application of Vetiver grass and also on further research.

Table of contents

Acknowledgements	i
Summary	ii
Table of contents	iv
List of figures	vii
List of tables	viii
List of symbols	ix
1. Introduction	1
1.1 Background.....	1
1.2 Problem definition.....	1
1.3 Approach.....	2
1.4 Objectives.....	2
1.5 Readers guide.....	2
2. Vetiver grass	3
2.1 Introduction.....	3
2.2 Classification.....	3
2.3 Morphological characteristics.....	3
2.3.1 Above ground.....	3
2.3.2 Below ground.....	4
2.4 Physiological Characteristics.....	4
3. Physical processes	5
3.1 Introduction.....	5
3.2 Vessel-induced loads.....	5
3.3 Erosion of cohesive banks.....	7
3.3.1 Introduction.....	7
3.3.2 Particle entrainment.....	7
3.3.3 Large scale mass failure.....	8
3.3.4 Small scale mass failure.....	10
3.3.5 Subaerial preparation.....	12
3.4 Vessel-induced failure mechanisms.....	12
3.5 Erosion models.....	14
3.6 Vegetation effects on bank erosion.....	15
3.6.1 Introduction.....	15
3.6.2 Subaerial preparation.....	15
3.6.3 Particle entrainment.....	15
3.6.4 Large scale mass failure.....	16
3.6.5 Small scale mass failure.....	18
3.7 Influence of Vetiver grass on bank erosion.....	18
3.8 Resulting tests.....	20
3.8.1 Introduction.....	20
3.8.2 Large scale mass failure.....	20
3.8.3 Small scale mass failure.....	22
4. Hypotheses	23
4.1 Influence of soil type and phreatic level on Vetiver grass.....	23
4.2 Influence of Vetiver grass roots on soil parameters.....	23
4.3 Bank retreat caused by water level changes.....	23

5. Influence of soil type and phreatic level on Vetiver grass	25
5.1 Introduction	25
5.2 Experiment.....	25
5.2.1 Soil type MX.....	25
5.2.2 Soil type C.....	26
5.3 Results.....	27
5.3.1 Soil type MX.....	27
5.3.2 Soil type C.....	30
5.3.3 Comparison soil types.....	32
5.4 Error analysis and assumptions.....	33
6. Large scale mass failure.....	35
6.1 Comparison of test methods.....	35
6.2 Experiment.....	36
6.3 Results.....	36
6.3.1 Fallow soil type C.....	36
6.3.2 Soil type C with Vetiver grass	37
6.3.3 Comparison.....	37
6.4 Error analysis.....	39
7. Small scale mass failure.....	40
7.1 Introduction	40
7.2 Experiment.....	40
7.2.1 Model design.....	40
7.2.2 Test setup	41
7.2.3 Runs.....	43
7.3 Results.....	44
7.3.1 Soil type C.....	44
7.3.2 Soil type MX.....	51
7.3.3 Comparison of soil type MX and C.....	55
7.3.4 Soil type SC	56
7.4 Error analysis.....	56
8. Conclusions.....	57
8.1 Physical processes	57
8.2 Influence of soil type and phreatic level on Vetiver grass.....	57
8.3 Large scale mass failure.....	58
8.4 Small scale mass failure.....	58
9. Recommendations	60
9.1 Influence of soil type and phreatic level on Vetiver grass.....	60
9.2 Large scale mass failure.....	61
9.3 Small scale mass failure.....	61
9.4 General.....	62
References.....	63
Appendices.....	66
Appendix A: Results of Vetiver grass root tensile strength measurements (from Hengchaovanich 1998).....	66
Appendix B: Diagram of Schijf ($\alpha=1,1$) (from Groenveld (2002))	67
Appendix C1: Grain size diagram for soil type MX.....	68
Appendix C2: Shear strength of soil type SC obtained with triaxial test.....	69
Appendix D: Classification of soil type C.....	70

Appendix E1: Cumulative length of the leaves at different groundwaterlevels (soil type MX)	73
Appendix E2: Cumulative length of the leaves at different groundwaterlevels (soil type C).	73
Appendix F: Testing of the hypotheses.....	74
Appendix G: MATLAB codes	78
Appendix H1: Bootstrap comparison ($\mu=1$) MX	80
Appendix H2: Bootstrap comparison growth rates MX	81
Appendix H3: Bootstrap new tillers MX.....	82
Appendix H4: Bootstrap comparison growth rates C	83
Appendix H5: Bootstrap comparison growth rates C and MX.....	84
Appendix I: Graphs rate of growth below-ground biomass	85
Appendix J: Root area ratios at 3 different heights of triaxial test samples (2, 4, 6 cm)	87
Appendix K: Bootstrap comparison undrained shear strength and specific weight.....	88
Appendix L: Sketch test setup	89
Appendix M: Forcing signal provided by the wave generator, measured by the wave height meter	90
Appendix N: Root area ratio (RAR) by depth for run 1 to 3 of soil type MX with Vetiver grass	91
Appendix O: Root area ratio (RAR) by depth for run 1 to 3 of soil type C with Vetiver grass	92
Appendix P: Small scale mass failure test results of soil type SC.....	93
Appendix Q: Proposal location further research, Delft, Schiekade	95

List of figures

- Figure 1.1: Erosion of a bank of the Mekong, Vietnam (from Le Viet Dung *et al* (2003))
- Figure 2.1: Vetiver grass distribution with active programs (adapted from [A1])
- Figure 2.2: *Vetiveria zizanioides* (from [B])
- Figure 2.3: Excavated root of 2-year old *Vetiveria zizanioides* in an arid climate (from [A2])
- Figure 3.1: Water movement around a ship on a restricted waterway (adapted from Groenveld (2002))
- Figure 3.2: Bank stability analysis of a characteristic geometry of natural, eroding riverbank (from Darby and Thorne (1996))
- Figure 3.3: Slip-circle failure (from Verruijt 1999)
- Figure 3.4: Mechanisms due to stratification of the soil
- Figure 3.5: Shear (above) and beam failure (below)
- Figure 3.6: Division of the slope in three zones (from CUR (1993))
- Figure 3.7: Phreatic levels in the soil just before a secondary wave breaks (above) and during waterlevel depression (below) (from CUR 1993)
- Figure 3.8: Schematic representation relevant ship-bank erosion relations
- Figure 3.9: Root-reinforcement model with a flexible elastic root aligned perpendicular to shear zone at start. Adapted from Abernethy and Rutherford (2001) after Gray and Leiser (1982)
- Figure 3.10: Variation in soil moisture under a Vetiver hedgerow (from Hengchaovanich 1998)
- Figure 3.11: Effects of Vetiver grass on bank erosion
- Figure 5.1: Test setup
- Figure 5.2: Sketch of the test setup (medium groundwater level)
- Figure 5.3: Results growth rates of the stems (MX)
- Figure 5.4: New tiller
- Figure 5.5: Increase in tillers per week (MX)
- Figure 5.6: Results growth rates of the stems (C)
- Figure 5.7: Increase in tillers per week (C)
- Figure 5.8: Small roots at the surface (soil type C)
- Figure 5.9: Overview results
- Figure 6.1: Different soil shear testing devices: 1.Vane test 2.Triaxial test 3.Direct shear test 4.Simple shear test (from Verruijt 1999)
- Figure 6.2: Test results triaxial tests for fallow soil and soil with Vetiver roots
- Figure 7.1: Water level change due to ship passage
- Figure 7.2: Sketch test setup
- Figure 7.3: Sketch of the equidistant measuring grid for profile measurements ($\Delta Z= 5\text{cm}$, $\Delta Y= 5\text{cm}$)
- Figure 7.4: Boxplots of soil type C, first and second run
- Figure 7.5: Total bank retreat of soil type C, two runs (both after 1300 cycles)
- Figure 7.6a: Boxplots of soil type C with Vetiver, first and second run
- Figure 7.6b: Boxplots of soil type C with Vetiver, third run
- Figure 7.7: Total bank retreat of soil type C with Vetiver , three runs (each 1300 cycles)
- Figure 7.8: Loss of bank material for fallow soil and for soil with Vetiver
- Figure 7.9: Position fallow soil type MX after five cycles
- Figure 7.10a: Boxplots of soil type MX with Vetiver, first run
- Figure 7.10b: Boxplots of soil type MX with Vetiver, third run
- Figure 7.11: Total bank retreat of soil type MX with Vetiver, 3 runs (after 1900 cycles)
- Figure 7.12: Loss of bank material for soil MX with Vetiver
- Figure 7.13: Comparison loss of bank material for soil type MX and C

List of tables

Table 5.1:	Initial values of growth test (MX)
Table 5.2:	Initial values of growth test (C)
Table 5.3:	Results growth rates of the stems and the leaves after 54 days (MX)
Table 5.4:	Increase in tillers per week (MX)
Table 5.5:	Rate of growth below-ground biomass
Table 5.6:	Results growth rates of the stems and the leaves after 54 days (C)
Table 5.7:	Increase in tillers per week (C)
Table 6.1:	Results triaxial tests fallow soil type C
Table 6.2:	Results triaxial tests soil type C with Vetiver grass
Table 7.1:	Number of holes and the corresponding loss of bank material

List of symbols

A_c	cross-sectional area of channel	$[m^2]$
A_r	cross-sectional area of roots intersecting the sample cross-section	$[m^2]$
A_s	cross-sectional area of ship	$[m^2]$
A_s	cross-sectional area of soil	$[m^2]$
a_i	average cross-sectional area of roots in size-class i	$[m^2]$
b	bank position	$[m]$
c	cohesion	$[Nm^{-2}]$
c'	effective cohesion	$[Nm^{-2}]$
C_{ic}	celerity of interference cusps	$[ms^{-1}]$
C_{pw}	celerity of primary wave	$[ms^{-1}]$
c_r	apparent cohesion due to roots	$[Nm^{-2}]$
c_u	undrained cohesion	$[Nm^{-2}]$
D	depth below the soil surface	$[m]$
d	grain diameter	$[m]$
d_r	root diameter	$[m]$
F_C	cohesive force per unit mass	$[N]$
F_{cp}	magnitude of the resultant hydrostatic confining pressure	$[Nm^{-2}]$
FD	resultant driving force acting on failure block	$[N]$
Fr	Froude number	$[-]$
FR	resultant resisting force on failure block	$[N]$
FS	stability factor or safety factor with respect to stability	$[-]$
FS_τ	factor of safety with respect to bank shear	$[-]$
f	coefficient of friction	$[-]$
f_{undr}	undrained shear stress	$[Nm^{-2}]$
g	gravitational acceleration	$[ms^{-2}]$
H	overall bank height	$[m]$
H_{ic}	wave height interference cusps	$[m]$
H'	uneroded bank height	$[m]$
\bar{h}	mean water depth	$[m]$
i	bank angle	$[^\circ]$
K	tension crack depth	$[m]$
K_h	relic tension crack depth	$[m]$
L_s	length of the vessel	$[m]$
L	length of failure plane	$[m]$
L_{ic}	wavelength interference cusps	$[m]$
L_{min}	minimum length	$[m]$
m_s	mass of a sediment particle	$[kg]$
n_i	number of roots in size-class i	$[-]$
R	empirical variable	$[Nm^{-2}s^{-1}]$
s	shear strength	$[Nm^{-2}]$
s_e	empirical erosion rate constant	$[ms^{-1}]$
s_{si}	distance from sailing line	$[m]$
s_u	undrained soil shear strength	$[Nm^{-2}]$
T	wave period	$[s]$
T_r	maximum tensile stress developed in the roots	$[N]$
u	pore water pressure	$[Nm^{-2}]$
U_r	return current	$[ms^{-1}]$
U_w	total pore-water pressure acting on failure plane	$[Nm^{-2}]$
V_{lim}	limit speed of a self-propelled ship	$[ms^{-1}]$
V_s	ship's service speed	$[ms^{-1}]$
W_t	weight of failure block	$[Nm^{-2}]$

Z	water-level depression	[m]
z	thickness shear zone	[m]
α	angle between direction of resultant of the confining pressure and a normal to the failure plane	[°]
α_c	correction factor	[-]
β	failure plane angle	[°]
ϕ	angle of internal friction	[°]
ϕ'	effective angle of internal friction	[°]
γ	specific weight or bulk density	[kgm ⁻³]
ζ	coefficient of proportionality for ships	[-]
λ	porosity of bank material	[-]
θ	angle of shear distortion	[°]
θ_{bank}	bank angle	[°]
ρ	specific weight	[kgm ⁻³]
ρ_s	bulk density of a sediment particle	[kgm ⁻³]
σ	normal or total stress on the plane	[Nm ⁻²]
σ'	normal (effective) stress on the plane	[Nm ⁻²]
τ_{bank} or τ	mean bank shear stress	[Nm ⁻²]
τ_{crit} or τ_c	critical bank shear stress for bank material	[Nm ⁻²]
τ_f	critical shear stress	[Nm ⁻²]
τ_{rs}	shear strength of the soil-root composite	[Nm ⁻²]

1. Introduction

1.1 Background

Bank erosion in rivers, canals and other waterways is a major concern, for engineering and environmental reasons, in many parts of the world. The erosion itself is not actually wrong, but it threatens interests situated near the waterway. Therefore, banks that consist of easily erodible material may have to be protected or strengthened in order to reduce erosion.

There are several ways of establishing a bank protection to prevent erosion. Which design is preferred depends mainly on the functionality for user and environment, the costs and the construction time [Schiereck 2004]. All these factors may depend on local conditions like availability of building materials, costs of manpower or hydraulic conditions (waves, currents etcetera). In countries like Vietnam heavy equipment and also the use of rock is relative expensive because of scarcity, while man power is relative inexpensive [Le Viet Dung *et al* 2003]. Therefore it may be worthwhile to employ so-called "environmentally friendly banks" in such countries. This method of bank protection is in this case probably cheaper, aesthetically more attractive and has a much smaller impact on the environment.



*Figure 1.1: Erosion of a bank of the Mekong, Vietnam
(from Le Viet Dung *et al* (2003))*

In a number of tropical countries Vetiver grass (*Vetiveria zizanioides*) is being used among others as a measure against top soil erosion of agricultural land and mountain- and hillsides for decennia now. More recently, it has also been tested as a bank protection. For this purpose Vetiver grass was planted on several test sites (in China, Vietnam, Australia and the Philippines) with quite good results [Ke *et al* 2003 Le Viet Dung *et al* 2003], whereupon it has been planted on several other locations. However, these tests were merely focused on if it works in practice and did not derive data for basic understanding of the processes and properties. Besides these tests, field tests and measurements have also been performed which were mainly focused on flow erosion [Dalton 1996, Ke *et al* 2003, Metcalfe *et al* 2003]. There is, up to now, no data available on the principles of reduction of vessel-induced bank erosion by Vetiver grass.

1.2 Problem definition

There is still a lack of qualitative and quantitative knowledge in which way Vetiver grass is able to withstand bank erosion caused by vessel-induced loads. Besides, river banks are pre-dominantly cohesive [Mosselman 1989] and therefore it is certainly of importance to gain more insight in the growth properties of Vetiver grass in clay. This Master of Science thesis therefore focuses on gaining more quantitative and qualitative insight on vessel-induced bank erosion of banks protected with Vetiver grass and growth properties of Vetiver grass in clay.

1.3 Approach

In order to tackle the first problem mentioned in paragraph 1.2, the following steps are to be taken:

1. Understand the erosion processes
2. Consider how each of these processes may be affected by vegetation in general
3. Determine the dominant properties of Vetiver grass which most affect these erosion processes
4. Try to quantify the effects of Vetiver grass on the processes in different circumstances
5. Attempt to use the results to set up a relation/model for the processes and properties

It is however impossible to deal with all of the aspects in these steps thoroughly and completely in this thesis, because of the limited time and resources. Therefore the activities are further defined in the objectives.

1.4 Objectives

The first three steps mentioned in paragraph 1.3 will be discussed in this thesis. This will lead to some hypotheses that will be tested as in step 4. However this thesis will not cover all processes and properties and won't cover step 5.

The following main objectives were defined for this thesis:

1. Setting up a qualitative description to gain a better understanding of the processes and properties of reduction of bank erosion by Vetiver grass.
2. Obtain qualitative and quantitative information on some specific processes and properties

The second main objective is defined into more detail after the analysis performed in chapter 3.

1.5 Readers guide

The first two chapters deal with the investigation of the processes involved. Chapter 2 is about some basic Vetiver grass properties, after which the relevant physical processes are described (chapter 3) resulting in aspects which should be investigated. Chapter 4 deals with the hypotheses which follow from the investigation performed in chapter 3. The description of the tests that were carried out, are given in chapter 5, 6 and 7. They deal respectively with the growth tests of Vetiver grass, the geotechnical tests performed to determine relevant soil properties on bank stability and the physical model test of small scale mass failure. Chapter 8 provides an overview on the conclusions to be drawn from the tests, and chapter 9 gives an overview of the recommendations based on this thesis study; for application of Vetiver grass and for further research.

2. Vetiver grass

2.1 Introduction

Vetiver grass is a typical bioengineering species. It is used for all kinds of purposes all over the world, mostly in relation with erosion control. An overview of countries where it is actively used is given in figure 2.1. This thesis focuses on the use of Vetiver grass as a bank protection. This chapter gives a brief introduction on Vetiver grass and some of its basic properties. For more background information on Vetiver grass is referred to, for example Maaskant (2005) or the website of the Vetiver network [A].



Figure 2.1: Vetiver grass distribution with active programs (adapted from [A1])

2.2 Classification

Vetiver grass is a clump-forming perennial grass, which presumably originates from the Asian continent. Vetiver is closely related to other fragrant grasses such as Lemon grass (*Cymbopogon citratus*) and Palmarosa (*Cymbopogon martinii*). There are twelve known varieties of Vetiver grass; the most relevant one for this thesis is *Vetiveria zizanioides* (L) Nash [Worldbank, 1993]. Especially the south Indian genotype of *Vetiveria zizanioides* is of interest, because it does very rarely form seeds and therefore has a very low weed potential. Anatomically Vetiver grass can be classified as a hydrophyte (an aquatic plant) because its roots possess aerenchyma-tissues¹ with air passages that enable flooded roots to snorkel air from above-water plant parts. This is why Vetiver grass is able to survive several months of submergence [Xia et al 2003, Ke et al 2003]. However, it is also known to thrive under xerophytic² conditions.



Figure 2.2: *Vetiveria zizanioides* (from [B])

2.3 Morphological characteristics

2.3.1 Above ground

The Vetiver grass above ground biomass consists of stems and leaves. The stems can be subdivided into two different groups: vegetative green stems (bundles of concentric leaf sheets) and woody stems. The green stems have several long narrow leaves (no more than 8 millimeters wide) that can become up to 2 m long. The stems are erect and are propagated by root divisions, or slips. Vetiver grass is often planted in hedges. These dense hedges are formed when planted close together. This is the most common configuration in which Vetiver grass is used. Vetiver grass stems have a high stiffness. Numerical values are mentioned by

¹ These type of cells enable gas exchange

² Areas with very little free moisture

Dunn and Dabney (1996), who evaluated among other things the moment of inertia and the modulus of elasticity associated with the elastic limit at several growth stages of a couple of grasses including Vetiver. The above ground parts are under good conditions very fast growing: growth rates of about 1-2 cm/day were reported by Yoon (1993) and Ke *et al* (2003). With higher average temperatures (25-30°C) the growth rate can become even higher.

2.3.2 Below ground

The below ground biomass of Vetiver grass consists of a strong dense, mainly vertical massive finely structured root system that can grow up to more than 3 m in length [e.g. Ke *et al* 2003]. Vetiver grass has neither stolons nor rhizomes. The below ground part is also very fast-growing under good conditions. As mentioned in the introduction, Vetiver roots are very strong and have a high mean tensile strength. Hengchaovanich (1998) recorded an average mean value of 75 MPa at 0.7-0.8 mm root diameter (appendix A) and Cheng *et al* (2003) recorded an average tensile strength of 85.10 ± 31.2 MPa at a root diameter of 0.66 ± 0.32 mm. This is very high compared to other grasses [Wu 1995]. Maaskant (2005) has carried out tests on the growth rate of Vetiver grass with varying groundwater levels. She concluded that a high groundwater level resulted in a smaller root length for a limit depth of 75 cm.



Figure 2.3: Excavated root of 2-year old Vetiveria zizanioides in an arid climate (from [A2])

2.4 Physiological Characteristics

Vetiver grass has a high tolerance level for all kinds of circumstances. It has a tolerance for extreme climatic variation such as drought, flood, submergence and high temperatures (up to 55°C), but thrives best in a climate with a mean temperature of 18-25°C. It is also known to be able to cope with a wide range of soil pH (3.0 to 10.5), a high level of sodicity and acidity and high levels of mineral toxicities (aluminium, manganese) [Truong 2000]. It has a high ability to regrow quickly after a period of bad growing circumstances. However, it is not suited for mild climates. Growth is very slow at low temperatures and it does not survive frost. It was also shown by Maaskant (2005) that Vetiver grass was able to survive mild saline conditions (9‰). However, at a higher salinity (35‰) the Vetiver grass did not survive.

3. Physical processes

3.1 Introduction

As mentioned in paragraph 1.3 we need to have a clear picture of the physical processes involved. There are different causes for hydraulic loads on banks, the main causes are: ship-traffic, wind, weather, tide and river-discharges. These result in a couple of eroding agents: waves, current, rainfall, runoff, weathering, or changing water levels. This thesis is focused on vessel-induced loads. First, a description is given of loads caused by ship traffic, after which erosion of unprotected cohesive banks is further investigated. Then the influence of vegetation and, more specific, Vetiver grass on these processes is treated. The last paragraph (3.8) deals with the experiments for this thesis following from this analysis.

3.2 Vessel-induced loads

The interaction between a sailing vessel and the direct surrounding water can be divided, according to Schiereck (2004), into 3 main components. Other authors (for example Groenvelde (2002)) use a different classification but describe the same phenomena. The three mentioned by Schiereck are:

- Primary wave
- Secondary wave
- Propeller wash

The primary wave consists of (figure 3.1):

1. Bow wave or front wave, first circumscription of the water-level depression
2. Water-level depression or drawdown, on both sides of the ship
3. Return current, on both sides and under the ship, opposite to the sail direction
4. Stern wave, last circumscription of the water-level depression
5. Return current, a current behind the ship and above the bank slope which has the same direction as the sail direction

According to CUR 201 (1999) 1 and 5 do not have a relevant influence on a bank.

The transverse and diverging waves caused by ships are called secondary waves. The combination of these two wave types result in

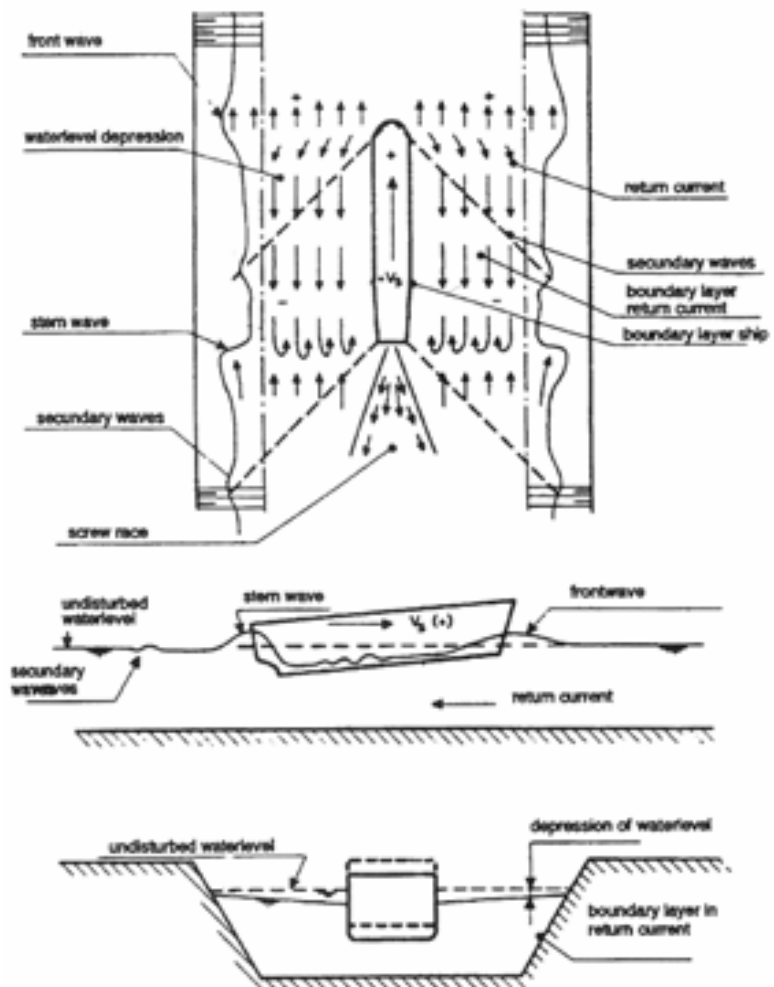


Figure 3.1: Water movement around a ship on a restricted waterway (adapted from Groenvelde (2002))

interference cusps. The secondary wave train usually consists of two higher waves followed by 10 to 15 smaller waves.

The propeller wash locally leads to very turbulent high flow velocities. Whether this phenomenon has any influence on the erosion of the banks depends on for example the distance ship-bank and the course of the waterway. The propeller wash is not taken into consideration in this thesis.

The magnitudes of the phenomena mentioned above are:

1. Vessel-related

- size of vessel (draft, length, beam width and tonnage)
- speed of the vessel
- hull shape

2. Channel-related

- size of channel (width, depth and cross-sectional area)
- bank height
- shape of channel

The limit speed is for self-propelled ships limited to its own generated primary wave speed, which is related to the length of the ship [Schiereck 2004].

$$V_{lim} = c_{pw} = \sqrt{\frac{gL_s}{2\pi} \tanh \frac{2\pi\bar{h}}{L_s}} \quad (3.1)$$

where c_{pw} = celerity of primary wave (ms^{-1}); L_s = length of the vessel (m); g = gravitational acceleration (m/s^2); and \bar{h} = mean water depth (m).

If the cross-sectional area of the ship is not negligible compared to the waterway's cross-sectional area, this approach is no longer valid. In order to determine the primary water movement in that case, Groenveld (2002) referred to Schijf (1949), who developed a method combining the theorem of Bernoulli and the equation of continuity. This method is called the method of preservation of energy. For a detailed description of the assumptions and derivations of the relations between the different phenomena is referred to for example Groenveld (2002).

The resulting relations between the ship's limit speed V_{lim} (ms^{-1}), water-level depression Z (m) and return current U_r (ms^{-1}) are graphically displayed in a dimensionless way as a function of the gravitational acceleration g (ms^{-2}), mean water depth \bar{h} (m), ship's service speed V_s (ms^{-1}) and the cross sectional ratio between ship and channel A_s/A_c in appendix B.

The factor α_c is a correction for the non-uniform distribution of U_r . It can be determined by:

$$\alpha_c = 1.4 - 0.4 \frac{V_s}{V_{lim}} \quad (3.2)$$

The value of $\alpha_c = 1,1$ stands for vessels with a sailing speed $V_s = 0,75 V_{lim}$, which is a commonly used value. The primary wave travels at the same angle with the bank as the propagation direction of the vessel, which is normally speaking parallel.

The interference cusps, which are the dominant load regarding secondary waves, do not propagate parallel to the bank. For moderate speed and for a bank parallel to the sailing direction their angle of approach is 55° . The wave height of the interference cusps can be described with the following relation [Schiereck 2004]:

$$\frac{H_{ic}}{h} = \zeta \left(\frac{s_{si}}{h} \right)^{-1/3} Fr^4 \quad \text{with} \quad Fr = \frac{V_s}{\sqrt{gh}} \quad (3.3 \text{ and } 3.4)$$

where H_{ic} = wave height (m); h = water depth (m); ζ = coefficient of proportionality (depending mainly on draught and shape of the bow); s_{si} = distance from sailing line (m); and Fr = Froude number. The wave period (T) and wavelength (L_{ic}) are related to the wave celerity (c_{ic}) by [Schierreck 2004]:

$$c_{ic} = \frac{gT}{2\pi} \quad \rightarrow T \approx 0.82 V_s \frac{2\pi}{g} \quad \text{and} \quad L_{ic} = c_{ic} T \quad (3.5, 3.6 \text{ and } 3.7)$$

3.3 Erosion of cohesive banks

3.3.1 Introduction

Erosion of cohesive banks is a very complex phenomenon in which a lot of factors have influence. Besides the different eroding agents, bank properties like bank material weight and texture, shear strength, cohesive strength, physio-chemical properties, bank height, cross-sectional shape, ground water level, permeability, stratigraphy, cracks and planes of weakness and the influence of living organisms can play a role in the erosion process.

Erosion of banks can be divided into two distinct processes: entrainment of particles or mass failure under the influence of gravity [e.g. Mosselman 1989, Duan 2005]. A third process, subaerial preparation [e.g. Abernethy and Rutherford 1998] is not mentioned by all authors, for it has no direct relation with river-processes. It is taken into account though, for it has an influence on the erosion of banks. With respect to mass failure difference is made between small scale and large scale mass failure. Large scale mass failure refers to deep-seated failure planes, while small scale mass failure refers to pushing off of material and shallow seated failure planes.

3.3.2 Particle entrainment

When speaking of particle entrainment, the balance between the fluid shear stress and the critical shear stress is of major importance. In contrary with fluvial entrainment of non-cohesive material, the mechanics of fluvial erosion of cohesive sediments is poorly understood [Millar and Quick 1998]. For cohesive bank material, electro-chemical interactions between particles result in a cohesive force on a grain that is being lifted by shear stress caused by flow and lift forces caused by turbulence. The cohesive force can be expressed by [Duan 2005]:

$$F_C = m_s f_c(d, \rho_s, \lambda, \dots) \quad (3.8)$$

where f_c = cohesive force per unit mass; m_s = mass of a sediment particle; d = grain diameter; ρ_s = bulk density of sediment particle and λ = porosity of bank material. From erosion tests, it is shown that when cohesive bank materials are entrained by flow, aggregates of grains (soil crumbs or peds) [ASCE 1998, CUR 1993] are detached. Whether or not erosion occurs can be expressed by a factor of safety (FS_τ) with respect to bank shear [Millar and Quick 1998]:

$$FS_\tau = \frac{\tau_{crit}}{\tau_{bank}} \quad (3.9)$$

where τ_{bank} = mean bank shear stress (Nm^{-2}); τ_{crit} = critical bank shear stress for bank material (Nm^{-2}). Erosion occurs whenever $FS_{\tau} < 1$.

Cohesive soils are normally speaking more resistant to particle entrainment than non-cohesive soils [ASCE 1998]. CUR (1993) after Riemdsijk and Van Eldik (1992) mentioned that the loads caused by currents (tested at 1.1 m/s) are too weak to significantly erode cohesive soils. A correct quantitative description of the critical shear stress is at this moment still lacking. CUR (1993) mentioned f_{undr} or the undrained shear stress, which in practice comes down to cohesion, as a possible estimate of the critical shear stress.

3.3.3 Large scale mass failure

The stability of a bank regarding mass failure depends on the balance between the driving force of bank failure and the bank resistance force on the most critical failure surface. This is expressed in the factor of safety or stability factor:

$$FS = \frac{FR}{FD} \quad (3.10)$$

where FS = factor of safety; FR = resultant resisting force on failure block (N); and FD = resultant driving force acting on failure block (N). Mass failure is considered to be a probabilistic event [e.g. Duan 2005], whenever $FS < 1$, failure is predicted to occur. The resisting force increases with increase in soil shear strength, whereas the driving force is directly proportional to specific weight γ , bank height H and slope i [Osman and Thorne 1988]. According to Coulomb, the critical shear stress in a soil body can be expressed in the following way [Verruijt 1999]:

$$\tau_f = c' + \sigma' \tan \phi' \quad (3.11)$$

in which τ_f = critical shear stress (Nm^{-2}), c' = effective cohesion (Nm^{-2}), σ' = normal (effective) stress on the plane (Nm^{-2}), ϕ' = effective angle of internal friction (degrees).

Mass failure stability of cohesive riverbanks can be estimated by a slope-stability analysis. Millar and Quick (1998) referred to the limit equilibrium methods (methods of slices by e.g. Bishop (1955), the slip-circle method by Taylor (1948) and planar failure by e.g. Lohnes and Handy (1968)) as the most commonly used methods. The local circumstances determine which method is the most suitable one.

Planar failure

According to Osman and Thorne (1988) steep slopes fail along an almost planar failure surface, while a gentle slope fails along a slip-circle. Most eroding river banks are very steep, often close to 90° . Consequently, their stability relations were only developed for steep banks ($>60^\circ$). The method was developed for homogeneous soil conditions.

The framework for the stability analysis of Darby and Thorne (1996) is illustrated in fig. 3.2. According to this analysis the driving force of bank failure is given by:

$$FD = W_t \sin \beta - F_{cp} \sin \alpha \quad (3.12)$$

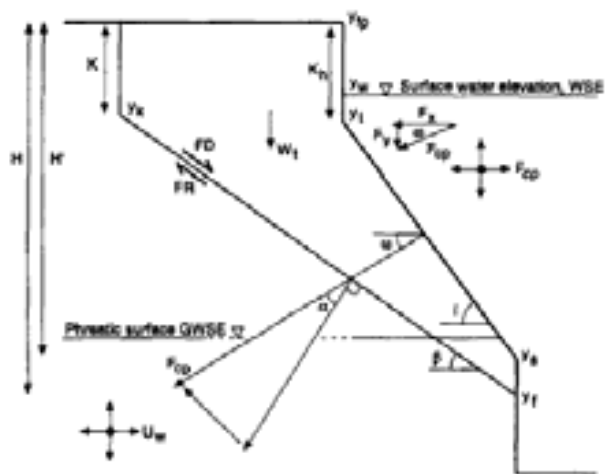


Figure 3.2 Bank stability analysis of a characteristic geometry of natural, eroding riverbank (from Darby and Thorne (1996))

where W_t = weight of failure block (Nm^{-2}); β = failure plane angle (degrees); F_{cp} = magnitude of the resultant hydrostatic confining pressure (Nm^{-2}); and α = angle between direction of resultant of the confining pressure and a normal to the failure plane (degrees).

The resisting forces, when taking into account the effects of pore-water and hydrostatic confining pressures, are given by:

$$FR = cL + [(W_t - U_w) \cos \beta + F_{cp} \cos \alpha] \tan \phi \quad (3.13)$$

where L = length of failure plane (m); U_w = total pore-water pressure acting on failure plane (Nm^{-2}). By geometry

$$W_t = \frac{\gamma}{2} \left(\frac{H^2 - K^2}{\tan \beta} - \frac{H'^2 - K_h^2}{\tan i} \right) \quad (3.14)$$

where γ = specific weight soil (Nm^{-3}); H = overall bank height (m); H' = uneroded bank height (m); K = tension crack depth (m); K_h = relic tension crack depth (m); i = bank angle (degrees)
The length of the failure plane is given by

$$L = (H - K) / \sin \beta \quad (3.15)$$

Substituting (3.14) and (3.15) through (3.12) and (3.13) into (3.10) results in

$$FS = \frac{FR}{FD} = \frac{\left(\frac{c(H - K)}{\sin \beta} + \left[\frac{\gamma}{2} \left(\frac{H^2 - K^2}{\tan \beta} - \frac{H'^2 - K_h^2}{\tan i} \right) - U_w \right] \cos \beta + F_{cp} \cos \alpha \right) \tan \phi}{\frac{\gamma}{2} \left(\frac{H^2 - K^2}{\tan \beta} - \frac{H'^2 - K_h^2}{\tan i} \right) \sin \beta - F_{cp} \sin \alpha} \quad (3.16)$$

In their paper Darby and Thorne (1996) also discussed the estimation of the failure plane angle, pore-water and hydrostatic confining pressure terms for a given bank situation. However, this is out of the scope of this thesis, as it is about the principles and it doesn't seek a stability analysis fitted for a specific location.

Method of slices

According to Verruijt (1999) there is a large variety of methods which in itself illustrates that none of them is exact. Most methods are based upon a slip-circle failure. The soil above the slip surface is subdivided into slices as shown in figure 3.3. Most methods are then based upon the momentequilibrium with respect to the midpoint of the circle. If all slices have an equal width, this results in the following expression for the factor of safety:

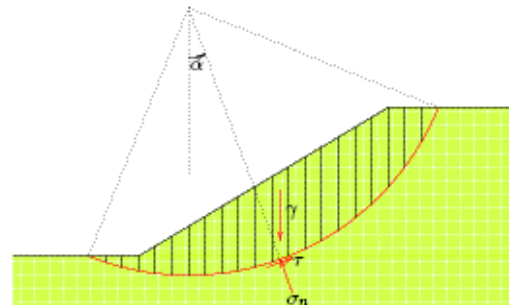


Figure 3.3: Slip-circle failure (from Verruijt 1999)

$$FS = \frac{\sum [(c + \sigma'_n \tan \phi) / \cos \alpha]}{\sum \gamma h \sin \alpha} \quad (3.17)$$

in which σ'_n = effective normal stress (Nm^{-2}); α = angle between vertical direction and the direction of the effective normal stress (degrees); h = height of slice (m)

The method of Bishop (Verruijt 1999) also takes into account the forces between the slices, which is one of the most often used methods. The resulting relation is:

$$FS = \frac{\sum \frac{c + (\gamma h - u) \tan \phi}{\cos \alpha (1 + \tan \alpha \tan \phi / FS)}}{\sum \gamma h \sin \alpha} \quad (3.18)$$

Non-homogeneous soil conditions can be taken into account in the unit weight, all contributions of each soil layer can be added.

Slip-circle method of Taylor

According to Millar and Quick (1998) after Taylor (1948), the factor of safety in undrained conditions with respect to height is defined as:

$$FS_H = \frac{N_s c_u}{H \gamma_{sat}} \quad (3.19)$$

The variation of N_s can be expressed by:

$$N_s = 3,83 + 0,052(90 - \theta_{bank}) - 0,0001(90 - \theta_{bank})^2 \quad (3.20)$$

where θ_{bank} = bank angle (degrees). The method was developed for homogeneous soil conditions. For stratified banks with varying soil properties average or representative values have to be used, which results in a lower level of accuracy.

3.3.4 Small scale mass failure

Shallow seated failure planes are in principle the same as deep seated failure planes, the same relations as mentioned in paragraph 3.3.3 are valid. However, when material is loose to some extent and for example a cantilever is formed, the balance of strength versus load is different. This process is usually induced by strong stratification and weathering of the soil which results in crack-forming. Layers of cohesive soil may become detached from layers below and above them, because of differences in erodibility. A schematisation of the mechanisms is shown in figure 3.4, in which shear failure and beam failure along a vertical plane are illustrated. Shear failure occurs when the weight of the lump exceeds the soil shear strength along a vertical plane, which results in a downwards slip of the lump. Beam failure occurs when disturbing moments about the neutral horizontal axis exceed restoring moments. This results in a

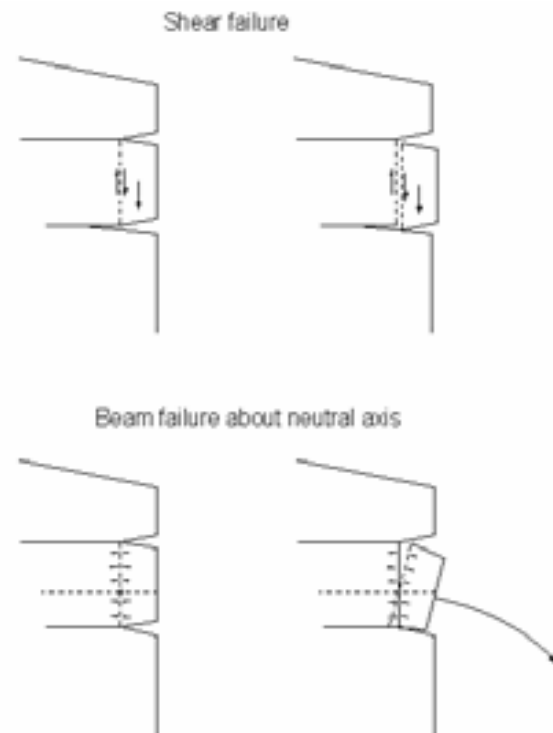


Figure 3.4: Mechanisms due to stratification of the soil

forward rotation of the soil lump. A rapid drawdown (further specification will be provided in paragraph 3.4) may have four different types of influence:

1. Loss of confining pressure provided by the surface water level
2. Positive pore pressures due to poor drainage resulting from the low permeability of the soil
3. Increases in the effective unit weight of the soil due to saturation
4. Cracks are filled up with water, which results in extra disturbing pressures on the clay

In the following approximations the soil block is considered to be a so-called black-box (no deformations of the block itself, rigid body approach) and is assumed only to be attached to the bank on the backside. When one would also consider a block which has binding with the soil besides it and not only at the back, the resisting force is increased for the shear zone is increased, while the extra attachment doesn't influence the driving force. This results in a higher stability and is not of interest in this study, for it only discusses the limit state of the material.

Shear failure

The driving force is determined by the soil weight and the dimensions of the block, while the resisting force is determined by size of the shear plane and the shear strength of the soil (figure 3.5):

$$\frac{FR}{FD} = \frac{\tau h_b}{b_b h_b \gamma_{sat}} \quad (3.21)$$

where τ = mean bank shear stress (Nm^{-2}); h_b = height of block (m); b_b = width of the block (m); γ_{sat} = saturated specific weight (Nm^{-3}). If a crack is present on plane AB, the shear plane surface is reduced and therefore the resisting force is reduced.

Beam failure

The driving force is determined by the soil weight and dimensions of the block, while the resisting force is determined by dimensions of the compression zone, the compression strength, the dimensions of the tension zone and the tensile strength (figure 3.5):

$$\frac{FR}{FD} = \frac{\sigma_t \frac{1}{2} v^2 + \sigma_c \frac{1}{2} w^2}{h_b \frac{1}{2} b_b^2 \gamma_{sat}} \quad (3.22)$$

where σ_t = tensile strength (Nm^{-2}); σ_c = compressive strength (Nm^{-2}); w = block height under compressive strength (m); v = block height under tensile strength (m). If a vertical crack is present, starting at A for example, the tension zone for the soil is reduced. If the crack is also filled up with water, an extra hydrostatic force is introduced, which adds an extra disturbing moment around the neutral axis C.

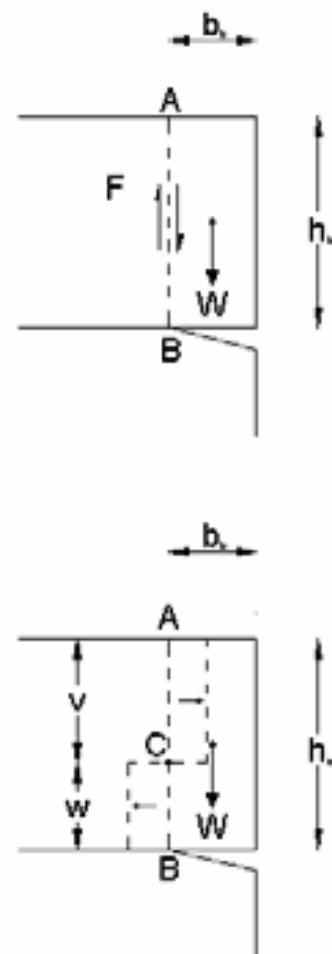


Figure 3.5: Shear (above) and beam failure (below)

It is stressed that for both schematisations the position of a crack often determines the position of the failure plane, which does not necessarily have the shape and angle as schematised above. The principle of driving force versus resisting force, however, does not change by position or angle of the failure plane.

3.3.5 Subaerial preparation

This process is primarily caused by the weather. All the mechanisms that cause this process are unrelated with ship traffic. Raindrop impact, surface run-off, freeze-thaw loads, wind erosion etcetera, may all cause subaerial preparation. The main processes are surface erosion by wind and run-off, an increase in crack forming by freeze-thaw loads and a decrease in permeability of the soil by raindrop impact, which influences the moisture content of the soil. The mass failure mechanism of pushing off of material is induced by forming of cracks or the presence of layers of different materials through the cohesive banks. In this respect, this can be considered as subaerial preparation. Parts of the soil which have no internal binding anymore, are being pushed off as a result of the presence of excess pressures caused by mechanisms described in paragraph 3.4.

3.4 Vessel-induced failure mechanisms

Among the mechanisms of riverbank erosion described in literature, erosion caused by the passage of vessels is quite important. Parchure *et al* (2001) referred to Maynard and Martin (1996) who reviewed literature on the possible impact of vessel wakes on bank erosion and described processes related to ship traffic and gave numerous examples of bank erosion studies carried out in the world over the past several years. According to Bauer *et al* (2002) there is by far no consensus on the subject of erosion by vessel-induced loads. This isn't very surprising considering the high amount of statistical, methodological and natural uncertainty.

When considering vessel-induced loads on unprotected banks, distinction has to be made in which zone the load acts. According to CUR (1993) the slope is divided into three parts (figure 3.6):

- I. Slope below the wave zone
- II. Slope in the wave zone
- III. Slope above the wave zone

Slope below the wave zone

- Particle entrainment caused by: the return-current and turbulence
- Mass failure caused by: Upwards water pressure gradient (for example water-level depression caused by a ship). Normally this load is relatively small in this zone.



Figure 3.6. Division of the slope in three zones (from CUR (1993))

When considering cohesive material the slope of the bank in this zone is of minor importance. When erosion occurs one does not speak of an equilibrium profile (as with non-cohesive material) but of an equilibrium situation (exercised shear stress = critical shear stress), so the shape of the profile is dominated by the loads.

Slope in the wave zone

The following loads are dominant in this zone:

- Wave-loads on the surface caused by the stern wave
- Wave-loads on the surface caused by secondary waves (interference cusps)
- Varying pressure differences in the ground caused by the water-level depression.

The limiting riverbank stability usually occurs when bank strength is reduced by increased unit weight of the soil and the excess pore-water pressures during a drawdown [Darby and Thorne 1996]. The phreatic water level is not able to follow the surface water level because

of the low permeability of cohesive soils. This results in an increase in head and an increase in pore water pressure, which reduces the effective shear stress, and therefore may result in mass failure. This is also the case just before a secondary wave breaks on the slope. Both are illustrated in figure 3.7. Because of the highly structured nature of the soil in this zone there is an increased chance of pushing off of pieces of clay, or the occurrence of shallow slips. However, when considering the latter, the lowest water level during the primary wave (water-level depression) is likely to be dominant because of the longer duration of exposure to the pressures. The amount of energy a soil is able to dissipate is not only determined by maximum shear strength, but also by allowable shear displacement [Ekanayake and Phillips (1999)].

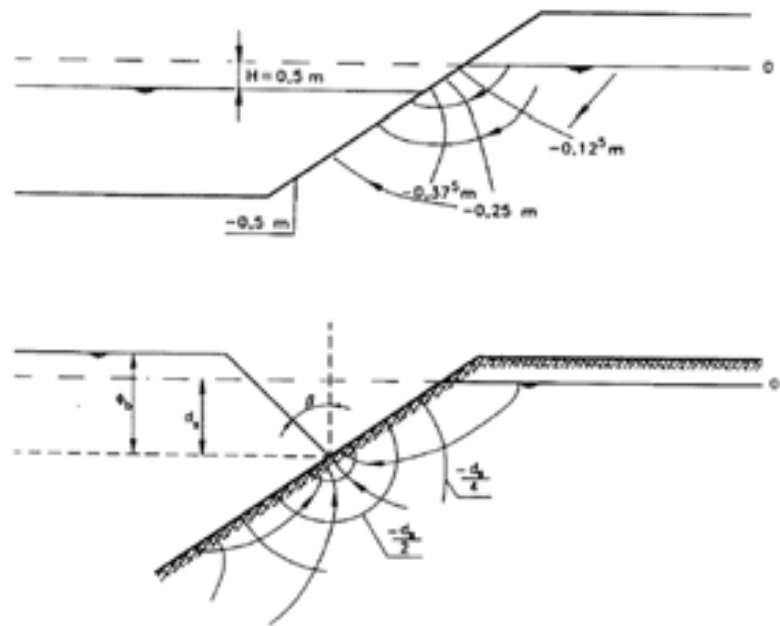


Figure 3.7: Phreatic levels in the soil just before a secondary wave breaks (above) and during waterlevel depression (below) (from CUR 1993)

According to CUR (1993) erosion of structured clay in aggregates of grains (soil crumbs or peds) was observed during tests. Water pressures propagate through cracks of clay and may push off these aggregates of soil and in so doing changing the load on the rest of the material. Usually the occurrence of mass failure like slip circles is a result of the undermining of a slope. The size of the erosion material is generally speaking larger than the material eroded in the zone under the wave zone, but still one has to speak of an equilibrium situation instead of an equilibrium profile.

Water pressures propagate through cracks of clay and may push off these aggregates of soil and in so doing changing the load on the rest of the material. Usually the occurrence of mass failure like slip circles is a result of the undermining of a slope. The size of the erosion material is generally speaking larger than the material eroded in the zone under the wave zone, but still one has to speak of an equilibrium situation instead of an equilibrium profile.

Slope above the wave zone

This zone is not influenced by passing ships.

Summary of the failure mechanisms

- | | |
|-----------------------------------|---|
| 1. Transport below the wave zone: | particle entrainment and slope instability |
| 2. Transport in the wave zone: | particle entrainment, pushing off and slope instability |
| 3. Transport above the wave zone | not influenced by ship traffic |

On each specific bank different failure mechanisms can be of importance. One way to quantify this is to look at the load/strength ratio of each separate failure mechanism. The execution of observations is another possibility to determine which mechanism is dominant. Besides the processes and mechanisms mentioned above, four other aspects should be taken notice of [CUR 1993]:

- Swell → reduction of effective stresses on a long time scale. Clay in Holland is known to be quite unsusceptible for swell. However, in those countries where Vetiver is used it is unknown. If swell does occur, the changes of small and shallow landslides (up to a couple of decimetres) increases. If the material also consists of sand- or gravel layers, there is an increased risk of local mass failure to a depth of approx. 1 m.

- Dispersion → the dissolving or the disintegration of aggregates of soil due to chemical reactions with substances which are dissolved in the water.
- Biodegradation → a process exclusively related to peat. It occurs when peat comes in contact with water with a high oxygen content, whereby it may lose its coherence
- Fluidisation → occurs whenever the effective stresses are reduced to zero, caused by an increase in pore water pressures. When speaking of river banks it is restricted to a thin surface layer of the bank.

Besides the secondary waves, the water-level depression and the return current also the stern wave has influence on the erosion process. It generates a long shore current, because it has a parallel propagation direction with the shore.

The schematic representation in figure 3.8 gives a short overview of the main ship-bank erosion relations.

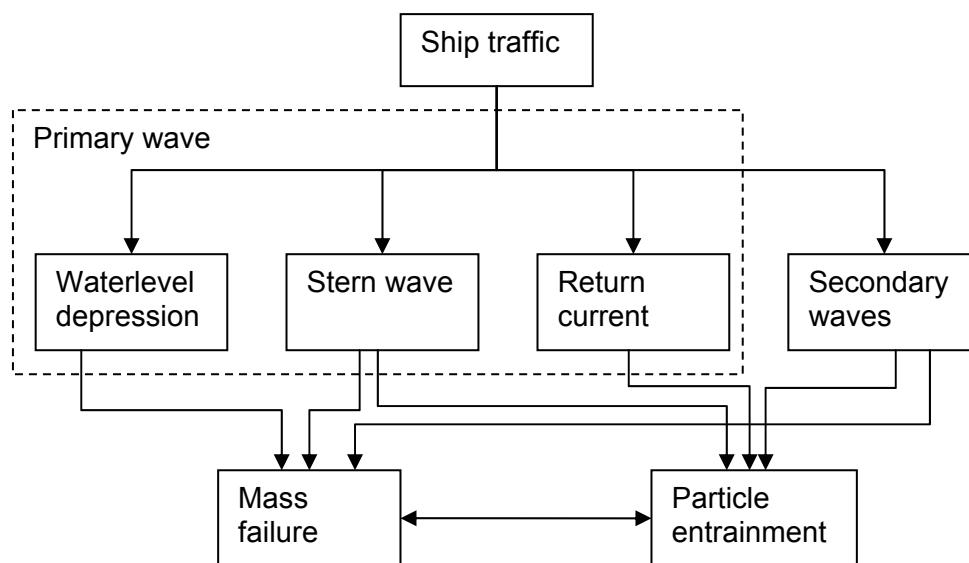


Figure 3.8: Schematic representation relevant ship-bank erosion relations

It is important to realize that failure mechanisms can have direct influence on each other. Particle entrainment can lead to mass failure and mass failure can influence particle entrainment.

3.5 Erosion models

CUR 96-7 (1996) reported that there is a lack of a correct transport formula for cohesive soils. Therefore a predictive model for erosion of unprotected banks is very hard to establish. Also the ASCE task committee (1998) mentioned this last fact. The causes are to be found in uncertainties in identification of failure mechanisms and erosion processes, size of dominant parameters and the heterogeneity of the soil, among others.

Alternatives for a transport model may be found in existing models like the commonly used erosion-rate-model (e.g. Osman and Thorne 1988, Mosselman 1989, CUR 1996, Parchure *et al* 2001):

$$\frac{db}{dt} = s_e * \left[\frac{\tau - \tau_c}{\tau_c} \right] \quad (3.23)$$

where db/dt = erosion rate (m/s); s_e = empirical erosion rate constant; τ = shear stress (Nm^{-2}); τ_c = critical shear stress for erosion. This model is based on the mean rate of bank retreat of cohesive banks with lateral erosion. In the paper by Osman and Thorne (1988) s is given by:

$$s = \frac{R}{\rho g} \quad (3.24)$$

with:

$$R = 0,364 \tau_c \exp(-1,3 \tau_c) \quad (3.25)$$

where ρ = specific weight of water (kg/m^3); $0,364$ = factor ($1/s$); $1,3$ = factor (m^2/N). CUR (1993) also investigated the use of the dune-erosion model DUROSTA to have a first indication about erosion rates. Blind runs did provide some reasonable results. The transport formulation remains the main problem when using this model, though.

3.6 Vegetation effects on bank erosion

3.6.1 Introduction

The effects of vegetation on the rate of erosion of cohesive sediments are complex and poorly understood. Vegetation can significantly influence particle entrainment as well as mass stability. However, whether vegetation increases or reduces e.g. bank stability is not always clear. The type, age, density and health of the vegetation all may have influence. Generally, a species with a dense network of fibrous roots is of more benefit than one with a sparse network of woody roots. In this paragraph the main processes mentioned in paragraph 3.3 are discussed.

3.6.2 Subaerial preparation

The foliage and plant residues intercept and absorb rainfall energy and prevent soil compaction by raindrop impact. Conclusively the infiltration capacity at the surface is raised and due to this a reduction of surface runoff is established. A reduction in surface run-off reduces topsoil erosion. The foliage also decreases near-ground wind velocities and provides a certain degree of protection against frost [Thorne 1990, ASCE 1998].

3.6.3 Particle entrainment

When the canopy is submerged it decreases the erosive forces by decreasing the near-bank velocities via an increase in hydraulic roughness. Plant stems also may dampen turbulence to reduce peak shear stresses. The boundary shear stress is proportional to the square of near bank velocity [e.g. Duan 2005]. Therefore a reduction of the velocity results in a high reduction in the eroding forces. Quantification remains however very difficult. A complicating factor is the bending of the material under flow conditions. Clearly the type of vegetation is very important. While grasses and shrubs are most effective at low velocities (relatively low level of bending), woody species are not very prone to bending, but may induce scouring by increasing the local acceleration. The density of the vegetation may play a role in this respect too. The rootsystem is also able to decrease near-bank or near-ground flow velocities and due to this it decreases the rate of particle entrainment. CUR 201 (1999) after RIZA and WL (1994) showed for example that the presence of reed resulted in an significant increase of

allowable velocity before erosion took place. To be effective, the roots must extend down the bank at least to the average low water level, otherwise the flow will undercut the root zone during significant flow events. In this respect, plants which are tolerant to submergence are more effective than plants which are not.

An aspect which influences both particle entrainment and mass stability, is the dissipation of wave energy by canopy. Wave dissipation caused by vegetation is discussed by several authors, e.g. Burger (2005) describes the wave energy dissipation by mangroves. No research has yet been performed to test wave energy dissipation by Vetiver grass.

Besides reducing the load on the bank, root networks also can physically restrain soil particles and increase critical shear stress via an apparent cohesion. Soil particles in fallow soil, which would have been removed by entrainment, are fixed on the bed by the filter-like functioning of the root network. The quantification of this process is very hard. Possible parameters are: Root density (e.g. Root-Area-Ratio), size of the erodible material and flexibility of the root network. Also, the increase in critical shear stress is very hard to define, as mentioned in paragraph 3.3.2.

3.6.4 Large scale mass failure

Vegetated banks are drier and much better drained compared with unvegetated banks. They are drier mainly because the canopy intercepts rain, and water is drawn from the soil by their roots. Drier banks are more stable, because of the decrease in bulk unit weight of the soil, while effective and apparent cohesion is increased. Roots and humus increase permeability and therefore reduce excess pore-water pressures.

Many studies have shown that tree roots improve soil strength and slope stability [e.g. Wu and Erb 1988, Wu and Watson 1998, Ekanayake and Phillips 1999, Simon and Collison 2002, Roering *et al* 2003]. The root system strengthens the soil by transferring the shear stress in the soil to tensile stress in roots via the skin friction of the root [e.g. Thorne 1990, Abernethy and Rutherford 2001]. In this way it introduces an extra cohesion over and above the intrinsic cohesion that the bank material may have. However, because of their random orientation, roots seem to have little effect on the frictional component of soil strength [Wu 1995]. Abernethy and Rutherford (2001) provided the following modified Mohr-Coulomb failure criterion for root-permeated soil:

$$\tau_{rs} = c' + c_r + (\sigma - u) \tan \phi' \quad (3.26)$$

where τ_{rs} = shear strength of the soil-root composite (Nm^{-2}); σ = normal stress on the plane (Nm^{-2}); u = pore water pressure with $\sigma' = \sigma - u$ (Nm^{-2}); and c_r = apparent cohesion due to roots (Nm^{-2}).

A simple model of a root-reinforced soil is shown in figure 3.9. During shear, the flexible, elastic root is stretched as it deforms across a planar shear zone with a certain thickness (z). When the soil deforms, tensile stress accumulates in the roots and mobilizes the shear strength of the interface between soil and root (τ_r). The tensile force can be resolved into normal and tangential components to the shear plane, whose

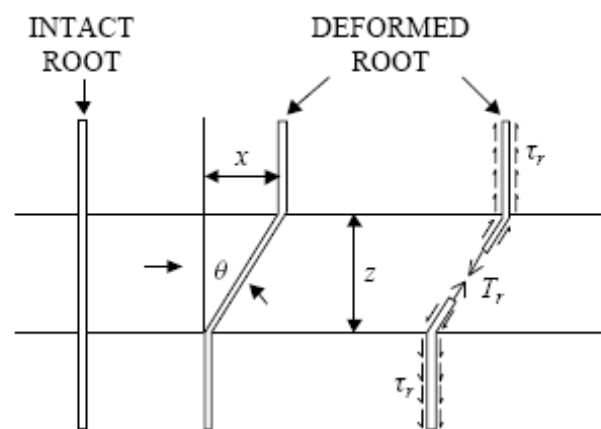


Figure 3.9: Root-reinforcement model with a flexible elastic root aligned perpendicular to shear zone at start. Adapted from Abernethy and Rutherford (2001) after Gray and Leiser (1982)

interactions produce the apparent cohesion due to roots. Abernethy and Rutherford (2001) give a description of the analysis and assumptions which lead to the following approximation of c_r :

$$c_r = T_r \frac{A_r}{A_s} (\cos \theta \tan \phi + \sin \theta) \quad (3.27)$$

where T_r = the maximum tensile stress developed in the roots (N); θ = the angle of shear distortion (*degrees*); A_r/A_s = the root area ratio (RAR), which is the sum of the cross-sectional area of the roots intersecting the sample cross-section A_r , expressed as a non-dimensional ratio of the total cross-section of the soil, A_s [adapted from Abernethy and Rutherford 2001 after Gray and Leiser 1982]:

$$\frac{A_r}{A_s} = \frac{\sum n_i a_i}{A_s} \quad (3.28)$$

where n_i = number of roots in size-class i ; and a_i = average cross-sectional area of roots in size-class i (calculated with the mid-point diameter of each size-class).

This model of c_r assumes that the full tensile strength is mobilized during failure. Therefore pulling-out of roots must be prevented by a minimum length given by [Abernethy and Rutherford 2001 after Gray and Sotir 1996]

$$L_{\min} = \frac{T_r d_r}{4\tau_r} \quad (3.29)$$

with:

$$\tau_r = D\gamma(1 - \sin \phi)f \tan \phi \quad (3.30)$$

where L_{\min} = minimum length (m) of roots of uniform diameter d_r (m) required to mobilize full tensile resistance and prevent pull-out; D = depth below the soil surface (m); f is coefficient of friction (set to 0.9 after Gray and Sotir 1996, p.82).

Ekanayake and Phillips (1999), however, used a different approach to calculate the increase in shear strength caused by roots. They used an energy approach (EA) instead of the limit equilibrium (LE) method, in which not only the increase in maximum shear was taken into account, but also the increase in length of shear displacement before failure. This method is limited to vegetated hillslopes where the stability analysis can be approximated by a simplified infinite slope model.

To increase the shear strength of the bank material, the roots must cross the most critical plane of failure. When the bank is relatively high or the rooting depth relatively low, the roots do not reinforce the soil against failure. Roots will still continue to prevent shallow slips and still bind the failure block together during and after collapse, so that failed blocks are more likely to remain at the toe and protect the intact bank from further failure, but are not able to prevent deep-seated soil slips. Research performed by Wood *et al* (2001) has shown the existence of apparent cohesion between failed, cohesive blocks without vegetation and their underlying surface, but disturbed soil is still less resistant to erosion than the original bank [Mosselman 1989]. In this respect vegetation may play a role in further increasing this apparent cohesion.

A negative effect of vegetation is the surcharge of a bank by the weight of vegetation [Thorne 1990]. Especially vegetation with a large above-ground biomass (especially trees) increase

the vertical load on the failure block and due to this increase instability. Vegetation exposed to wind transmits dynamic forces into the slope. Other causes of reduction of stability by vegetation are related to reduction of internal bonds of the soil and increasing pore pressures. Decayed dead roots will leave voids and holes, reducing cohesion and allowing of water inflow that can result in freeze–thaw damage [Thorne 1990]. Desiccation of the soil from trees and other vegetation can occur particularly during droughts, resulting in crack forming.

However, it is likely that vegetation in fact reduces the forming of cracks [Micheli and Kirchner (2002)]. The forming of cracks is induced by tension in the soil. While soil is weak in tension and strong in compression, plant roots are strong in tension but weak in compression. It was for example reported in studies of alluvial bank materials that the tensile strength of rooted samples was on average ten times that of unrooted samples [Thorne 1990 after Thorne, Murphy and Little 1981].

3.6.5 Small scale mass failure

Again, when considering shallow seated failure planes they are in principle the same as deep seated failure planes. With respect to the other failure mechanisms mentioned in paragraph 3.3.4, the roots will increase shear stress (shear failure) and will increase the tensile strength (beam failure). Micheli and Kirchner (2002) assumed that gains in the shear strength due to roots are primarily tensile. Even if there isn't any connection left between the bank and the material being pushed off, roots may still prevent failure, but again only if the roots have enough tensile strength and are not being pulled-out. Probable parameters are: root density (RAR), root tensile strength, size of the failure block, bulk density of the material and the size of the external loads (e.g. waves). It is also possible that fatigue of the roots will play a role when considering the external loads. No data is available on this topic at this moment.

3.7 Influence of Vetiver grass on bank erosion

The question presents itself which properties of Vetiver grass would make it suitable for bank protection and which limitations and problems may occur when applying Vetiver grass. The following salient properties will very likely contribute to the reduction of bank erosion.

- Fast growing plant (under good conditions)
- Soil moisture depletion (figure 3.10)
- Herbaceous root system (high density of fibrous roots with a small mean diameter)
- Deep vertical rooting depth up to 3 m depending on the soil type
- Relatively tolerant to submergence
- Stiff (especially just above ground level) and dense upright hedges
- Dense system of stems and leaves
- High root tensile strength (appendix A)
- Relatively low above-ground biomass

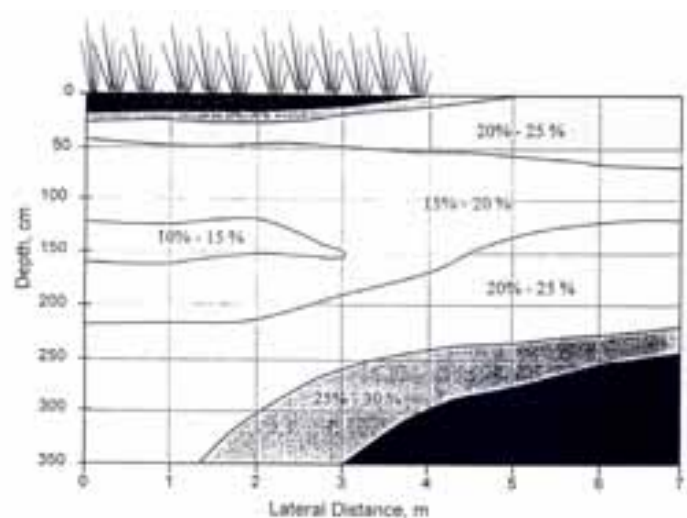


Figure 3.10: Variation in soil moisture under a Vetiver hedgerow (from Hengchaovanich 1998)

An overview of all the processes involved in the protection of riverbanks by Vetiver grass (including the adverse ones) is given in figure 3.11.

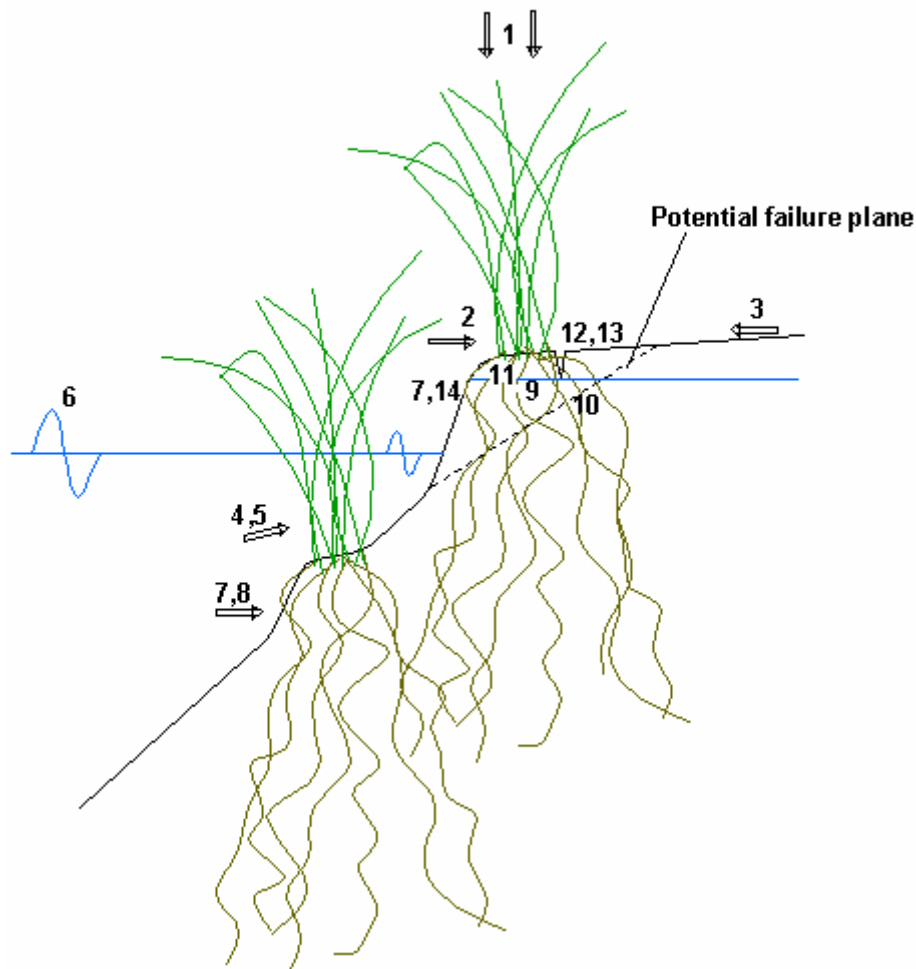


Figure 3.11: Effects of Vetiver grass on bank erosion

		Influence
	Subaerial preparation	
1	Canopy intercepts rainfall, which dissipates raindrop energy and reduces rainfall available for infiltration	A
2	Canopy reduces wind erosion by stabilizing the surface and decreasing near-surface wind velocities, but the canopy exposed to wind transmit dynamic forces into the slope	A/B
3	The stems reduce run-off erosion by reducing flow velocities but at the same time increase infiltration	A/B
	Particle entrainment	
4	Submerged canopy reduces near-bank flow velocities	A
5	Submerged canopy damps turbulence, which results in a reduction of peak shear stresses	A
6	Submerged canopy, especially the stems dissipate wave energy	A
7	The rootsystem physically restrains soil particles	A
8	The rootsystem provide an apparent cohesion, which increases critical shear stress	A
	Mass failure	
9	Rootsystem increases drainage and permeability which results in a decrease of excess pore pressures	A

- List continues on next page -

10	The rootsystem increases soil shear strength via apparent cohesion and therefore the probability of the occurrence of a landslide is reduced	A
11	Decayed roots reduce cohesion and increase the change on freeze-thaw damage	B
12	Depletion of soil moisture may accentuate desiccation cracking in the soil, resulting in higher infiltration capacity	B
13	The tensile strength of the roots hinder crack forming	A
14	The tensile strength of the roots hinder pushing off of aggregates of soil	A

Legend: A = Adverse to erosion
B= Beneficial to erosion

3.8 Resulting tests

3.8.1 Introduction

This study is focused only on vessel-induced loads. As mentioned in paragraph 3.3.5, subaerial preparation is not influenced by ship traffic at all and, as found in paragraph 3.3.2, cohesive banks have a high resistance to partial entrainment. The main focus of this thesis is pointed on the aspects of mass failure as it may be dominant, also because there is a lack of time to investigate all other aspects.

3.8.2 Large scale mass failure

Two alternatives have been examined:

- Execution of a physical model test (replica of a river bank with Vetiver)
- Comparison of relevant properties of cohesive material with and without Vetiver

When considering a physical model test on cohesive material 1g-testing will in any case not be possible (it is impossible to scale cohesion). The biggest problem encountered when performing a scale test with soil is that the mechanical properties of that soil often depend upon the state of stress, which is determined largely by the weight of the soil itself. In a scale model, the stresses are much smaller than in reality, which implies that it is not a good reproduction of reality. In order to obtain a good reproduction of the stresses, the volumetric weight has to be increased, without changing the material. This can be achieved by placing a scale model in a centrifuge. Because of the high rotation speed that then can be obtained (by the centripetal acceleration), it appears as if gravity is magnified. In this way, all stresses in the model are the same as in reality, which more or less guarantees that the soil in the model behaves as it would do in reality. For more details about the centrifuge is referred to, for example Verruijt (1999). The test in the centrifuge is for this thesis not possible because of the unavailability of a centrifuge, at least until June 2006. Without these practical limitations, the main problem of this scale test would be how to scale the Vetiver roots. More research has to be performed in order to make further statements on this.

A different way to investigate large scale mass failure would be to obtain the values for the relevant properties for slope stability of two different types of samples, one of these samples consisting of cohesive soil and the other one consisting of that same soil but now with fully-grown Vetiver roots in it. It is important to understand which parameters mentioned in the methods in paragraph 3.3.3 are relevant. When considering vessel-induced loads, all phenomena have relative short timescales (seconds to minutes). Experience provides us with estimates of the period of drawdown, which is normally speaking between 10 to 60 s depending on vessel speed and vessel size. Because of the very low permeability of cohesive soils it is assumed that the phreatic level will not be able to respond in this very

short timescale. It is therefore very likely that the soil behaves in an undrained way, which implies that the stability of the bank could be analysed on a total stress basis. Darby *et al* (2000) referred to this state of a bank as a "worst-case scenario". The Mohr-Coulomb theory then describes the following relation:

$$s = c + \sigma \tan \phi \quad (3.31)$$

in which s = shear strength (Nm^{-2}), c = cohesion (Nm^{-2}), σ = total stress (Nm^{-2}), ϕ = angle of internal friction (degrees).

The undrained shear strength is independent of σ . During undrained testing of a saturated sample, σ' remains constant despite changes in σ , because any increase in σ is taken up as an increase in the pore-water pressure. This results in the $\phi=0$ analysis. Actually, the soil is not taken frictionless, but it indicates that the undrained shear strength is independent of the applied total stress σ . The undrained shear strength of saturated soil s_u can therefore be represented in terms of total stress by the undrained cohesion c_u .

Planar failure

Equation (3.16) can then be rewritten in:

$$FS = \frac{FR}{FD} = \frac{\left(\frac{c_u (H - K)}{\sin \beta} \right)}{\frac{\gamma}{2} \left(\frac{H^2 - K^2}{\tan \beta} - \frac{H'^2 - K_h^2}{\tan i} \right) \sin \beta - F_{cp} \sin \alpha} \quad (3.32)$$

The terms which depend on geometry (H, i), failure plane angle and water level (α, β, F_{cp}) are not directly influenced by Vetiver grass. Also, in paragraph 3.4.4 it is stated that it is likely that vegetation reduces the forming of cracks [Micheli and Kirchner (2002)]. However, no direct proof has been provided to continue on this. Neglecting the influence of Vetiver on crack forming, and replacing all terms independent of Vetiver grass related to resistance by R and related to driving force by D results in:

$$FS = \frac{FR}{FD} = \frac{c_u * R(H, K, \beta)}{\gamma * D(H, K, H', K_h, \beta, i, F_{cp}, \alpha)} \quad (3.33)$$

Method of slices

When considering Bishop's method, equation (3.18) can be rewritten in:

$$FS = \frac{\sum \frac{c_u}{\cos \alpha (1/FS)}}{\sum \gamma h \sin \alpha} \quad (3.34)$$

Slip-circle method by Taylor

This method is already based upon the undrained conditions (equation (3.19)).

For all three methods the undrained shear strength and the bulk density of the soil are directly related to bank stability. The undrained shear stress is linearly related to the safety factor, while the bulk density is inversely proportional to the safety factor. The Vetiver grass will influence the water content of the soil. It is however very hard to determine the hydrological influence of Vetiver grass, especially within the time restrictions of this thesis.

Therefore only the direct influence of the roots on the bulk density and the (suspected) increase in undrained shear strength by Vetiver roots will be investigated.

3.8.3 Small scale mass failure

Because of the lack of an existing model on small scale mass failure, a physical model test seemed the most obvious way to obtain a first quantification of the influence of Vetiver grass on this phenomenon. However, because of the much smaller zone to be tested, 1:1 testing should be possible. A description of the test is given in chapter 7. The results of the tests for the large scale mass failure may provide indications on the improvement of small scale stability also, as shown in the analysis in paragraph 3.3.4.

4. Hypotheses

4.1 Influence of soil type and phreatic level on Vetiver grass

Maaskant (2005) found different growth rates with varying phreatic levels of Vetiver grass in potting compost. The growth rate of Vetiver grass is known to be around 1-2 cm/day, depending on the conditions. When using a different type of soil (classification of soil type MX (mixture) and C (clay) is given in appendices C and D), it is to be expected that the growth rates will differ. Therefore the first two hypotheses for soil type MX are:

1. A low phreatic level will result in a normal growth rate
2. The rate of growth of plants with a substantial different phreatic level will differ significantly from each other

However, Kirby and Bengough (2002) reported that growth rates decrease with increasing soil strength. Therefore it is to be expected that the growth rate of Vetiver grass in clay (soil type C) is significantly lower than the growth rate of Vetiver grass planted in soil type MX. Another difference may be the capillary action of clay, which will probably be higher and therefore may result in less pronounced differences between plants with different phreatic levels. This leads to the following hypotheses for soil type C:

3. The rate of growth of plants with a substantial different phreatic level will not differ significantly from each other
4. The rate of growth of Vetiver grass will be significantly lower than the growth rates of Vetiver grass in soil type MX under the same conditions.

4.2 Influence of Vetiver grass roots on soil parameters

It is to be expected that the Vetiver grass roots will significantly increase the undrained shear strength of the soil type, whereas it is expected to have no significant direct influence on the specific weight of the soil. The hypotheses are:

5. The undrained shear strength of soil type C with and without Vetiver grass roots will differ significantly from each other
6. The specific weight of soil type C with and without Vetiver grass roots will not differ significantly from each other

4.3 Bank retreat caused by water level changes

It is expected that Vetiver grass has a significant influence on the bank retreat for each type of bank material. Therefore the following hypothesis will be tested:

7. Vetiver grass reduces bank retreat caused by vessel-induced water level changes significantly

When considering erosion of cohesive banks, mass failure is very important and particle entrainment is less influential as it is with non-cohesive banks. Non-cohesive soils are generally speaking highly permeable. Therefore excess pore water pressures are not as easily established in non-cohesive soils as in cohesive soils. Vetiver grass is unable to reduce the load caused by rapid drawdown, while it most probably is able to reduce near-

bank flow velocities and wave heights. The question rises if the physical process behind the protection of a bank by Vetiver grass is dependent on bank material. It is hard to make quantitative statements on this, but qualitative observations may provide more insight.

5. Influence of soil type and phreatic level on Vetiver grass

5.1 Introduction

It is already known to some extent what kind of influence the groundwater level has on the growth of Vetiver grass in potting compost [Maaskant 2005]. However, the soil of the river banks on which Vetiver grass may be used mainly consists of materials with loam/clay-like properties. The influence of soil type and groundwater level on the growth rate of Vetiver was tested. Two different soil types were used in this experiment.

5.2 Experiment

5.2.1 Soil type MX

Experiments were carried out in the Botanical Garden - Delft University of Technology. Three Vetiver plants (obtained by splitting full-grown Vetiver plants and, as far as possible, washing out the material between the roots) were planted into a pot filled with soil. This soil type (MX) was a mixture of organic material (about 20%) clay, silt, sand and small gravels. A grain size diagram of the non-organic material in the soil has been made by sieving of the material and is shown in appendix C1. The stems of the Vetiver grass were cut off at a length of around 30 cm, while the roots were cut off at a length of 20 cm, both measured from the surface level. The pots (\varnothing 32 cm, h = 51 cm) were put into PVC pipes (\varnothing 50 cm, h= 51 cm) that were watertight with a PVC plate at the bottom. The three PVC pipes were filled with water up to three different levels. The pots with



Figure 5.1: Test setup

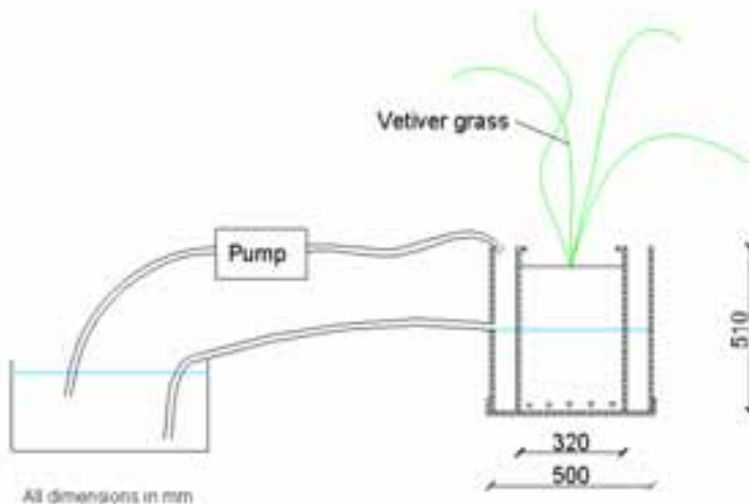


Figure 5.2: Sketch of the test setup (medium groundwater level)

the Vetiver grass had holes in the bottom through which the water could penetrate the pot. In this way the water level in the PVC pipe corresponded with the groundwater level in the pot. The water was circulated regularly to reduce algal growth and to be sure that the water level was constant, otherwise the water level might have dropped because of evaporation and water use by the Vetiver grass. An illustration of the test setup is given in figure 5.1, while a principle sketch is given in figure 5.2. The test setup for all three plants was situated in a greenhouse to provide a good

(tropical) growing climate. This means that the temperature was kept approximately at 20-25°C (with the use of heating lamps) and that the atmospheric humidity was also kept high. A couple of initial values related to the water levels and the condition of the plants have been measured and are shown in table 5.1.

	Pot #1	Pot #2	Pot #3
Water level in PVC-pipe (ø 50 cm)	8 cm	24 cm	43 cm
Difference between height pot and surface level in pot	7 cm	8 cm	5 cm
Groundwater level (in cm - surface level)	35 cm	18 cm	1 cm
Number of green stems	16	11	16
Number of green stems shorter than 30 cm	3	2	2

Table 5.1: Initial values of growth test (MX)

Each stem has several leaves and each leaf is measured individually from the cut (so 30 cm above surface level) to the top. Because of the inaccurate way the stems were cut off at the end (order of 1 cm), the uneasy way of measuring (which results in inaccuracy), and because of the growing number of leaves (and therefore growing number of measurements), it was decided to use a certain bin width. The considerations that lead to the size of the bin width were mainly practical. When using a too large bin width this would result in useless data, however, a too small bin width would still require an unnecessary high accuracy. Therefore it was decided to use a bin width of 3 cm (so 0-3, 3-6, 6-9 ...). The number of leaves in each category as well as the number of fresh stems was tallied per pot. This routine was executed 2 times a week for a period of 54 days. Also the water levels in the PVC pipes were inspected once a week too ensure that the water levels stayed constant. After this test period the (new) roots were washed out and the increase in length of the roots with a diameter $d_r > 0.5$ mm was measured.

5.2.2 Soil type C

The same test setup and procedure was used as described in paragraph 5.2.1, except for the type of soil used. The soil used in this test setup was clay retrieved from the field. The location is shown in appendix D. A classification is also provided in appendix D. The initial values related to the water levels and the conditions of the plants have also been measured for this test and are shown in table 5.2.

	Pot #4	Pot #5	Pot #6
Water level in PVC-pipe (ø 50 cm)	8 cm	24 cm	43 cm
Difference between height pot and surface level in pot	2 cm	2 cm	2 cm
Groundwater level (in cm - surface level)	40 cm	24 cm	5 cm
Number of green stems	14	20	20
Number of green stems shorter than 30 cm	5	3	2

Table 5.2: Initial values of growth test (C)

5.3 Results

5.3.1 Soil type MX

Growth rates stems and leaves

The cumulative length of the leaves is graphically displayed in appendix E1. It is quite clearly visible that the Vetiver grass with a low groundwater level has a higher growth rate than the plants with a high or medium groundwater level. However, this gives a distorted view of reality because, as shown in table 5.1, the initial conditions were not equal for all three pots. Therefore, the average length increase per stem per day was determined.

With the cumulative length increase per measurement per pot the mean rate of growth in cm/day per stem was determined (number of stems, number of leaves and number of days was known). The results are shown in table 5.3 and figure 5.3.

	Pot 1 (low)	Pot 2 (med)	Pot 3 (high)
Total cumulative length increase leaves	4354,5 cm	2755,5 cm	2619 cm
Total number of new leaves	97	69	86
Mean rate of growth per stem (in cm/day ± s.d.)	1,03 ± 0,13	0,93 ± 0,16	0,72 ± 0,14
Slope of trend line rate of growth	-0,0309	-0,0371	-0,0322

Table 5.3: Results growth rates of the stems and the leaves after 54 days

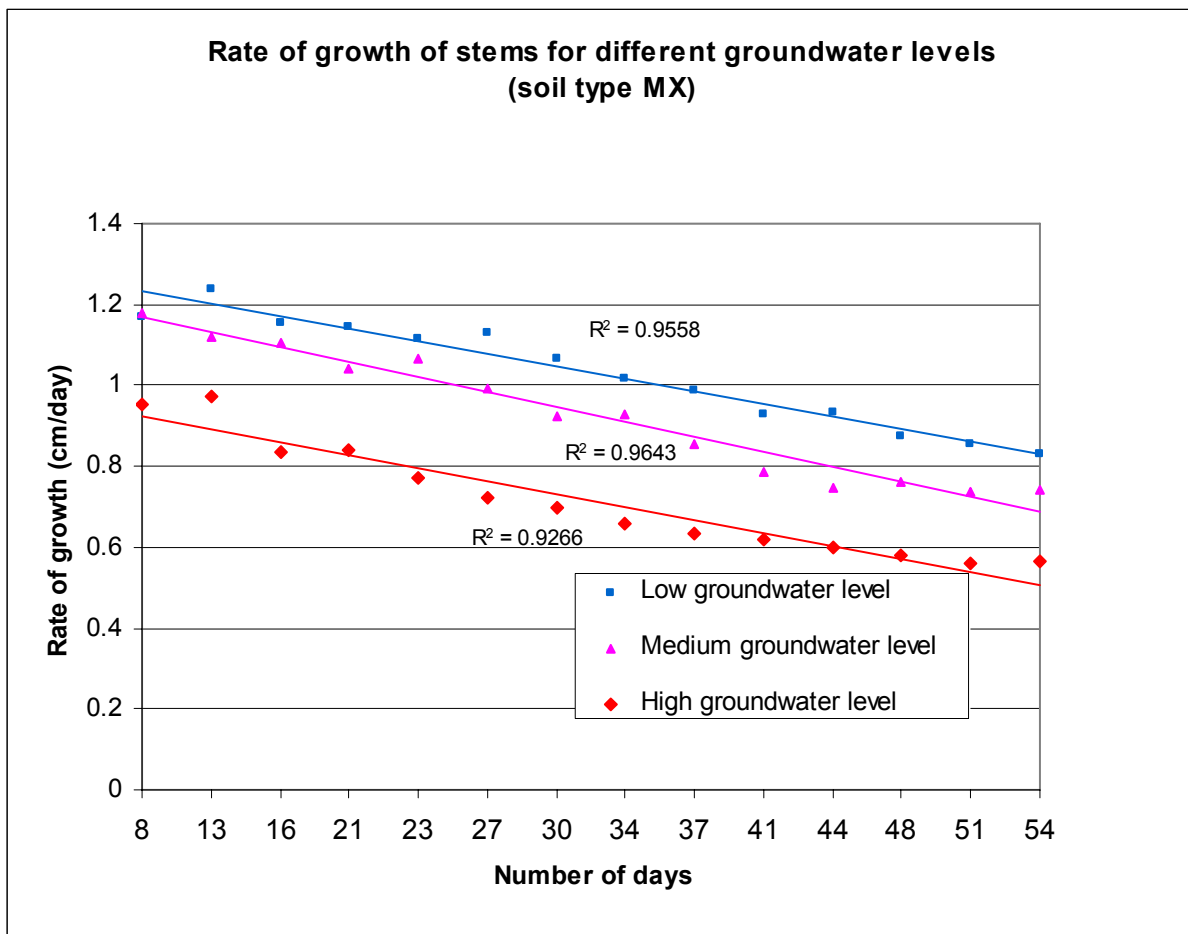


Figure 5.3: Results growth rates of the stems

The Vetiver grass with a low groundwater level did have a higher rate of growth than the plants with a medium (10%) and with a high groundwater level (30%). The plant with the high

groundwater level did have the lowest rate of growth considering length increase (20% lower than medium groundwater level). But when observing the increase in number of leaves, the high groundwater level had a higher growth rate than the medium groundwater level (again the low groundwater level had the highest growth rate). A possible explanation of the decrease in growth rate at a higher groundwater level may be the lower level of available oxygen for the roots. Another possible explanation may be that the roots grow towards the groundwater level as quickly as possible, in search of water. Therefore the presence of water in the starting phase (high groundwater level) will then result in a lower growth rate.

To be able to test the hypotheses 1 and 2, MATLAB codes for two different bootstraps were written. A description of this procedure and the results of these bootstraps are given in appendices F-H3. The results with regard to the hypotheses are:

Hypothesis 1:

The H_0 -hypothesis can't be rejected on basis of this data ($P=0,186$) and the sample mean lies in the expected range (1-2 cm/day).

Hypothesis 2:

The growth rates with the low and medium groundwater levels ($P<0,05$), the medium and high groundwater levels ($P<0,01$) and with the high and the low groundwater levels ($P<0,01$) differ significantly or even very significantly for this experiment.

It was also observed that there seemed to be a linear decrease in rate of growth over time. For all three plants there was a decrease of 30-40% in the rate of growth of the stems in 54 days. The explanation and investigation of this decrease is out of the scope of the goal of this test.

New tillers

The results are shown in figure 5.5 and in table 5.4

	Pot 1 (low)	Pot 2 (med)	Pot 3 (high)
Total number of new tillers after 54 days	7	6	3
Mean growth rate (new tillers/week \pm s.d.)	0,88 \pm 0,6	0,75 \pm 0,9	0,38 \pm 0,5

Table 5.4: Increase in tillers per week

The discrete nature of the results and the limited number of measurements are the main problems with the interpretation of these results. However, to have an indication whether or not the results match the expectation, which is around 1 new tiller per week, a parametric bootstrap was performed. It is not very accurate to retrieve a P-value from these bootstraps, because of the discrete nature of the data. Still one can get an indication whether or not the pattern gives reason to cast doubt on the hypotheses 1 and 2 from the histograms in appendix H3.



Figure 5.4: New tiller

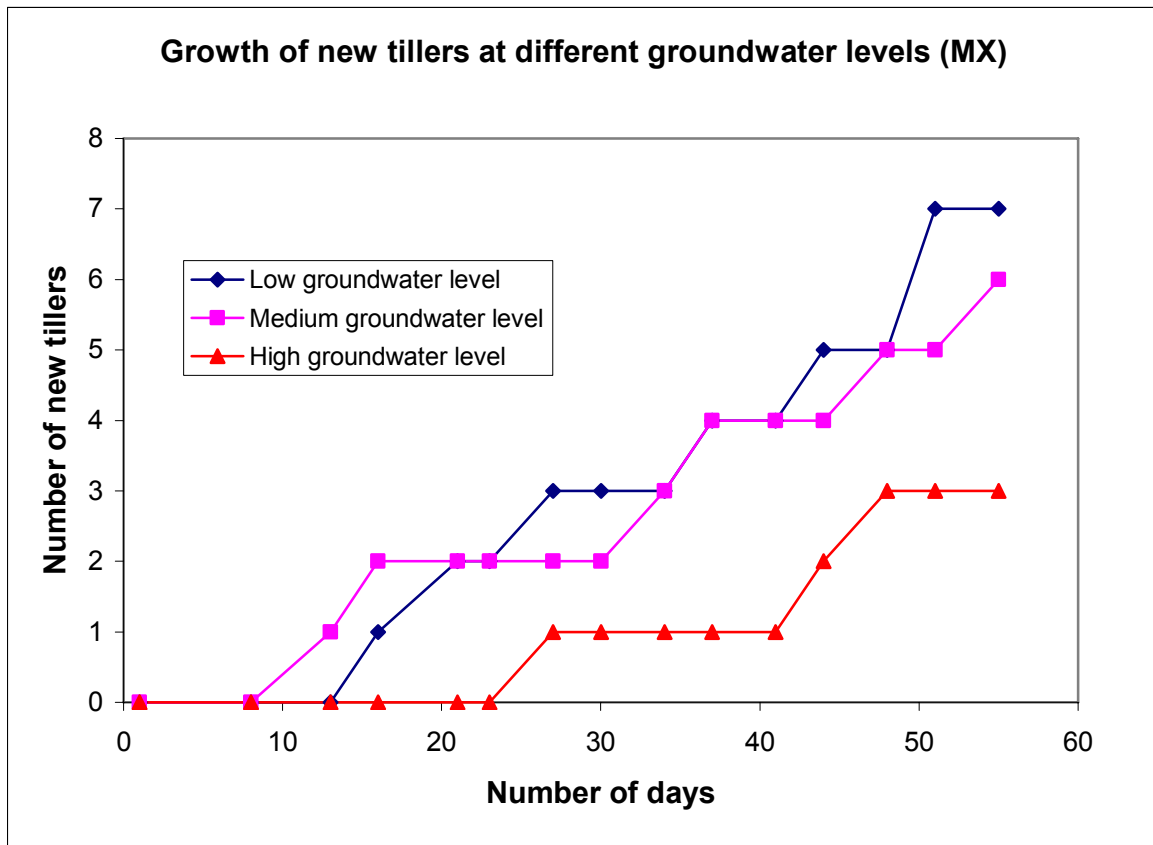


Figure 5.5: Increase in tillers per week

Again the Vetiver grass with the low groundwater level has the highest growth rate and the one with the high groundwater level the lowest growth rate. No evidence was found in order to reject the hypotheses 1 and 2 on basis of these results.

Below-ground biomass

As mentioned in paragraph 5.2 the length increase of the roots was only measured once for practical reasons. All the root lengths mentioned in this paragraph have been measured from the initial length (20 cm below ground level for all 3 pots). Only roots with a diameter $d > 0,5$ mm were measured. The results are graphically displayed in appendix I and numerically in table 5.5.

	Pot 1 (low)	Pot 2 (med)	Pot 3 (high)
Groundwater level	35	18	1
Number of new shoots	91	75	58
Total cumulative length increase	1919 cm	703 cm	538 cm
Mean length increase per root \pm s.d. (cm)	21,1 \pm 7,5	9,4 \pm 4,6	9,3 \pm 4,7
Depth range of intense root hair growth	30-40 cm	20-25 cm	-

Table 5.5: Rate of growth below-ground biomass

The same pattern as with the growth rates of the leaves and the new tillers is found. The below-ground growth of the Vetiver with a low groundwater level is highest, the growth at a medium groundwater level comes second, and the high groundwater level has the lowest growth rate. It is impossible to make quantitative statements about the growth rates of these roots because they were only measured twice, at the start and in the end. However, the root lengths provide evidence in favor of hypotheses 1 and 2.

It was also observed that in a zone of approximately 5 cm above and 5 cm below the groundwater level a very high density of small roots ($d < 0.5$ mm) was present for pot 1. But below this zone the density of these small roots dropped to zero. Pot 2 did show the same below-groundwater-level-zone (5 cm), but it was due to the presence of the old, very dense root system impossible to check whether it showed the same above-groundwater-level-zone. For pot 3 there wasn't a possibility to do this observation at all for the same reason as for pot 2.

5.3.2 Soil type C

Growth rates stems and leaves

The cumulative length increase of the leaves is given in appendix E2. The mean rate of growth in cm/day per stem was determined. The results are shown in table 5.6 and figure 5.6.

	Pot 4 (low)	Pot 5 (med)	Pot 6 (high)
Total cumulative length increase leaves	1555,5 cm	1642,5 cm	1254 cm
Total number of new leaves	63	69	62
Mean rate of growth per stem (in cm/day \pm s.d.)	0,35 \pm 0,05	0,44 \pm 0,04	0,37 \pm 0,04

Table 5.6: Results growth rates of the stems and the leaves after 54 days

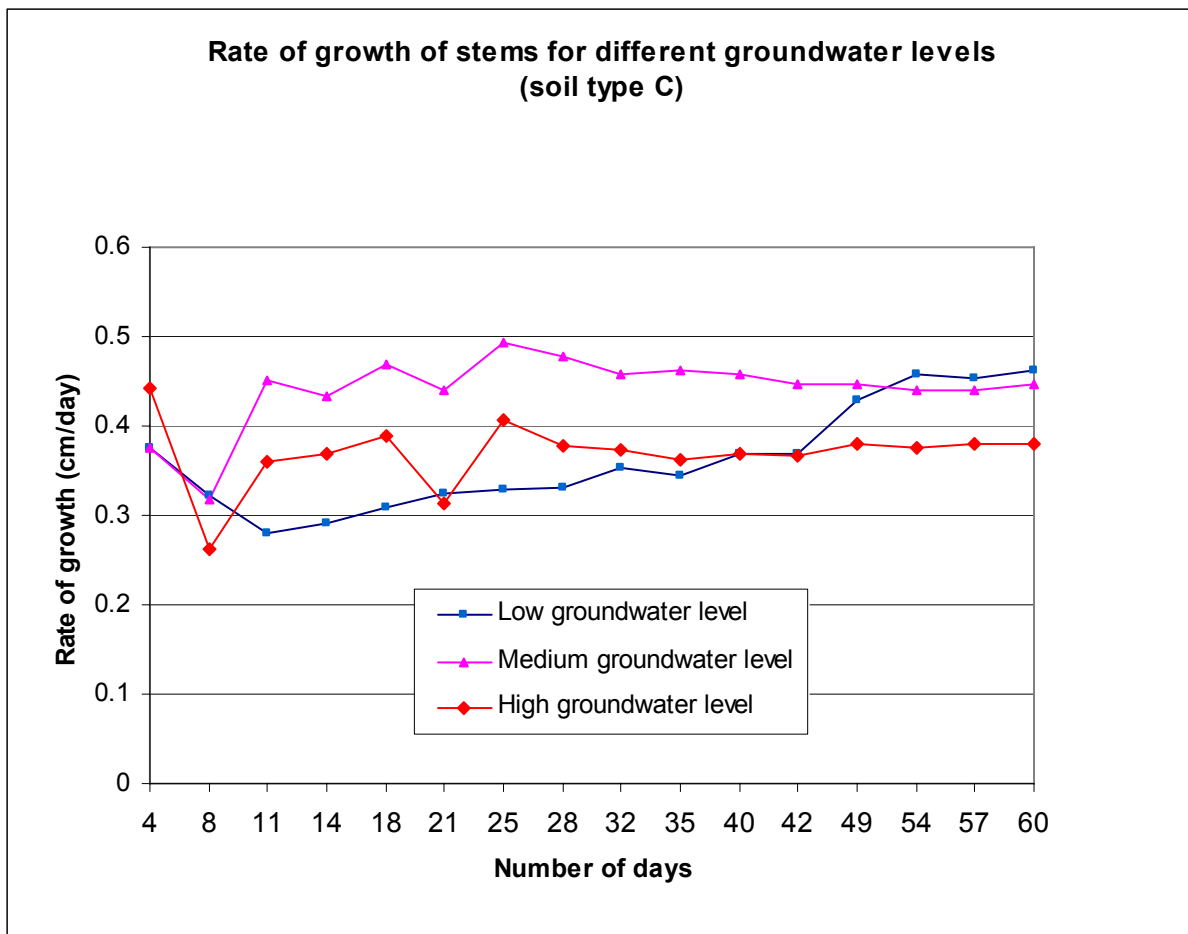


Figure 5.6: Results growth rates of the stems

The sudden increase in growth rate of the pot with the low groundwater level around 42 days is probably caused by a lower level of light intensity, while the other pots did have full light availability. However, the cause of this light interception (another Vetiver grass plant) was removed after 42 days after which the light intensity became equal again for all three pots. The high level of sensitivity of local circumstances on the growth rate of the plants is clearly to be seen in figure 5.6. The experiment was continued for 6 days extra in order to get a confirmation on the higher growth rate. The same pattern as with soil type MX emerged again: A high groundwater level results in a low growth rate. All comparisons were executed with the results after 54 days. The results of the pot with the low groundwater level were not included in the comparison. The plant with the high groundwater level did have a lower mean rate of growth than the medium groundwater level (17%).

The testing of the hypothesis was performed in the same way as with soil type MX. The results of the bootstrap for hypothesis 3 are given in appendices F, G and H4. The results with regard to the hypothesis are:

Hypothesis 3:

The growth rates with the high and medium groundwater levels differ very significantly for this experiment ($P < 0,01$). The H_0 -hypothesis is rejected on basis of this data. Therefore one can conclude that there is a strong indication that the third hypothesis has to be rejected.

New tillers

The results are shown in figure 5.7 and in table 5.7

	Pot 4 (low)	Pot 5 (med)	Pot 6 (high)
Total number of new tillers after 54 days	1	1	2
Mean growth rate (new tillers/week \pm s.d.)	0,11 \pm 0,33	0,11 \pm 0,33	0,22 \pm 0,44

Table 5.7: Increase in tillers per week

Because of the low number of new tillers a comparison via a bootstrap or any other quantitative statements are impossible.

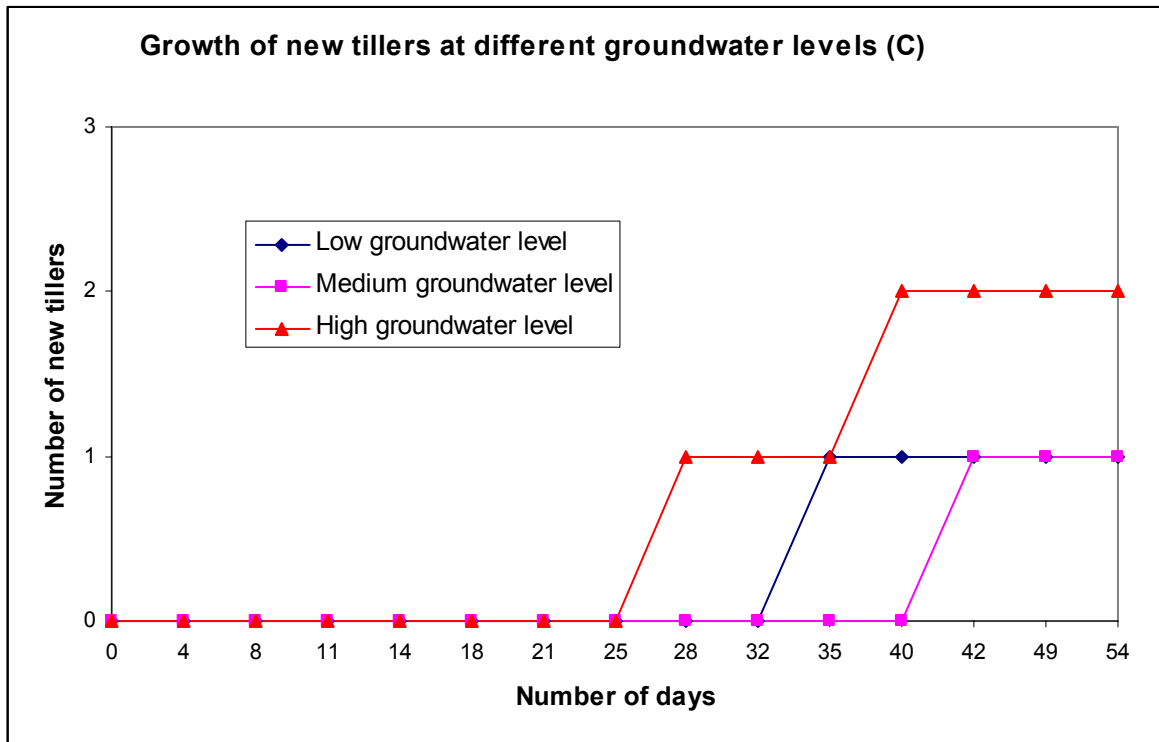


Figure 5.7: Increase in tillers per week

Below-ground biomass

Because of the impossibility of washing out the clay between the roots, no accurate measurements were possible. However, by removing clay from the bottom up to the first observed roots, the following rough indications about maximum root length were obtained:

- Low groundwater level: 45 cm
- Medium groundwater level: 40 cm
- High groundwater level: 30 cm

This provides evidence that the same growth relations as with soil type MX are valid.

It was observed that small roots ($d < 0.5$ mm) in contrary with soil type MX were present from the tips of the thicker main roots up to the surface level of the soil, illustrated in figure 5.8. No clearly defined zone was present; the roots did have a much wider distribution with soil type C.



Figure 5.8: Small roots at the surface (soil type C)

5.3.3 Comparison soil types

The comparison of the two soil types is focused on the growth rates at equal groundwater levels. The testing of hypothesis 4 was performed in the same way. The results of the bootstrap for hypothesis 4 are given in appendices F, G and H5. The results with regard to the hypothesis are:

Hypothesis 4:

The growth rates with a high groundwater level (pot 3 and 6) as well as with the medium groundwater level (pot 2 and 5), differ very significantly for this experiment ($P < 0,01$). The H_0 -

hypothesis is rejected on basis of this data. The mean growth rates of Vetiver grass with a high groundwater level as well as with a medium groundwater level were reduced by approx. 50% when growing in soil type C instead of soil type MX. Again no comparison for pot 4 (and therefore also pot 1) was performed.

Figure 5.9 illustrates the different relations found during this experiment.

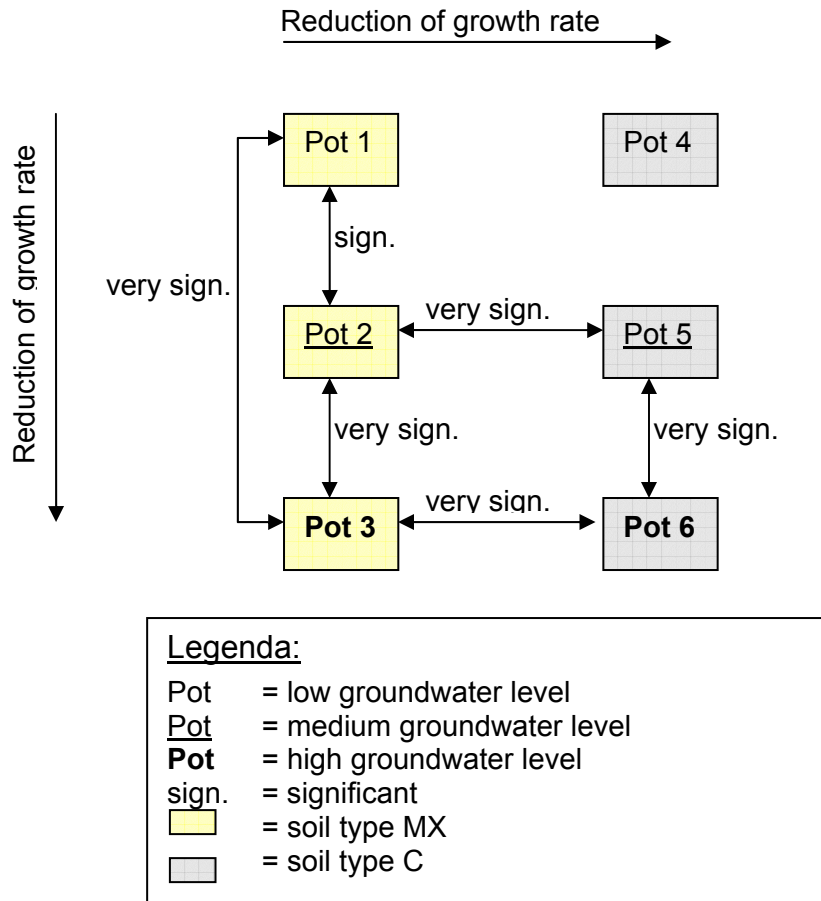


Figure 5.9: Overview results

5.4 Error analysis and assumptions

The growth rate of leaves and stems are assumed to be representative for the growth rate of the Vetiver grass. Furthermore it is assumed that the conditions for all three plants are equal during the experiment. The sudden increase of growth rate of pot 4 has shown that a small difference may result in mayor differences in results. Other general types of possible shortcomings are:

- Each phreatic level was tested only with one plant, which might lead to false conclusions
- The duration of the test may be too short, especially with the run with clay, for the phreatic level will possibly take more time to adjust
- Only shallow differences in phreatic level were tested, deeper phreatic levels may result in different trends

Above-ground biomass measurement errors

Possible measuring errors are all related to length measurements. The precision of the measuring rod (0,1 cm) is not expected to have any influence on the results, for the lengths were categorized in bins of a much larger size (3 cm). However, the results were obtained by multiplying the number of roots in a category with the mid-point length of that specific category. The assumed uniform distribution (U(0,3)) may give a false signal at small numbers. Especially at the start of the experiment, when the number of leaves was limited, the influence of a single leaf is relatively large. This is illustrated by the larger spread of data at the start of the experiment. This potential error will most probably result in an underestimation of the significance level, for a larger spread of data results in a higher P-value. It is not expected that errors were made when counting the new tillers.

Below-ground biomass

Possible measuring errors are again related to length measurements. The measurement error of the root length is related to the precision of the measuring equipment (0,1 cm). However, the conclusions are not based on these results, therefore the influence is small (merely indicative).

6. Large scale mass failure

6.1 Comparison of test methods

Four different types of test methods for the undrained shear strength were compared, the vane test, direct shear test, simple shear test and triaxial test. All four tests are well-known tests; for a full description is referred to for example Verruijt (1999).

The vane test is specifically developed for in-situ measurements. In this case, in-situ measurements are not possible because Vetiver grass doesn't thrive in the Dutch climate. Besides, it is quite easy to obtain samples for laboratory tests, it is not known how well the vane test can be performed on soils in pots, and there is a lot of uncertainty concerning the implementation and the results of this test when applied on the root system of the Vetiver grass.

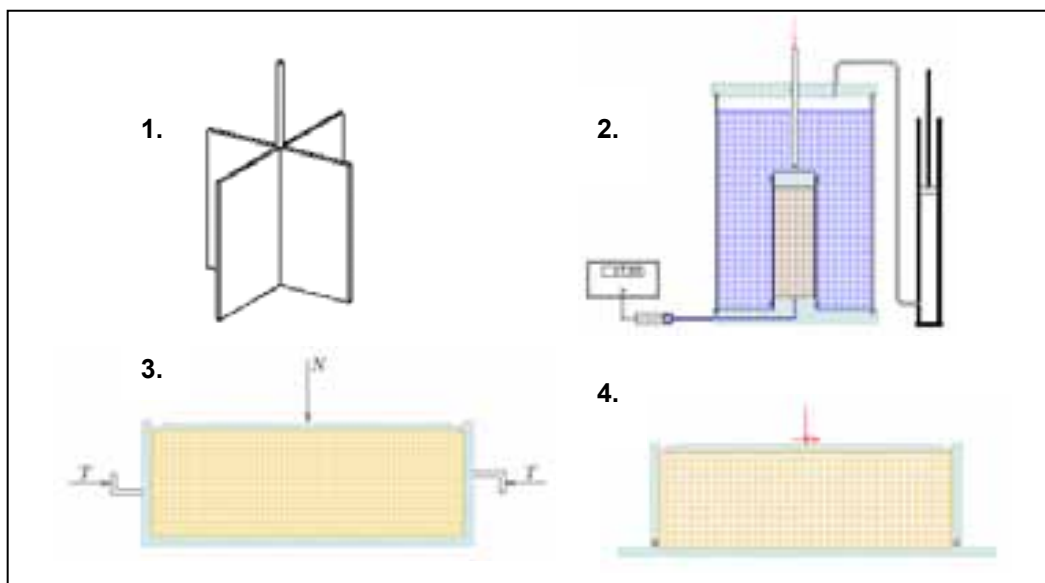


*Figure 6.1: Different soil shear testing devices: 1.Vane test 2.Triaxial test
3.Direct shear test 4.Simple shear test (from Verruijt 1999)*

Both simple as direct shear test are based upon the notion that the failure of a soil by sliding along a plain is caused by reaching a maximum value of the shear stress. In these tests a sample is loaded and failure is expected to be on a given sliding plane where one part of the sample slides over another part. One of the problems experienced with the direct shear test is that the deformation is strongly non-homogeneous. This lead to a different box layout, in which the deformations are more or less homogeneous: the simple shear test. A disadvantage of both shear tests is that it is assumed that the deformations will be in horizontal direction, while it is also possible that there will be deformations in vertical direction. When performing a shear test the state of stress is not fully known, while with a triaxial test it is. This may lead (in practice it actually did several times (Verruijt 1999) to a lower (incorrect) estimated strength than the strength estimated by a triaxial test on the same soil. The results of a shear test also have a wider distribution than the results of a triaxial test. The triaxial test was therefore chosen as testing method.

6.2 Experiment

All tests were performed in the Laboratory of Geomechanics - Delft University of Technology. The tests were executed on a total stress basis in order to retrieve the undrained shear stress of a soil sample. This type of test is called an UU-test, which stands for undrained unconsolidated. In total 20 samples were tested, 10 samples of fallow soil type C and a total of 10 samples of soil type C with Vetiver roots. All samples ($\phi=3,8$ cm) were retrieved with a sampling tube. Sample height and diameter fulfilled the criteria stated for example by TAW (1988). The "undisturbed" samples were loaded quickly after installation. Pore water pressures (precision $0,1 \text{ N/m}^2$), vertical loading (precision $0,01 \text{ kg}$) and displacement (precision $0,05 \text{ mm}$) were measured during the tests. Pore water pressures are not taken into account with tests on a total stress basis, but they were nevertheless measured in order to get some insight into the nature of the material (e.g. occurrence of dilatancy).

The samples of the fallow soil were weighted after loading (precision $0,001 \text{ kg}$) with which the saturated bulk density of the soil was determined, after which they were dried (105°C for 24 hours). The dried samples were weighted which resulted in the dry bulk density. The samples with Vetiver roots were also weighted after loading in the triaxial test. The RAR (root-area-ratio) was determined by counting the roots present in the sample at 3 different depths of the sample. The roots were categorized into four classes: $0-0,5 \text{ mm}$, $0,5-1,0 \text{ mm}$, $1,0-1,5 \text{ mm}$ and $>1,5 \text{ mm}$. The area of the sample ($\phi=3,8 \text{ cm}$) is known, so the RAR can be determined by equation (3.28). After this these samples were dried also (105°C for 24 hours) to determine the dry bulk density.

6.3 Results

6.3.1 Fallow soil type C

The results of the triaxial tests on fallow soil type C are given in table 6.1.

Sample:	Sample height (cm)	Max. shear displacement (mm)	Max. shear stress s_u (kN/m^2)	Saturated specific weight γ_{sat} (kN/m^3)	Dry specific weight γ_{dr} (kN/m^3)
1 (C)	8,0	13,0	32,6	17,3	12,0
2 (C)	7,5	14,0	37,55	16,8	-
3 (C)	8,0	12,5	27,6	17,1	-
4 (C)	7,9	13,5	36,4	16,8	11,3
5 (C)	7,9	9,0	30,05	17,1	11,7
6 (C)	8,0	10,5	30,7	17,2	11,7
7 (C)	8,0	11,0	35,1	17,0	11,8
8 (C)	7,6	10,0	29,7	17,2	11,8
9 (C)	7,8	11,5	35,95	17,4	11,8
10 (C)	8,0	12,0	31,35	17,0	11,4
Mean \pm s.d.	$7,9 \pm 0,2$	$11,7 \pm 1,6$	$32,8 \pm 4,8$	$17,1 \pm 0,2$	$11,7 \pm 0,2$

Table 6.1: Results triaxial tests fallow soil type C

The mean undrained shear stress of fallow soil type C is estimated at $32,8 \pm 4,8 \text{ kN/m}^2$ and the samples had a mean shear displacement of $11,7 \pm 1,6 \text{ mm}$. The saturated and dry specific weight are respectively $\gamma_{\text{sat}} = 17,1 \pm 0,2 \text{ kN/m}^3$ and $\gamma_{\text{dr}} = 11,7 \pm 0,2 \text{ kN/m}^3$.

No clear signs of dilatancy were observed, so there are no indications of overconsolidation of the soil.

6.3.2 Soil type C with Vetiver grass

The results of the triaxial tests on soil type C with Vetiver grass are given in table 6.2. The results of the RAR measurements are displayed in appendix J.

Sample:	Sample height (cm)	Max. shear displacement (mm)	Max. shear stress s_u (kN/m ²)	Saturated specific weight γ_{sat} (kN/m ³)	Dry specific weight γ_{dr} (kN/m ³)
1 (C)	8,0	15,5	37,3	16,2	10,4
2 (C)	8,0	14,0	30,05	18,1	11,8
3 (C)	8,0	14,0	33,1	15,8	10,3
4 (C)	8,0	15,5	45,1	15,1	9,9
5 (C)	8,0	12,5	32,7	17,2	11,5
6 (C)	8,0	16,0	49,72	16,8	11,1
7 (C)	8,0	14,5	48,2	17,0	11,2
8 (C)	8,0	12,0	40,1	17,3	11,7
9 (C)	8,0	11,5	31,4	17,3	11,6
10 (C)	8,0	12,0	37	17,0	10,9
Mean \pm s.d.	8,0 \pm 0	13,7 \pm 1,7	38,5 \pm 7,1	16,8 \pm 0,9	11,0 \pm 0,7

Table 6.2: Results triaxial tests soil type C with Vetiver grass

The estimation of the undrained shear stress of soil type C with Vetiver grass is $38,5 \pm 7,1$ kN/m² and a shear displacement of $13,7 \pm 1,7$ mm. The saturated and dry specific weight are respectively $\gamma_{sat} = 16,8 \pm 0,9$ kN/m³ and $\gamma_{dr} = 11,0 \pm 0,7$ kN/m³.

6.3.3 Comparison

The results of shear displacement and undrained shear strength are plotted together in figure 6.2. At first sight it looks like Vetiver grass improves the undrained shear strength of the soil. When comparing both means, an increase of approximately 17% was found. Hypothesis 5 was tested via a bootstrap (appendix F).

The results with regard to the hypothesis are:

Hypothesis 5:

The result is not significant ($P=0,0543$) for this data. Therefore the H_0 hypothesis cannot be rejected ($H_0: \mu_1=\mu_2$). With this data it is not proven that Vetiver grass increases the undrained shear strength significantly.

When considering the specific weight of the soil, only the specific saturated weight is of interest. The comparison of the specific dry weight is not useful, for the strongly horizontal layering of clay almost always results in a natural moisture content, so dry conditions are very rare. Besides, the comparison is focused on undrained conditions (paragraph 3.8.2), which is only possible when the soil is saturated.

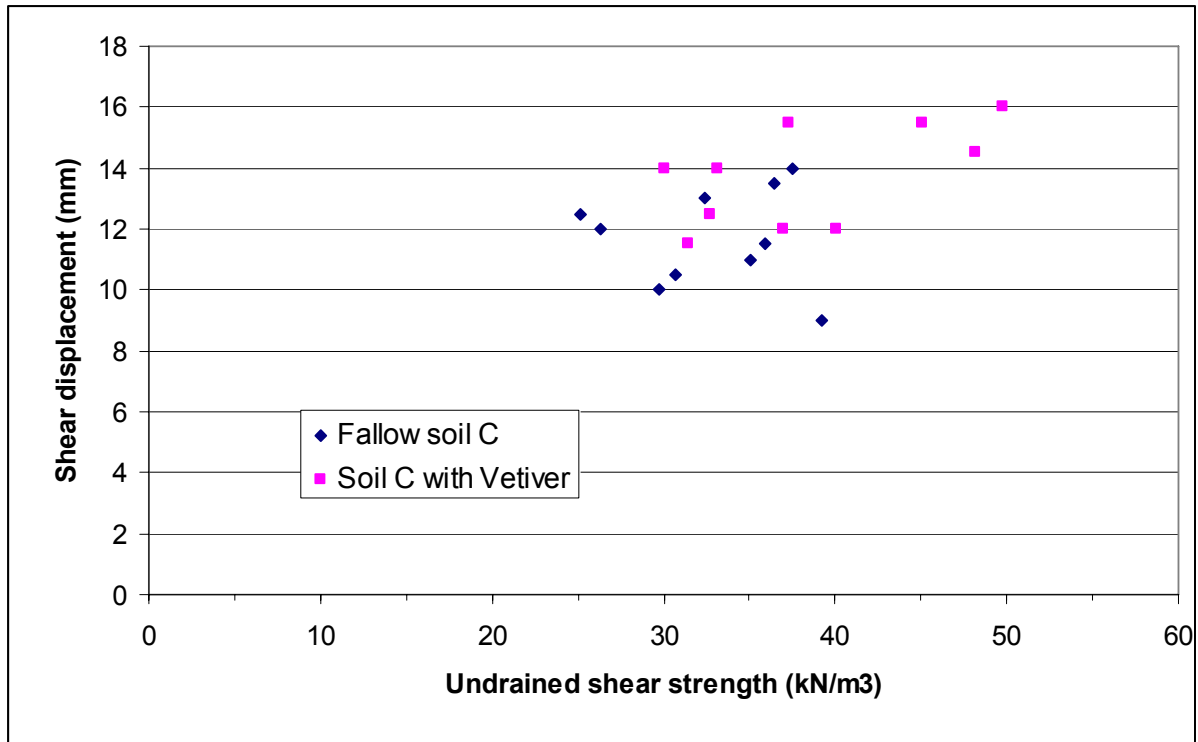


Figure 6.2: Test results triaxial tests for fallow soil and soil with Vetiver roots

The results with regard to the hypothesis are (appendix F):

Hypothesis 6:

The result is not significant (P=0,131) for this data. This means that there are strong indications that hypothesis 6 is true; Vetiver grass does not have a significant direct influence on the specific weight of the soil.

The overall result for the increase in safety factor (equations (3.19), (3.33), (3.34)) purely based on the results of the performed tests is:

$$\frac{FS_{vet}}{FS_{fal}} = \frac{\left(\frac{c_{u,vet}}{\gamma_{sat,vet}}\right) * \frac{R}{D}}{\left(\frac{c_{u,fal}}{\gamma_{sat,fal}}\right) * \frac{R}{D}} = 1,19 \quad (6.1)$$

where the subscript "vet" refers to soil with Vetiver roots and "fal" refers to fallow soil;
R = contribution of the components resisting failure but independent of Vetiver grass;
D = contribution of the components driving failure but independent of Vetiver grass.

It should be emphasized that the results of both factors are not significant, so these results are not to be used. The comparison is purely indicative.

6.4 Error analysis

The main errors in the determination of the undrained shear strength are not expected to be the result of inaccuracy of the measuring equipment. The difference in soil samples and testing conditions will most probably have a bigger influence:

- Disturbance of the sample is fully reflected in the results of an UU-test. Especially the samples with roots are very likely not undisturbed, because the roots have to be cut when obtaining the samples.
- The samples will most probably contain some air during the testing, which may lead to incorrect measurements of the pore pressures.
- The samples are non-homogeneous.
- Because of the small size of the samples, the condition for pulling out of roots as mentioned in equation (3.29) may not be fulfilled for all roots. This will result in an underestimation of the shear strength with Vetiver roots.

7. Small scale mass failure

7.1 Introduction

The water level change due to a passing ship is given in figure 7.1.

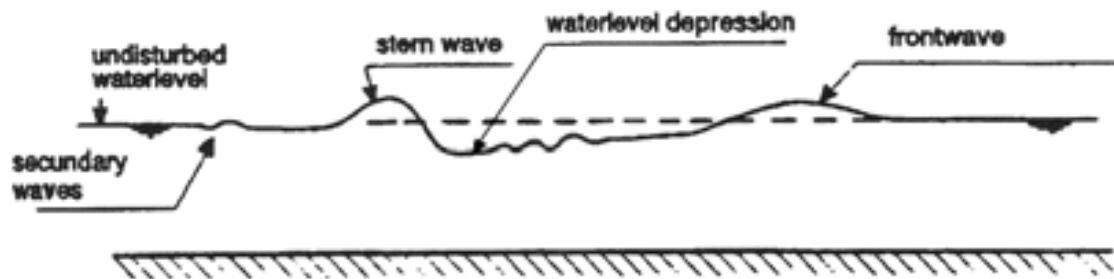


Figure 7.1: Water level change due to ship passage

Eventually the main forcing causing small scale mass failure may be related only to the rapid drawdown during a ship passage. This may well be simulated by a less complex signal than given in figure 7.1. A test setup was made in which multiple water level changes related to ship traffic could be simulated in succession. It should be mentioned that the combined effect of all eroding agents is more complex than their individual effect, and therefore the results of this test cannot be extrapolated to the general performance of Vetiver grass as a river bank protection. It is merely focused on gaining insight on the specific processes and mechanisms mentioned above.

7.2 Experiment

7.2.1 Model design

For the same reason mentioned in paragraph 3.6.2, 1-g testing was only possible in a 1:1 test. No existing test setup was available to perform this simulation, so it had to be designed. For this design a list of requirements was created, consisting of quantitative (based on the parameters of interest, for example water-level difference or speed of the drawdown) and qualitative demands (based on practical considerations).

Quantitative demands

The goal of this test was to test the soil-root system. Because of the limited available time and the beforehand unknown growth rate of the Vetiver roots the bank height was restricted to about 25 cm, which was expected to be sufficient to study small scale phenomena.

The most critical point for mass failure is expected to be just after the establishment of the head difference, after which the pore water pressures will only decrease. It was therefore decided to use the shortest common period of water level depression. Because of the high number of cycles, a short forcing period would also gain a lot of time. The period of the stern wave is normally about 2-3 seconds. Therefore the water level change (from high to low) had to take place in 1-1,5 seconds. Summarizing:

1. The water-level changes should be established in 1-1,5 seconds
2. The maximum head difference had to be smaller than 0,25 m
3. The period of the drawdown was estimated on approximately 10 s

The number of samples was limited, therefore only one forcing signal was used, of which a representative graph of the resulting water levels in time are shown in appendix M.

Qualitative demands

As mentioned before, the qualitative demands were mainly given by practical considerations.

1. It had to be possible to perform the test indoors, because the test would be executed during winter (risk of frost)
2. Because the profile of the soil with Vetiver was determined a couple of times per run, this part of the test setup had to be easily accessible
3. Attention had to be paid on preventing big lumps of clay jamming the test.
4. Model effects like artificial oscillations and turbulence near the samples had to be limited.

Hydraulic wave generator

In principle an axial pump, a plunger with a hydraulic arm and a hydraulic wave generator were able to produce the desired signal. Because of specific circumstances preference was given to the hydraulic wave generator. The principle of the test setup is based on the change of shape of the basin volume in front of a construction with an artificial top of a bank (with and without Vetiver grass). When the hydraulic wave flap was at its rest position (0-signal), the water level was constant in front as well as behind it. Whenever the hydraulic wave flap was given a positive signal it was forced forwards, which resulted in a higher water depth in front and a lower water level behind it, whereas a negative signal resulted in an opposite water position as illustrated in figure 7.2. The connection between hydraulic wave flap and the basin walls was not watertight, therefore compensation of leakage under and along the hydraulic wave flap was required in order to maintain a steady water level.

Beforehand four test signals were used with a wooden board as an artificial slope to investigate the limitations of the test setup. Special attention was paid on the possible occurrence of artificial oscillations. The straight rectangle-shaped form in which the water is forced into movement and the very limited amount of damping may cause unwanted oscillations. During these test runs it was observed that oscillations occurred whenever the forcing signal included short sinusoidal-like periods. It was decided to use the signal as given in appendix M because of the good representation of the desired forcing and because of the low amplitude of the oscillations. The amplitude of the water movement was 20,5 cm with a standard deviation of 2,4 cm. The period of high water level was 8,4 s, the drawdown was established in 1,0 s the period of low water level was again 8,4 s and the period of rising water level was 2,7 s. In total a single cycle took 20,5 s.

7.2.2 Test setup

Experiments were carried out in a wave flume at the Laboratory of Fluid Mechanics - Delft University of Technology. A sketch of the test setup without dimensions is given in figure 7.2, while a sketch with dimensions is shown in appendix L. The woodwork was kept in its place by concrete blocks and by supporting water at the backside. The position of the hydraulic wave flap was adjustable into detail in x-direction and in time (Dasylab 32-bit). The soil samples were placed on the wooden construction as illustrated in figure 7.2. The intention was to place the fallow soil types S and SC as one coherent block. Unfortunately in practice this couldn't be achieved; the samples with the Vetiver grass were placed in pairs. So each run 2 Vetiver grass samples were tested. The Vetiver grass with soil type MX was planted 3 months beforehand in pots which didn't have the exact shape of the space on top of the "shelf" in the test setup, which implies that the samples in the test setup did not fill the "shelf", therefore the gaps had to be filled manually before the start of the test.

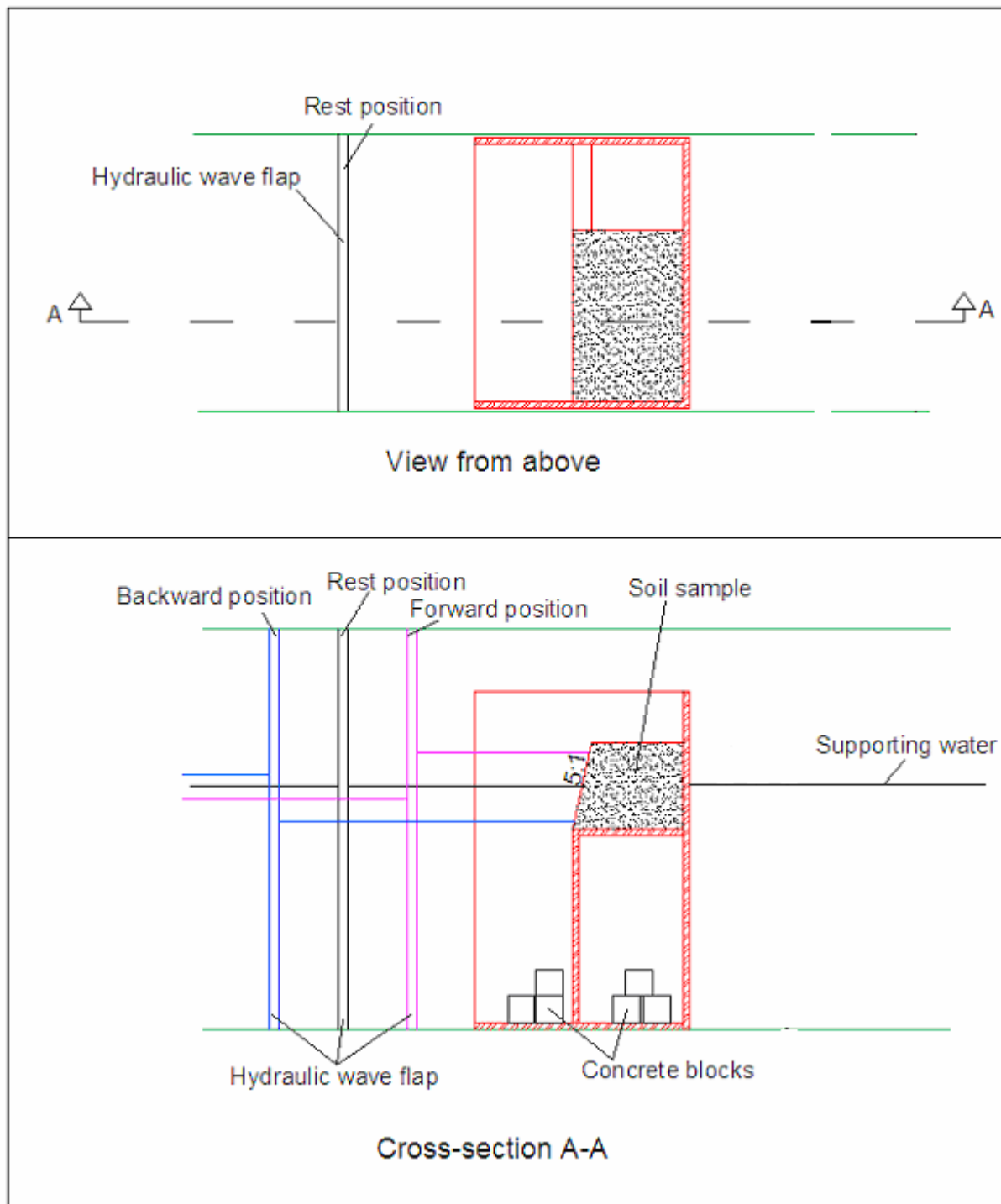
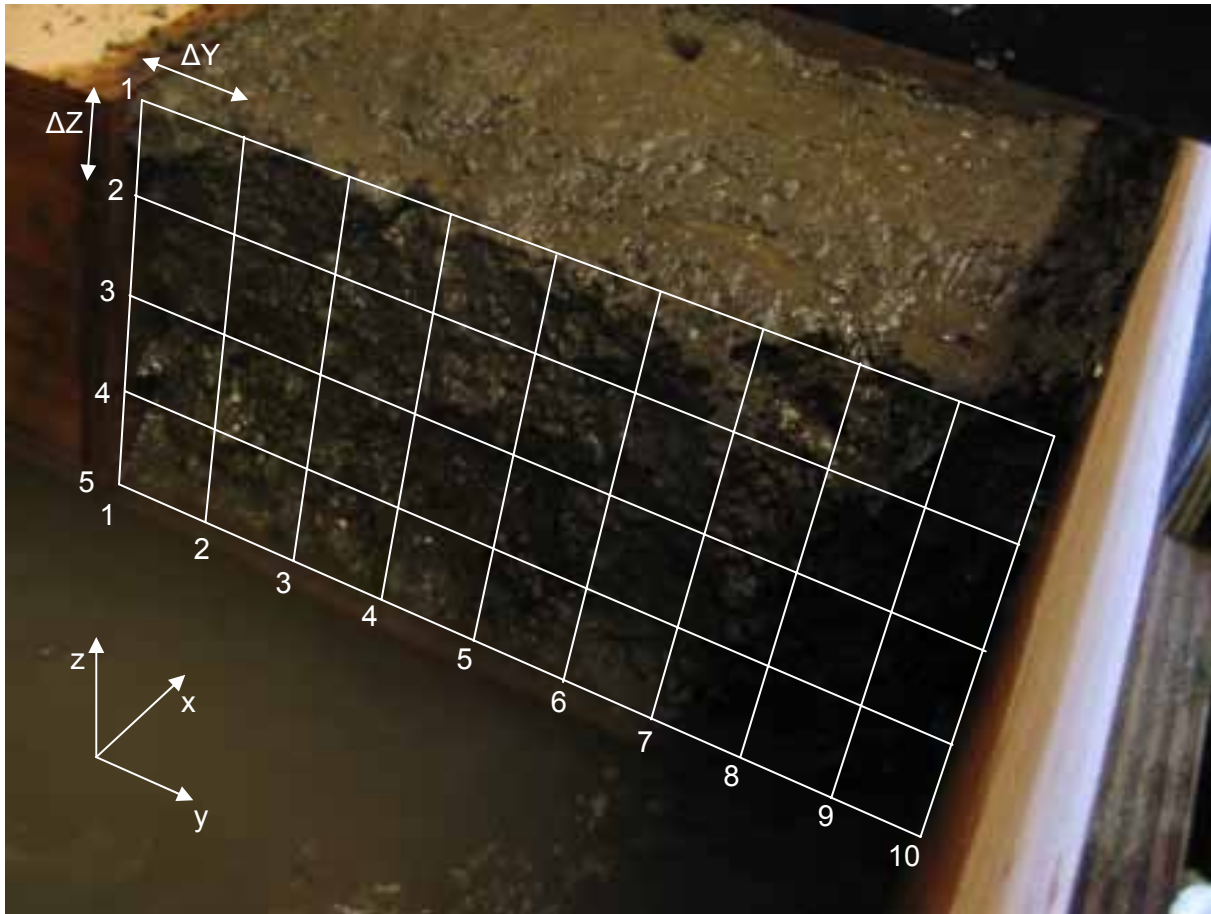


Figure 7.2: Sketch test setup

The Vetiver grass in soil type C was planted 2 months beforehand. Full-grown Vetiver grass plants were split in two and, as far as possible, material between the roots was washed out. The leaves were cut off at a length of approximately 0,50 m in order to reduce the evaporation surface and also to monitor growth. The plants were planted in cubes of polystyrene (inner dimensions: 0,25x0,25x0,25 m) filled with soil type C. The cubes were placed in a basin in a greenhouse of the Botanical Garden - Delft University of Technology with a water level of approximately 22 cm below the topside of the cubes.

After placement of the soil the surface water level was raised up to half of the height of the soil sample. The initial topography of the slope was determined at equidistant intervals of 0,05 m parallel (horizontal y-direction) and vertically (z-direction) in reference to the slope,

with a horizontal measuring needle (precision 0,001 m) in the horizontal direction incident on the slope (x-direction), as illustrated in figure 7.3.



Figur 7.3: Sketch of the equidistant measuring grid for profile measurements ($\Delta Z = 5\text{ cm}$, $\Delta Y = 5\text{ cm}$)

A wave height meter (precision 0,0005 m) was connected to a computer to acquire data regarding the number of simulated ship passages and the water level changes. The groundwater level at 0,25 m behind the slope was measured before the start of the test to check whether or not the groundwater level corresponded with the water level in front of the slope. These measurements were performed with a measuring rod (precision 0,001 m) in a borehole (\varnothing 0,02 m). The test was started at the moment the groundwater level and the surface water level were equal. During the test with soil types C and SC the groundwater level was measured regularly (after each 100 cycles) to check if it remained constant. If the groundwater level showed fluctuations after some time during the forcing, this would have given indications about the possible presence of cracks or holes reaching far into the soil. At several moments during the experiment, after a certain number of cycles, as specified in paragraph 7.3, the experiment was paused. The hydraulic wave generator was brought back into its resting position and the topography of the soil was measured, after which the experiment continued. After performing the experiment on the soils with Vetiver grass, the RAR at different heights in the soil was determined in the same way as described in paragraph 6.2.

7.2.3 Runs

At first, the experiment was carried out with fallow soil type C and MX. Also fallow soil type SC was tested once, after which soil type MX and C were tested with Vetiver grass. To obtain more reliability of the data most tests were executed two or three times. In total the following runs were executed:

1. Fallow soil type C (2 times) and soil type C with Vetiver grass (3 times)
2. Fallow soil type MX (2 times) and soil type MX with Vetiver grass (3 times)
3. Fallow soil type SC (1 time)

7.3 Results

The results are described in the paragraphs below. Two important remarks regarding the contourplots in figure 7.5, 7.7 and 7.11 are made:

- As mentioned in the title of each plot, they are interpolated contour plots, which means that values between the grid points may differ from reality. Only the values on the grid points are actually measured. The contour plots are nevertheless interpolated to provide a clear visual presentation of the bank retreat.
- The scales of the contour plots are not equal, so one must be careful when comparing those plots.

7.3.1 Soil type C

A qualitative description of the observations during the test is given, after which the quantitative results are shown. The temperature of the water during the runs with fallow soil were respectively approximately 17,5°C and 18,0°C. The runs with Vetiver grass were performed in water with a temperature of respectively 18,0°C, 17,5°C and 17,5°C.

Qualitative description erosion fallow soil C

The adjustment of the groundwater level took about 16 hours for both runs. At first it looked like a thin layer of clay showed signs of dispersion, although it might very well be possible that it was a result of the damage caused by the placement of the sample. Anyhow, it led to very fine erosion material (order of grain size). This process did not continue, however. The groundwater level didn't respond on the surface water level during the start of the experiments. After the forcing was started it didn't take long for small scale mass failure to occur. Lumps of clay (around 0,5 cm to 5 cm) fell off almost immediately after a drawdown. A couple of times a small crack or an irregularity was observed on the failure plane. It was also observed that the loss of a big lump of clay almost immediately led to failure of smaller parts in the surrounding area. After about 350 cycles for the first run and about 550 cycles for the second run, the groundwater level corresponded more and more with the movement of the surface water level. This was probably caused by small tunnels and cracks which were formed (or already present) in the clay. Therefore local flow velocities seemed to grow especially in and out of the cracks and holes. This resulted in erosion of small clay lumps out of the holes which induced an even higher level of correspondence between the groundwater level and the surface water level. Most of the erosion took place in the mid part of the slope. It is uncertain whether this may be a model effect or if this had a relation with the non-homogeneity of the soil. The erosion rate dropped and less signs of mass failure were observed later on during the experiment.

Quantitative description erosion fallow soil C

Standard boxplots were created for the bank retreat per measuring point after a certain number of cycles, as specified in figure 7.4. From these figures it is clearly to be seen that the erosion was locally higher which implies erosion of holes. Also, the reduction of erosion over the number of cycles is observed from the fact that the increase of the median does not follow the increase in number of cycles. The spread of datapoints is higher in the first run than in the second run, while the latter has more outliers. The bank topography at the end of the experiment is displayed in a contour plot in figure 7.5 in which the above mentioned holes are clearly to be seen.

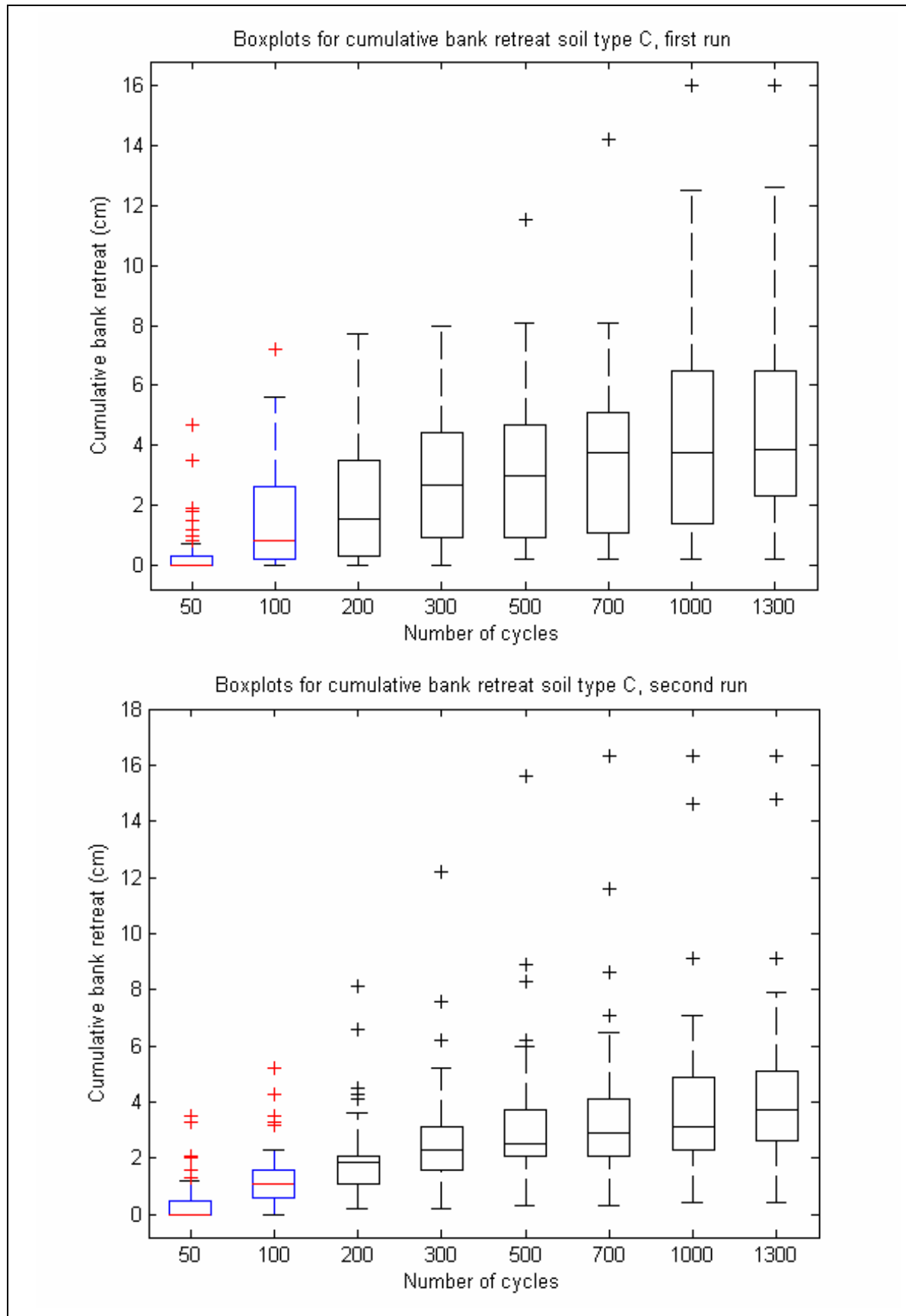


Figure 7.4: Boxplots of soil type C, first and second run

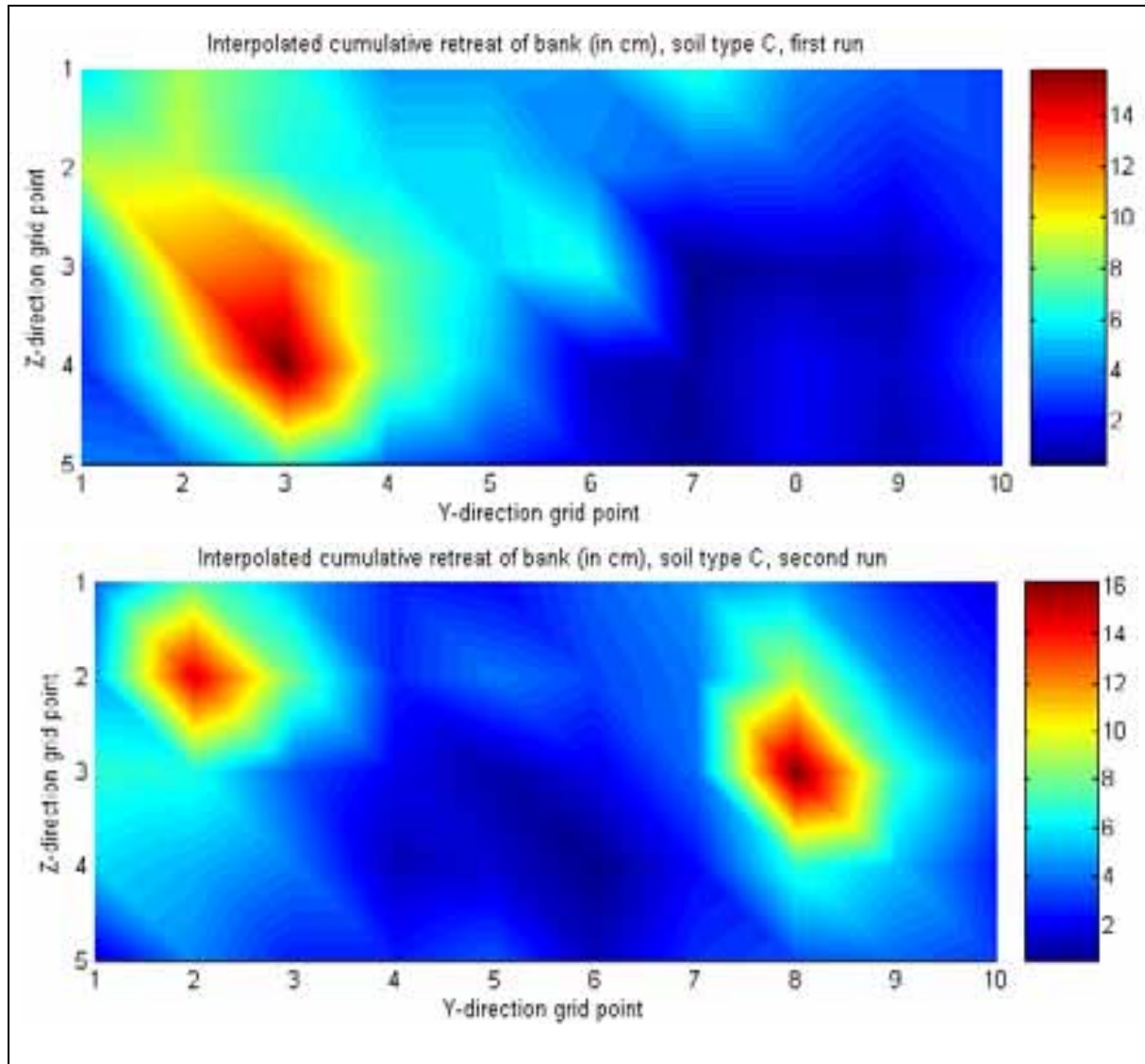


Figure 7.5: Total bank retreat of soil type C, two runs (both after 1300 cycles)

Qualitative description erosion soil C with Vetiver grass

At first there was some erosion in poorly rooted parts, especially at the interface of the two samples or on the interface between the wood and the samples. The groundwater level didn't respond at all to the fluctuations of the surface water level for the entire experiment for all three runs, though. Erosion rates decreased very quickly (within the first 500 cycles) and almost came to a full stop. Some cracks were observed, but unlike during the tests with the fallow soil those cracks didn't lead to failure. Apparently the roots kept the soil in its place, even after a long time. The highest erosion rates were observed at the interface between the two samples.

Quantitative description erosion soil C with Vetiver grass

Standard boxplots were created for the bank retreat per measuring point after a certain number of cycles, as specified in figure 7.6a and 7.6b. From these figures it is clearly to be seen that the spread for all three runs was quite low, with a high number of outliers. This implies very local erosion which implies forming of holes. In this case these holes were observed especially at the interface of the two samples, as mentioned in the qualitative description. The reduction of erosion over the number of cycles is mainly to be seen in the increase of number and size of outliers. The median has a very low level of increase.

The bank topography at the end of the experiment is displayed in a contour plot in figure 7.7 in which the above mentioned holes are clearly to be seen.

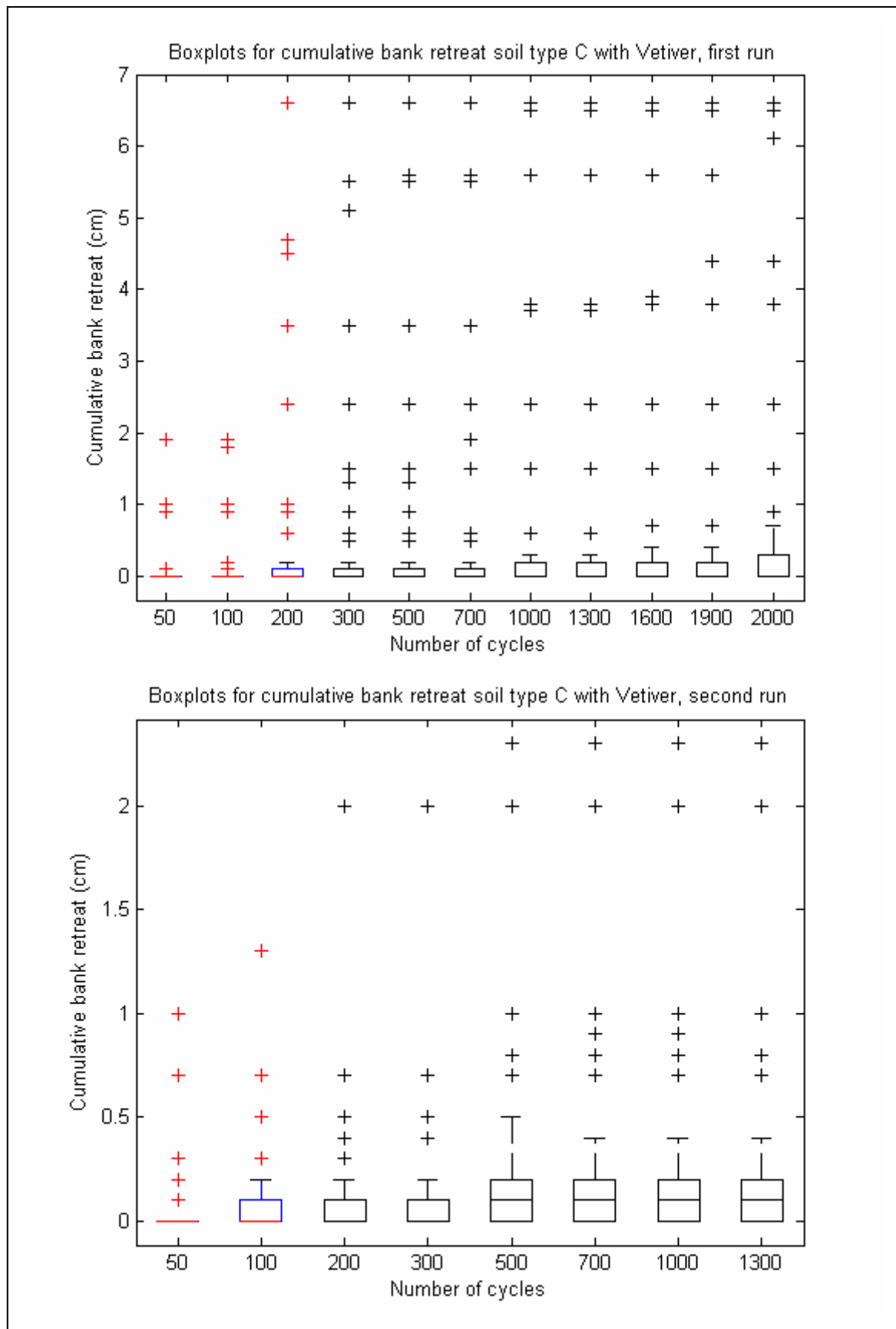


Figure 7.6a: Boxplots of soil type C with Vetiver, first and second run

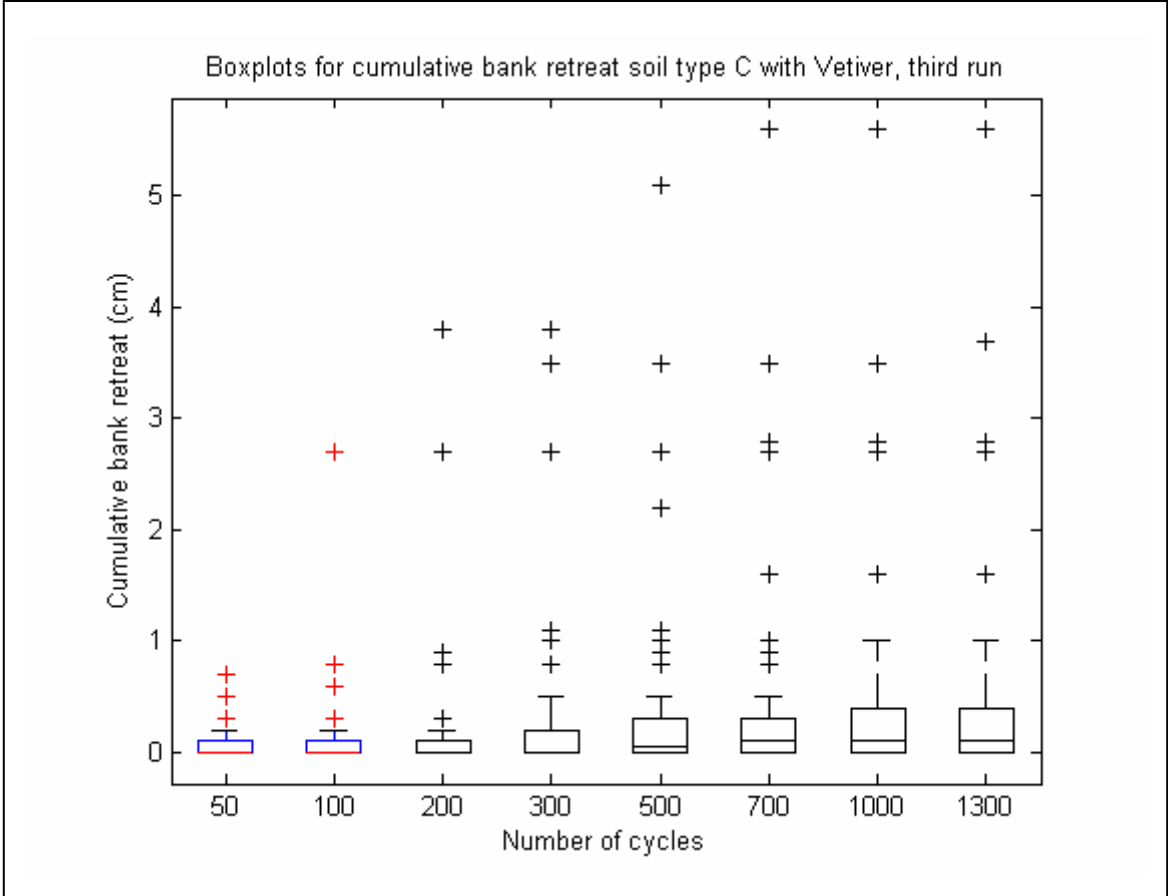


Figure 7.6b: Boxplots of soil type C with Vetiver, third run

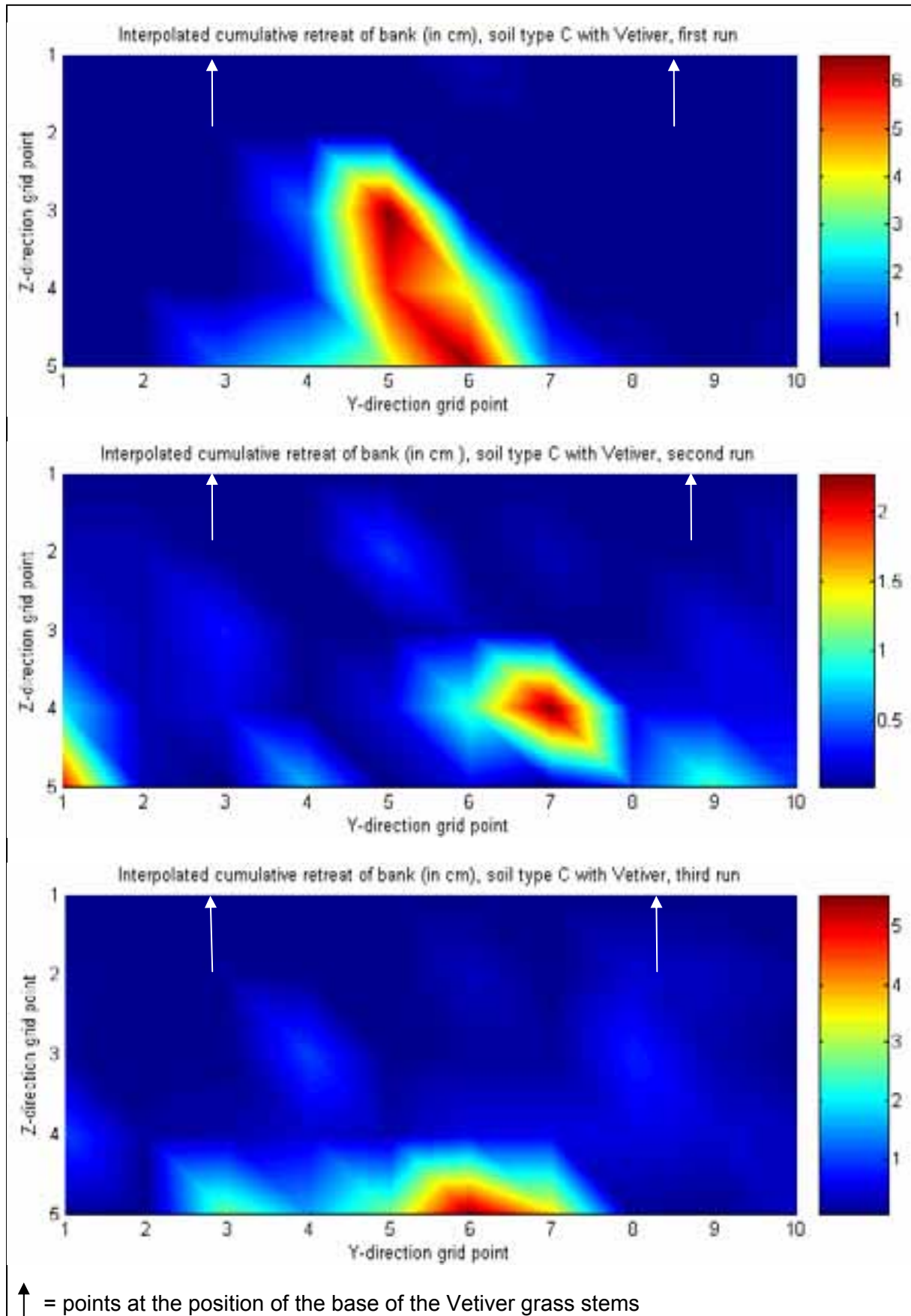


Figure 7.7: Total bank retreat of soil type C with Vetiver, three runs (each after 1300 cycles)

Comparison

The results presented in the boxplots (figure 7.4, 7.6a and 7.6b) show great differences between the amount of erosion and the spread of erosion rates between the fallow soil and soil with Vetiver grass. However, to obtain a parameter for all runs which is comparable, the amount of loss of bank material was calculated. The volume of lost bank material was obtained by double integration of the contour plots with respect to the plane $x=0$, in which $x=0$ was taken to be the initial value of the bank. The lost amount of material in cm^3 over the amount of cycles is shown in figure 7.8. The amount of loss of material is solely meant as an indication because the contour plots were interpolated, which implies that the actual loss of material may be different from the numbers shown in figure 7.8. The differences are not expected to be very large, because comparison of the contour plots with observations during the tests did not show mayor differences. It is clearly shown in figure 7.8 that the amount of erosion is very much reduced by the presence of Vetiver grass. Also, there are indications that the erosion of the fallow soil keeps continuing, while the erosion of the soil with Vetiver grass almost comes to a full stop after approximately 1000 cycles.

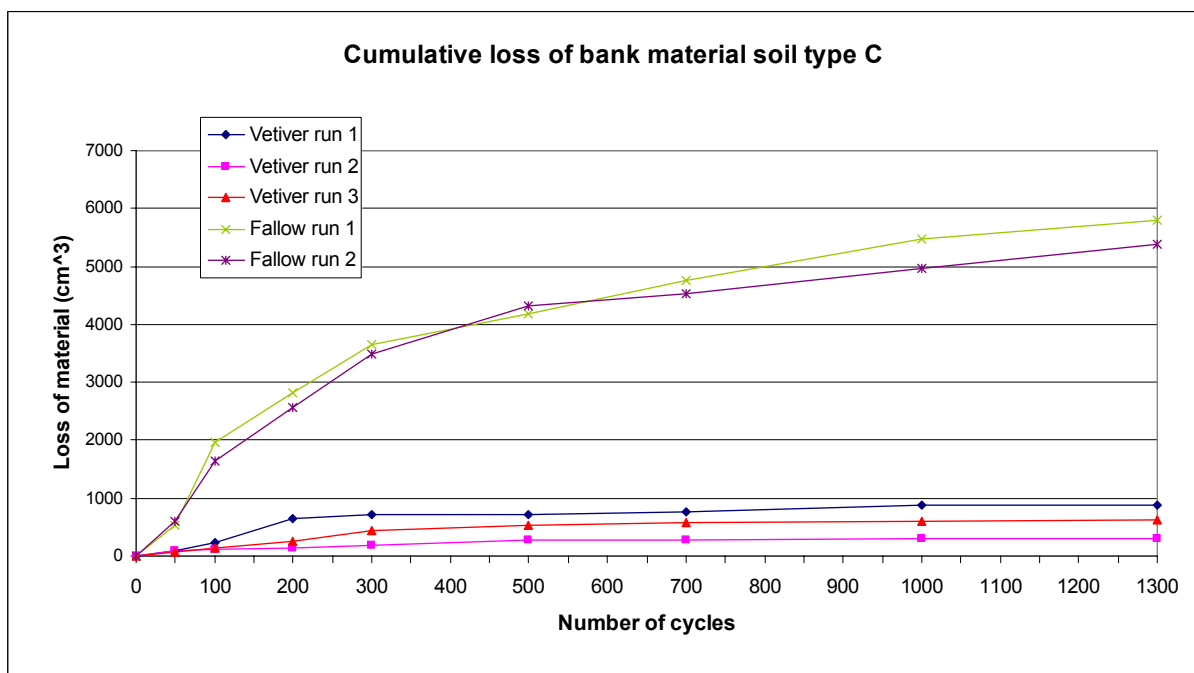


Figure 7.8: Loss of bank material for fallow soil and for soil with Vetiver

There is not enough data to perform a reliable investigation of the significance level. When the mean of material loss for fallow soil and for soil with Vetiver are compared, the erosion rate was approximately 8-10 times lower, which is purely an indicative number, no further conclusions can be drawn from this.

To obtain some insight into the quantitative properties of the erosion of holes, investigation of the frequency of level crossings and the corresponding loss of bank material was investigated for two levels. The results are displayed in table 7.1. Connected gridpoints which did have a bank retreat larger than the mentioned level, were counted as one hole. In the columns with the number of holes, an estimation of the size of the holes in cm^2 is given between brackets.

It was observed that the number of holes did not show any mayor differences while the size of the holes (especially depth) was much larger with fallow soil than with soil with Vetiver grass.

	Level crossings > 2cm		Level crossings > 5cm	
	Number of holes (surface in cm ²)	Loss of material (cm ³)	Number of holes (surface in cm ²)	Loss of material (cm ³)
Vetiver run 1	1 (150)	415	1 (75)	90
Vetiver run 2	1 (25)	8	0	0
Vetiver run 3	2 (25 and 75)	170	1 (25)	15
Fallow run 1	Not definable	3540	1 (450)	1410
Fallow run 2	Not definable	3010	2 (150 and 200)	995

Table 7.1: Number of holes and the corresponding loss of bank material

7.3.2 Soil type MX

A qualitative description of the observations during the test is given, after which the quantitative results are shown.

Qualitative description erosion fallow soil MX

The adjustment of the groundwater level was due to the high permeability of the soil finished immediately. As to be expected the soil was not stable at a slope of 5:1. Before the test was started, the slope already decreased in steepness. Apparently, virtually no cohesion was present in the soil. At the moment the forcing was turned on, the instability of the bank was directly visible and after 5 cycles, there was virtually no "bank" left, as shown in figure 7.9. Both runs provided more or less the same results.



Figure 7.9: Position fallow soil type MX after five cycles

Quantitative description erosion fallow soil MX

The temperature of the water during run 1 and 2 was respectively approximately 17 °C and 17,5 °C. Because of the immediate failure of the bank, it is impossible to make statements on the quantitative erosion.

Qualitative description erosion soil MX with Vetiver grass

No time was needed for the adjustment of the groundwater level due to the high permeability. Erosion took place at those points where the root intensity appeared to be low. The erosion process was clearly to be defined as washing out and did not have a clear relation with pore water pressures. The changing water level did provide an in- and outflow at weak spots which were enlarged until it reached soil with a higher root intensity. The erosion on locations with a high root density came to a full stop after the first 1 or 2 cm of soil was washed out between the roots. It might very well be possible that the organic content in the soil provided extra stability. At those spots where the soil consisted of mainly organic material, virtually no erosion took place. Most of the erosion took place at the interface of the two samples and on the side of the samples (figure 7.11) where no roots were present.

Quantitative description erosion soil MX with Vetiver grass

The temperature of the water during run 1, 2 and 3 was respectively approximately 17 °C, 17,5 °C and 18,0°C. Standard boxplots were created for the bank retreat per measuring point after a certain number of cycles, as specified in figure 7.10a and 7.10b. From these figures it is clearly to be seen that the spread for all three runs was quite low, with a high number of

outliers. This implies very local erosion which implies forming of holes. This is also to be seen by the very low level of increase of the median. Holes were observed especially at the interface of the two samples, as mentioned in the qualitative description. The bank topography at the end of the experiment is displayed in a contour plot in figure 7.11 in which the above mentioned holes are clearly to be seen. The mean RAR of each run is given in appendix M. They are very susceptible for the presence of occasional large roots. From a depth of approx. 10 cm the amount of small roots was almost equal for each sample (mean 24 ± 2), but the presence of thicker roots scatters the RAR considerably.

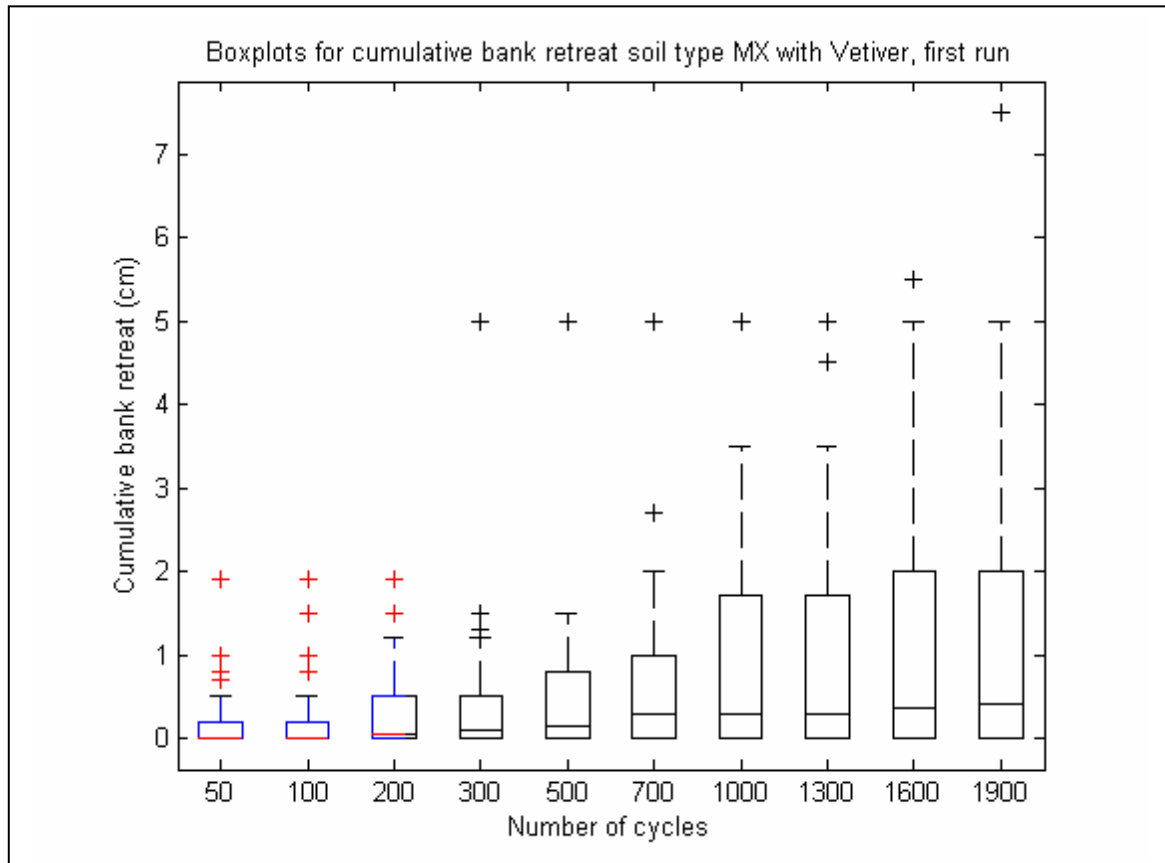


Figure 7.10a: Boxplots of soil type MX with Vetiver, first run

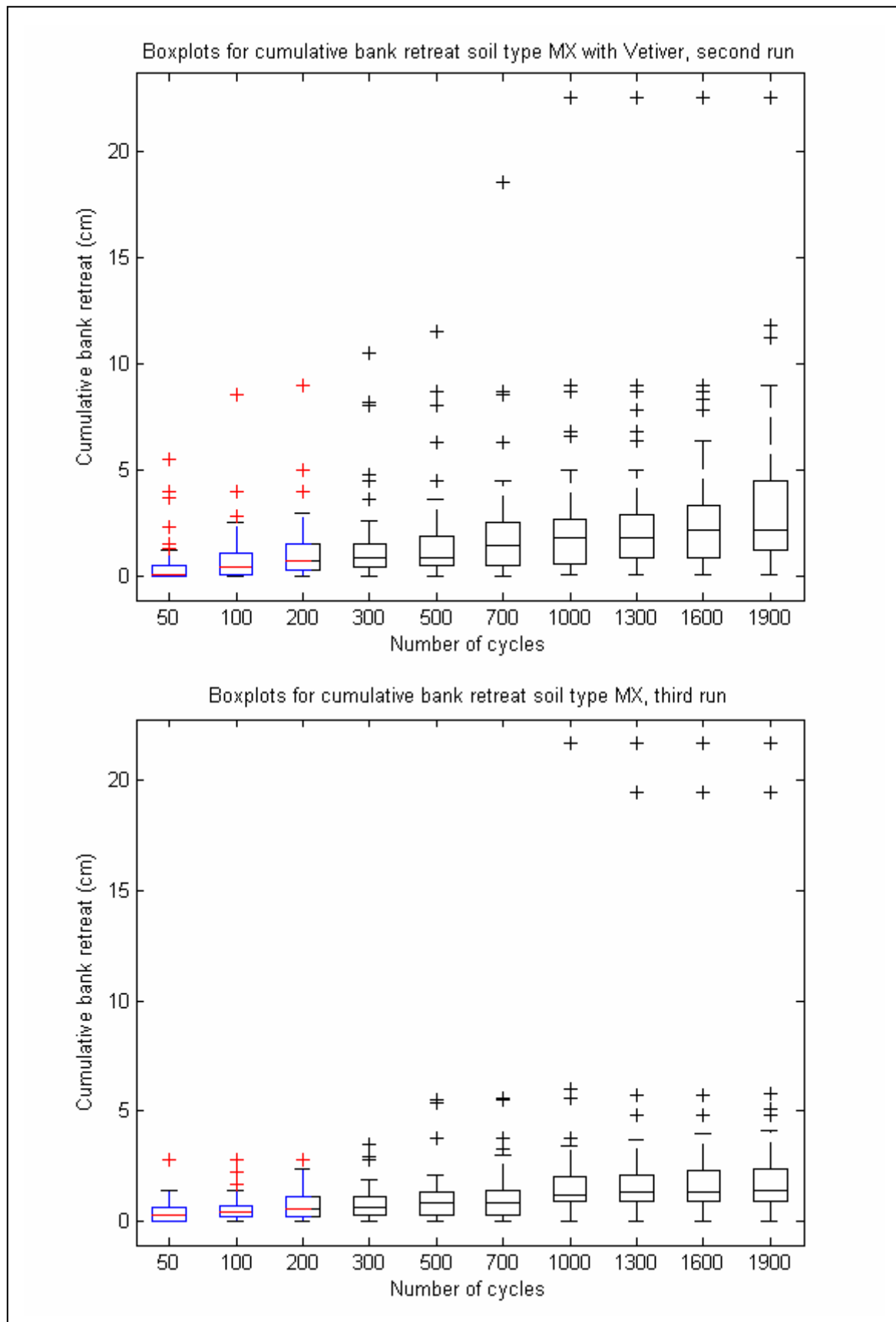


Figure 7.10b: Boxplots of soil type MX with Vetiver, third run

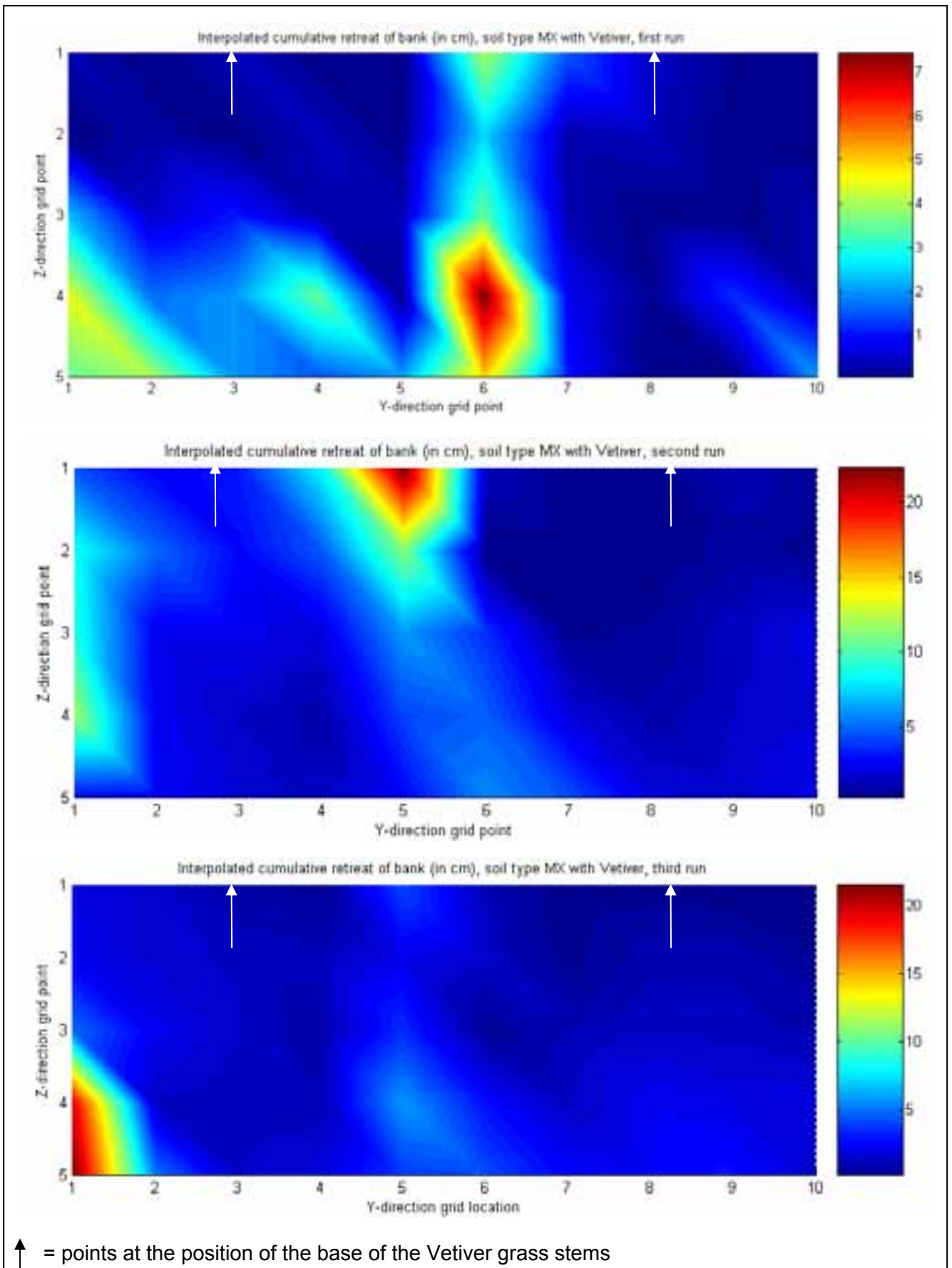


Figure 7.11: Total bank retreat of soil type MX with Vetiver, 3 runs (after 1900 cycles)

Comparison

Because of the absence of reliable data concerning the erosion of fallow soil MX, a quantitative comparison as well as a significance analysis is not possible. However, there are very strong qualitative indications that Vetiver grass significantly reduces the erosion rate. The loss of bank material of soil type MX with Vetiver grass was obtained the same way as described in paragraph 7.3.1 and is illustrated in figure 7.12.

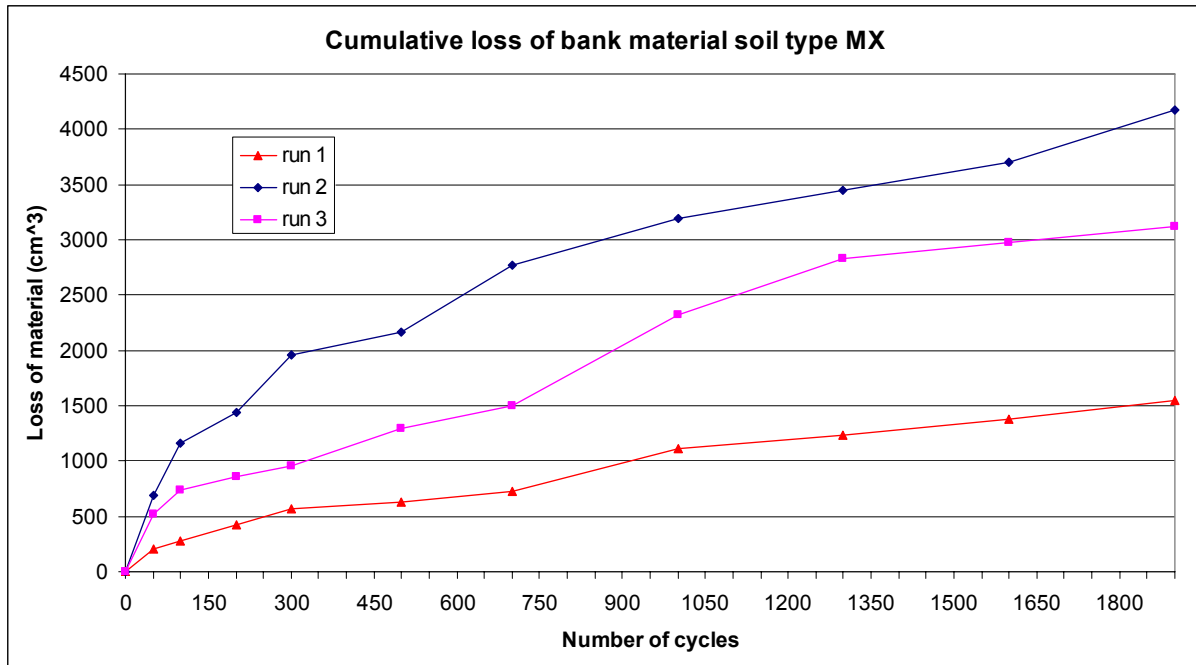


Figure 7.12: Loss of bank material for soil MX with Vetiver

7.3.3 Comparison of soil type MX and C

In order to compare the two soil types, figure 7.8 and 7.12 are combined in figure 7.13.

The erosion of soil type C with Vetiver almost comes to a full stop after approximately 1000 cycles, while the erosion of soil type MX with Vetiver still continues. The average amount of erosion of soil type MX with Vetiver is also higher than the amount of erosion of soil type C with Vetiver. Both observations may well be related to the differences in failure mechanisms. Soil type MX is very permeable and is mainly eroded by critical flow velocities and reduction of the shear strength by reducing the effective internal friction angle by porewater pressures. Soil type C on the other hand has a very low permeability and is eroded by different processes as described in paragraph 3.3. Because of the lack of sufficient data it is impossible to test the significance level.

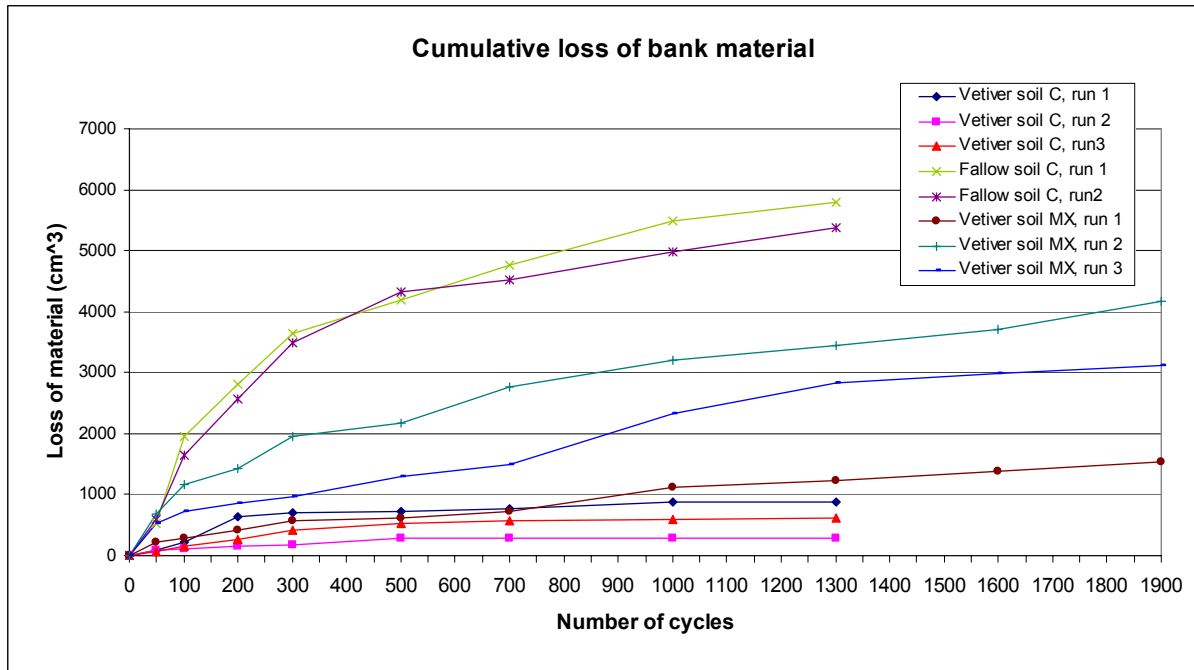


Figure 7.13: Comparison loss of bank material for soil type MX and C

7.3.4 Soil type SC

The qualification "soil type SC" refers to sandy clay. This soil type is not classified, but definitely has at first sight a higher amount of sand than soil type C and has a much lower cohesion, which follows from appendix C2. This soil type was tested once, the results are shown in appendix P. The results may be of interest when considering the erosion of unprotected banks, but are not further investigated in this thesis.

7.4 Error analysis

First of all the test setup was not supposed to be testing non-cohesive material like soil type MX, but was designed solely to test cohesive soil. Because of circumstances however, the first set of samples with Vetiver grass did not contain cohesive soil. Therefore the experiment was executed on both soil types C and MX. One can also consider this as an advantage, because in this way a comparison between two soil types is possible.

The main errors in the determination of erosion rates in this experiment are not expected to be the result of inaccuracy of the measuring equipment. Other aspects will most probably contribute for a much larger part to inaccuracy. Possible causes of errors are:

- Non-homogeneity of the samples
- Possible model effects caused by the small size of the samples
- The intention was to place the fallow soil types S and SC as one coherent block. Unfortunately in practice this couldn't be achieved. Therefore cracks at the interface were already present before loading
- Loose soil tends to form an equilibrium profile when loaded. However, in this test setup that was not possible, through which the erosion rate of fallow soil MX may be exaggerated
- The filling of the samples with soil type MX was artificial and may provide false conclusions, especially at the interfaces between wood and sample

8. Conclusions

In this chapter the conclusions are presented. In the first paragraph two conclusions related to the analysis performed in chapter 3 on the possible influence of Vetiver grass on bank erosion are given. After this, the conclusions drawn from the results of the three experiments are described.

8.1 Physical processes

- The salient properties of Vetiver grass ought to make it suitable for a bioengineering solution against bank erosion.
- The influence of Vetiver grass on bank erosion caused by vessel-induced loads is very diverse; 14 different adverse and/or beneficial effects were found.

8.2 Influence of soil type and phreatic level on Vetiver grass

With respect to the hypotheses the following conclusions can be drawn:

1. Hypothesis 1: "*A low phreatic level will result in a normal growth rate (soil type MX)*" is accepted at a significant level ($P < 0,05$).
2. Hypothesis 2: "*The rate of growth of plants with a substantial different phreatic level will differ significantly from each other (soil type MX)*" is accepted at a very significant level ($P < 0,01$)
3. Hypothesis 3: "*The rate of growth of plants with a substantial different phreatic level will not differ significantly from each other (soil type C)*" is to be rejected at a significant level ($P < 0,05$)
4. Hypothesis 4: "*The rate of growth of Vetiver grass in soil type C will be significantly lower than the growth rates of Vetiver grass in soil type MX under the same conditions*" is accepted at a very significant level ($P < 0,01$)

Shallow phreatic level differences (up to 0,5 m) have significant or even very significant influence on the growth rate of Vetiver grass. A decrease in phreatic level of approx. 0,17 m resulted in an increase in growth rate of 10-20% for both soil types. The growth rate of Vetiver grass is strongly influenced by soil type. The application of Vetiver grass in soil type C resulted in a decrease in growth rate of approx. 50% compared to soil type MX, which was a very significant result.

These results give reason for the following statements.

When applying Vetiver grass as a bank protection, attention has to be paid on the bank material and groundwater level:

- Cohesive soils reduce growth rates. An overestimation of the growth rates and therefore the rate of protection of the rootsystem, especially in the planting stage and a couple of months hereafter, may be a potential problem. The establishment of Vetiver grass as a bank protection, will take more time when applying it on cohesive banks and the phase in which the new planted slips are most vulnerable for being washed away, lasts longer.
- When established, the Vetiver grass in cohesive soil has a higher level of spreading of small roots ($d_r < 0,5$ mm) throughout the soil, whereas in non-cohesive soil distinct high density root zones were found. In the top 10 cm of non-cohesive soil barely any

small roots were present, while with cohesive soil the Vetiver grass did have small roots up to the surface level.

- High phreatic levels reduce growth rates. The reinforcement against the occurrence of deep-seated failure planes by the presence of Vetiver roots will be lower or even absent when the phreatic level is high.
- The slips planted in the wave zone will be longer vulnerable for being washed away, for the rooting depth and growth rate in the planting stage and a couple of months hereafter will be relatively low.

An unplanned observation was made on the high sensibility of Vetiver grass on shade. A small reduction in light availability resulted in a relatively high decrease in growth rate.

8.3 Large scale mass failure

With respect to the hypotheses the following conclusions can be drawn:

5. Hypothesis 5: "*The undrained shear strength of soil type C with and without Vetiver grass roots will differ significantly from each other*" is rejected on basis of this data, because $P > 0.05$. It may very well be possible that this is caused by the errors discussed in paragraph 6.4 and therefore one can cast serious doubt on whether or not the triaxial test with a small diameter is really suitable to perform this comparison. However, undrained shear tests in general are known to have a tendency to produce results with a high variance [e.g. Millar and Quick 1998]. Although not significant, the results still show indications that the factor of safety with respect to undrained large scale mass failure of a bank which consists of clay is improved by Vetiver roots ($FS_{\text{Vet}} = 1,19 \cdot FS_{\text{fal}}$) by an increase in undrained shear strength.
6. Hypothesis 6: "*The specific weight of soil type C with and without Vetiver grass roots will not differ significantly from each other*" is accepted. The direct influence of Vetiver grass roots on specific weight is negligible (high P-value (0,131), despite a relatively low variance).

8.4 Small scale mass failure

First of all the conclusion with respect to the hypothesis:

7. Hypothesis 7: "*Vetiver grass reduces bank retreat caused by vessel-induced water level changes significantly*" couldn't be tested because of a too small dataset.

However, even after relatively short growing periods, the influence of Vetiver grass was clearly observed. The following conclusions regarding erosion can be drawn:

- Vetiver grass reduces small scale mass failure of cohesive soil type C caused by vessel-induced waterlevel changes.
 - The amount of eroded material in time was for this experiment on average approximately 8-10 times lower for the soil with Vetiver grass than with fallow soil.
 - Erosion came to a full stop after approx. 800-1000 cycles for all three runs with Vetiver grass, while erosion continued throughout the experiment when testing the fallow soil.
 - Even with the presence of cracks, the roots were able to keep the soil in its place (increase of the tensile strength with respect to beam failure)

- Vetiver grass has a large influence on erosion of non-cohesive soil type MX by vessel-induced waterlevel changes.
 - The stability of the soil was increased by the presence of the Vetiver grass roots. Fallow soil was already unstable before the loading started until its slope reached an angle of approx. 30°, while with Vetiver the soil was stable at an angle of 90°.
 - Erosion rates considerably dropped. After 5 cycles the fallow soil was almost completely washed away, while with Vetiver grass after 1900 cycles only limited amounts of erosion were recorded.
- Which physical process causes the reduction of erosion by Vetiver grass depends on soil type. Proof for this conclusion is found in the qualitative observations during the experiments. When observing the erosion of soil type C small scale mass failure was clearly observed whereas with soil type MX the process should be described rather as particle entrainment or washing away of material.
- The amount of erosion is lower when applying Vetiver grass on cohesive soil than on non-cohesive soil. Comparing the quantitative results of soil type MX and C with Vetiver grass, the following distinct differences were found:
 - Erosion continued after 1900 cycles for soil type MX with Vetiver, while with soil type C with Vetiver the erosion came to a full stop after approx. 800-1000 cycles.
 - Average amount of erosion, although hard to compare because of the large spread, was approx. 2-4 times higher when comparing soil type C with MX both with Vetiver grass.

9. Recommendations

In this chapter the recommendations based on the experiments and some general recommendations are presented. These are divided into recommendations concerning the application of Vetiver grass and in recommendations for further research.

9.1 Influence of soil type and phreatic level on Vetiver grass

Application

- Because of the reduction in growth due to a high phreatic level, the planting of Vetiver grass on a river bank is preferred to take place at the start of the time of year with a low river discharge. The Vetiver grass should then be able to obtain a deep root system in the first couple of months after planting.
- The distance between the Vetiver hedge rows should be smaller in the wavezone then higher up the slope because of reduction in growth caused by a high phreatic level. The density of the root-network of a single hedge will be lower in the wavezone, especially in the planting phase.
- Vetiver grass is usually planted in dense hedges at a certain distance between the hedges and is not applied as a ground-covering species. Therefore, after some time other types of vegetation may grow between the Vetiver hedges. As observed in the experiment the reduction of light availability strongly influences the growth rate of Vetiver grass, therefore high vegetation has to be removed. When the Vetiver grass is also planted with the purpose of improving large scale mass stability, the rooting depth must be large. This increases the necessity of maintenance.

Further research

- To retrieve more reliable data, the experiment should be carried out on a larger number of plants and/or with a longer duration of the experiment.
- To investigate whether the same relations and trends are also valid for lower phreatic levels (>0,5 m below surface level) the same experiment could be carried out with lower phreatic levels. A different test setup may be necessary then, because of the extended root length during the experiment. It might then be useful to use pots with a wider diameter, for the root system of Vetiver grass is known to have a cone-like shape.

If further research is desired, one has to consider performing the experiment on location (for example in Vietnam). The experiment is then not restricted by space, thus a large amount of samples can be tested, but mainly because of the natural conditions in which the Vetiver grass will be tested then. It was namely observed that a small difference in conditions may lead to large differences in the results (paragraph 5.3.2). The mayor advantage of performing the test in a green house, however, is the fact that the conditions are much more controllable, and due to this it is easier to isolate a single variable to be tested.

9.2 Large scale mass failure

Further research

The testing of the undrained shear strength in the experiment described in chapter 6 did not provide significant results. The results may be improved by execution of:

- standard UU-tests on larger samples ($\varnothing=6,6$ cm)
- CU triaxial tests, which reduces the influence of disturbances, after which the undrained shear strength can be estimated by a standard analysis (e.g. Verruijt 1999)
- a higher number of UU-tests to increase accuracy
- a different type of test. In-situ direct shear tests on river banks may potentially provide more accurate results.

Parameters which are neglected in the analysis of paragraph 3.8 may be of importance for large scale mass failure:

- The hydrological influence of Vetiver grass in cohesive soil should be investigated to have an estimation of the influence on bank stability.
- The reduction of crack forming by Vetiver grass roots should be investigated, not only for large scale mass stability, but it may be of great influence on small scale mass failure too.

9.3 Small scale mass failure

Application

- The combination of Vetiver grass on a cohesive soil provides the best protection against bank erosion. The properties of the cohesive soil and the properties of the Vetiver grass complement each other well.
- When applying Vetiver grass on banks, the construction or initial phase is normally speaking the most vulnerable phase. The slips are not yet able to strengthen the bank and are therefore themselves also vulnerable for erosion. Also, erosion may take place between two Vetiver grass slips as observed during the experiments, making the slips themselves more vulnerable for erosion. It is necessary to prevent initial erosion in this stage. Possible solutions might be the use of (permanent) reinforcement (e.g. rock) or a temporarily protection in combination with Vetiver grass. The first solution is not very useful in this case, for the advantages of application of Vetiver grass will then be (partially) countered. The second solution might be very useful, especially when considering a protection which does not have to be removed, but disintegrates after some time (for example a wooden construction or a filter consisting of jute cloth). The required service time for this protection depends on the erodibility of the soil, the type and size of the (hydraulic) loads and the growth rate of the Vetiver grass. The latter depends on local conditions like groundwater level and soil type as observed in the experiments (paragraph 8.2). But even in strong cohesive soils, the growth rate of Vetiver grass is quite high, and the roots are distributed well through the soil, as observed in the experiments. If a temporary reinforcement is applied, this may become redundant relatively quickly.

Further research

- The same test setup principle could be used to obtain more data, or to perform tests on larger samples to reduce the influence of possible model effects.
- Erosion tests on soil type MX should be carried out with a larger bank, such that an equilibrium profile can be established. This would be a better representation of the properties of erosion of non-cohesive soil.
- The test setup used in this experiment is not suitable to represent physical phenomena with a sinusoidal-like forcing and a relatively short period, as for example the stern wave. It is namely very susceptible to artificial oscillations.

9.4 General

Further research

- In this thesis attention is paid only on waterlevel changes for it was assumed to be dominant for cohesive soils. Further research can be conducted on other aspects of vessel-induced loads like return current and breaking secondary waves in order to test this assumption.
- As mentioned in paragraph 7.1 the combination of all phenomena related to erosion of banks by vessel-induced loads is more complex than their individual contribution. Further research could therefore very well be aimed at the total signal of loads caused by ships. It is, however, hard to get a good representation of the full forcing of a ship in an experimental setup. Therefore field research may provide better testing conditions. In order to obtain a reliable dataset concerning the loads related to ship passages, an interesting experiment would be to test on a location where the exact dimensions and loading of the passing ships is known. Such a location is given in appendix Q. On this location the dimensions and tonnage of each ship is recorded by the personnel who operate the bridges in this stretch of the channel. Of course there are other difficulties when performing such a field test, for example: creating a representation of a bank with Vetiver grass or executing measurements of the bank erosion and/or the hydraulic conditions may be quite troublesome. But it may be worthwhile for this experimental test setup should be able to keep artificial effects to a minimum and thus provide a better insight on the full loads of vessels, and their effects on a bank.

References

1. **Abernethy, B. and Rutherford, I.D. (2001)**. "The distribution and strength of riparian tree roots in relation to riverbank reinforcement". *Hydrol. Process.*, 15: 63-79
2. **ASCE Task Committee on Hydraulics, Bank Mechanics and Modeling of River width adjustment (1998a)**. "River width adjustment. I: Processes and mechanisms". *J. Hydraul. Engrg.*, 124(9): 881-902
3. **Barker, D.H., Watson, A.J., Sombatpanit, S., Northcutt, B. and Maglinao, A.R. (eds) (2004)**. "Ground and water bioengineering for erosion control and slope stabilization", Science publishers, Plymouth, UK, ISBN 1-5788-209-9
4. **Bauer, B.O., Lorang, M.S. and Sherman, D.J. (2002)**. "Estimating boat-wake-induced levee erosion using sediment suspension measurements", *J. Waterway, Port and Coast. Engrg.*, 128(4), 152-162
5. **Burger, B. (2005)**. "Wave attenuation in mangrove forests". Msc Thesis, Delft University of Technology
6. **Cheng, H., Yang, X., Liu, A., (2003)**. "An experimental study on mechanic performance and mechanism of soil-reinforcement by herb root system". *Proc. Third Int. Conference on Vetiver, Guangzhou, China, October 2003*
7. **Coops, H., Geilen, N., Verheij, H.J., Boeters, R., Velde, G. van der, (1996)**. "Interactions between waves, bank erosion and emergent vegetation: an experimental study in a wave tank", *Aquat. Bot.*, 53: 187-198
8. **Cornforth, D.H., (2005)**. "Landslides in practice: Investigation, analysis and Remedial/preventative options in soils", John Wiley & Sons, New Jersey, USA, ISBN 0-471-67816-3
9. **CUR (1993)**. "Modelleren gedrag onverdedigde oevers". Stichting CUR, Gouda, Werkrapport. (in Dutch)
10. **CUR 168 (1995)**. "Natuurvriendelijke oevers". Stichting CUR, Gouda, (in Dutch)
11. **CUR 96-7 (1996)**. "Erosie van onverdedigde oevers". Stichting CUR, Gouda, (in Dutch)
12. **CUR (1996)**. "Onderhoudsmodellen voor oevers". Stichting CUR, Gouda, Evaluatienotitie, (in Dutch)
13. **CUR 201 (1999)**. "Natuurvriendelijke oevers, belasting en sterkte". Stichting CUR, Gouda, (in Dutch)
14. **Dalton, P.A., Smith, W.J., and Truong, P.N.V. (1996)**. "Vetiver grass hedges for erosion control on a cropped flood plain: hedge hydraulics", *Agric. Water Managem.*, 31: 91-104.
15. **Darby, S.E. and Thorne, C.R., (1996)**. "Development and testing of riverbank-stability analysis", *J. Hydraul. Engrg.*, 122(8): 443-454
16. **Darby, S.E., Gessler, D. and Thorne, C.R. (2000)**. "Computer program for stability analysis of steep, cohesive riverbanks". *Earth Surf. Process. Landforms*, 25: 175-190
17. **Dekking, F.M., Kraaikamp, C., Lopuhaa, H.P., Meester, L.E., (2003)**. "Kanstat: Probability and statistics for the 21st century", Lecture notes WI3102, Delft University of Technology
18. **Duan, J.G. (2005)**. "Analytical approach to calculate rate of bank erosion", *J. Hydr. Engrg.*, 131(11), 980-990
19. **Dunn, G.H. and Dabney, S.M. (1996)**. "Modulus of elasticity and moment inertia of grass hedge stems", *Transactions of the ASAE*, 39(3): 947-952
20. **Ekanayake, J.C. and Phillips, C.J. (1999)**. "A method for stability of vegetated hillslopes : an energy approach", *Can. Geotech. J.*, 36: 1172-1184
21. **Gaskin, S.J., Pieterse, J., Al Shafie, A. and Lepage, S. (2003)**. "Erosion of undisturbed clay samples from the banks of the St. Lawrence River", *Can. J. Civ. Eng.* 30: 585-595

22. **Groenveld, R. (2002)**. "Inland Waterways", Lecture notes CT4330, Delft University of Technology
23. **Hengchaovanich, D. (1998)**. "Vetiver grass for slope stabilization and erosion control", Tech. Bull. No. 1998/2, Pacific Rim Vetiver Network (PRVN), Bangkok, Thailand, ISBN 974-7773-71-6
24. **Ke, C.C., Feng, Z.Y., Wu, X.J., and Tu, F.G. (2003)**. "Design principles and engineering samples of applying Vetiver eco-engineering technology for land landslide control and slope stabilization of riverbank", *Proc. Third Int. Conference on Vetiver, Guangzhou, China, October 2003*
25. **Kirby, J.M. and Bengough, A.G. (2002)**. "Influence of soil strength on root growth: experiments and analysis using a critical-state model". *Europ. J. Soil Science*, 53: 119-128
26. **Le Viet Dung, Luu Thai Danh, Truong, P. and Le Thanh Phong (2003)**. "Vetiver system for wave and erosion control in the Mekong delta, Vietnam". *Proc. Third Int. Conference on Vetiver, Guangzhou, China, October 2003*.
27. **Maaskant, I. (2005)**. "Toepassingsmogelijkheden van vetiver gras en *Cyperus rotundus* op dijken". Msc Thesis, Delft University of Technology (in Dutch)
28. **Metcalfe, O., Smith, R. and Truong, P. (2003)**. "Hydraulic characteristics of vetiver hedges in deep flows", *Proc. Third Int. Conference on Vetiver, Guangzhou, China, October 2003*.
29. **Micheli, E.R. and Kirchner, J.W. (2002)**. "Effects of wet meadow riparian vegetation on streambank erosion. 2. Measurements of vegetated bank strength and consequences for failure mechanisms". *Earth Surf. Process. Landforms* 27: 687-697
30. **Millar, R.G. and Quick, M.C. (1998)**. "Stable width and depth of gravel-bed rivers with cohesive banks". *J. Hydraul. Eng.*, 124(10): 1005-1013
31. **Morgan, R.P.C. and Rickson, R.J. (eds) (1995)**. "Slope stabilization and erosion control: A Bioengineering approach", F.N. Spon/Chapman and Hall, London, UK, ISBN 0-419-15630-5
32. **Mosselman, E. (1989)**. "Communications on hydraulic and geotechnical engineering", Report No. 89-3 Faculty of Civil Engineering, Delft University of Technology
33. **Osman, A.M. and Thorne, C.R. (1988)**. "Riverbank stability analysis. I: Theory", *J. Hydraul. Eng.*, 114(2): 134-149
34. **Parchure, T.M., McAnally Jr., W.H., Teeter, A.M., (2001)**. "Desktop method for estimating vessel-induced sediment suspension", *J. Hydr. Engrg.*, 127(7), 577-587
35. **Roering, J.J., Schmidt, K.M., Stock, J.D., Dietrich, W.E. and Montgomery, D.R. (2003)**. "Shallow landsliding, root reinforcement, and the spatial distribution of trees in the Oregon Coast Range", *Can. Geotechn. J.*, 40: 237-253
36. **Schiereck, G.J. (2004)**. "Introduction to bed, bank and shoreprotection". Delft University Press, ISBN 90-407-1683-8
37. **Simon, A. and Collison, A.J.C., (2002)**. "Quantifying the mechanical and hydrological effects of riparian vegetation on streambank stability", *Earth Surf. Process. Landforms*, 27: 527-546
38. **Soest, J. van, (1997)**. "Elementaire statistiek", Delft University press, Delft (in Dutch), ISBN 90-407-1270-0
39. **TAW (1988)**. "Leidraad cel- en triaxiaalproeven", Technische Adviescommissie voor de Waterkeringen (TAW), Waltman, Delft, ISBN 90-212-3146-8 (in Dutch)
40. **Truong, P. (2000)**. "An Overview of Research, Development and Application of the Vetiver Grass System (VGS) Overseas and in Queensland", *Vetiver Workshop, Toowoomba, Qld, Australia, November 2000*
41. **Thorne, C.R. (1990)**. "Effects of vegetation on riverbank erosion", in: Thornes, J.B. (ed), "Vegetation and erosion: Processes and environments". John Wiley & Sons, Chichester, UK, ISBN 0-471-92630-2
42. **Verruijt, A. (1999)**. "Grondmechanica", Delft University Press, Delft (in Dutch)

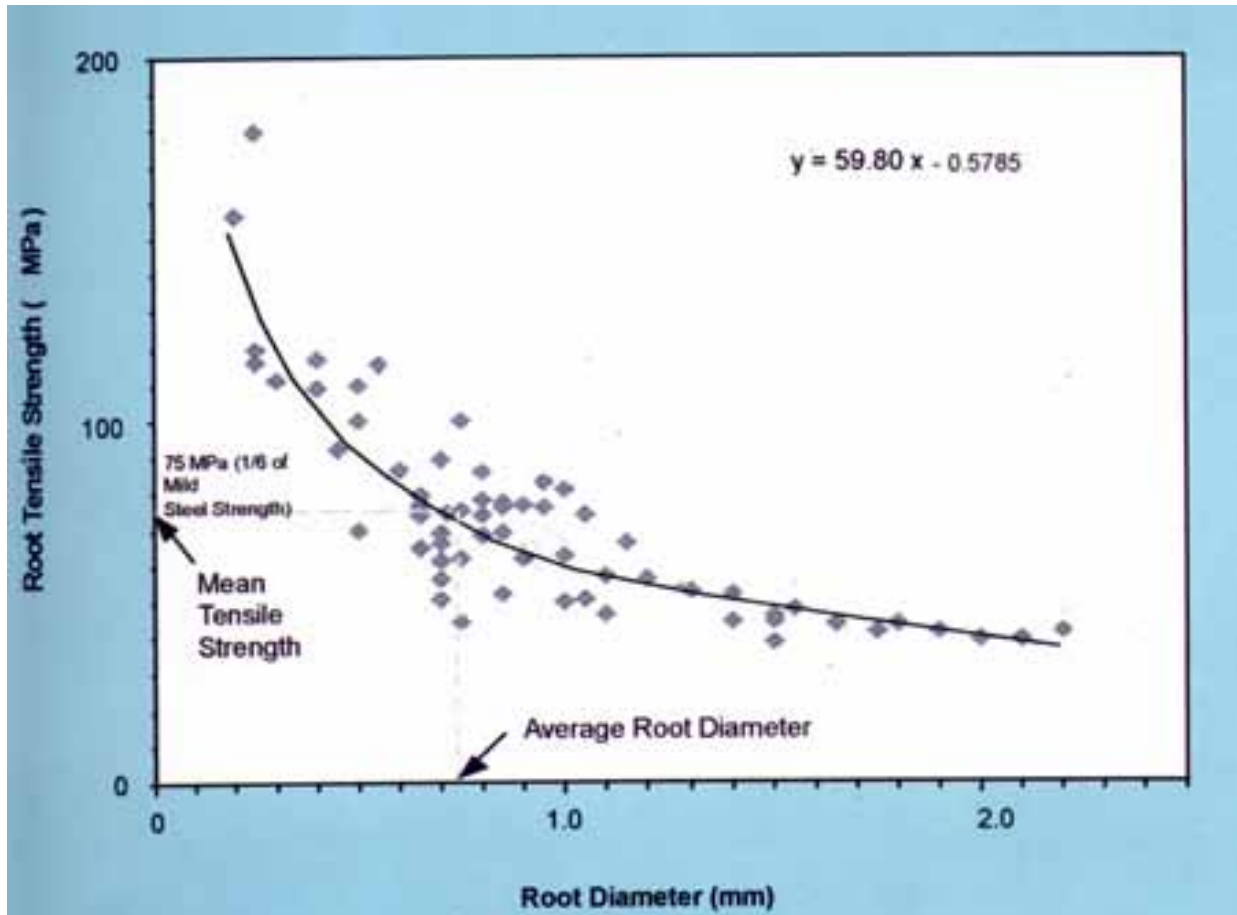
43. **Verwaal, W., Mulder, A.**, "Soil mechanics: Test procedures", Lecture notes, Delft University of Technology
44. **Vietmayer, N.D. (1993)**. "Vetiver grass, a thin green line against erosion", National Research Council, Washington, ISBN 0-309-04269-0
45. **Wood, A.L., Simon, A., Downs, P.W., and Thorne, C.R. (2001)**. "Bank-toe processes in incised channels: the role of apparent cohesion in the entrainment of failed bank materials", *Hydrol. Process.*, 15: 39–61
46. **Worldbank, (1993)**. " Vetiver grass: a hedge against erosion", Worldbank, Washington, DC, ISBN 0-8213-1405-X
47. **Wu, T.H. and Erb, R.T. (1988)**. "Study of soil-root interaction" *J. Geotechn. Eng.*, 114(12): 1351-1375
48. **Wu, T.H. (1995)**. "Slope stabilization", in R.P.C. Morgan and R.J. Rickson (eds). "Slope stabilization and erosion control: A Bioengineering approach". F.N. Spon/Chapman and Hall, London, UK
49. **Wu, T.H. and Watson, A. (1998)**. "In situ shear tests of soil blocks with roots", *Can. Geotech. J.*, 35: 579-590
50. **Xia, H.P., Lu, X., Ao, H., and Liu, S. (2003)**. " A preliminary Report on Tolerance of Vetiver to Submergence". South China Institute of Botany, Chinese Academy of Sciences, Guangzhou, China
51. **Yoon, P.K. (1993)**. "A look-see at Vetiver grass in Malaysia". First and second progress report, Worldbank, Washington, DC

Websites:

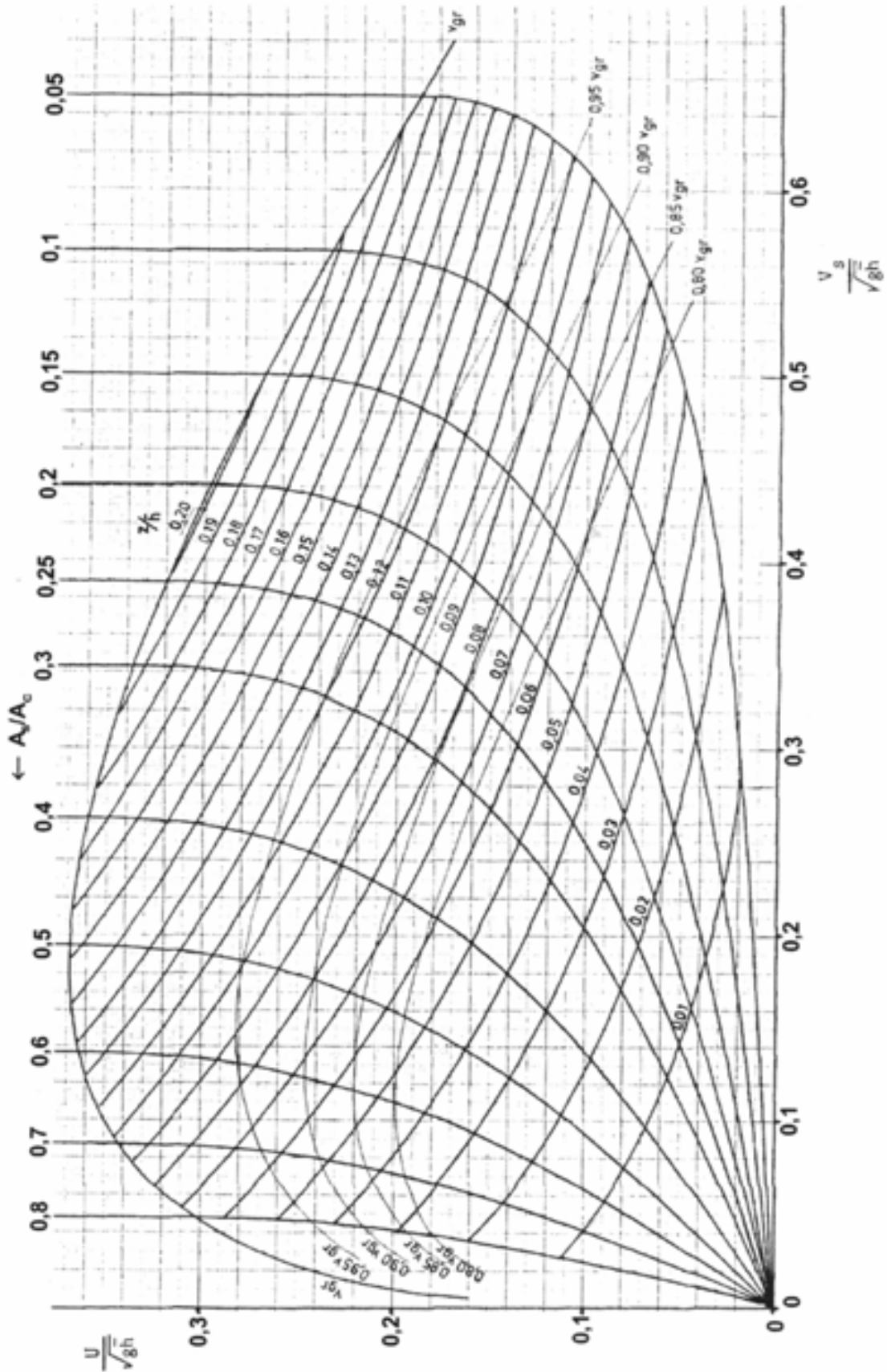
- | | | |
|----|---|------------------|
| A | http://www.vetiver.org | (september 2006) |
| A1 | http://www.vetiver.org/TVN_distribution.htm | (january 2006) |
| A2 | http://www.vetiver.org/TVN_FRONTPAGE_ENGLISH.htm | (january 2006) |
| B | http://en.wikipedia.org/wiki/Vetiver | (january 2006) |

Appendices

Appendix A: Results of Vetiver grass root tensile strength measurements (from Hengchaovanich 1998)



Appendix B: Diagram of Schijf ($\alpha=1,1$) (from Groenvelde (2002))



Appendix C2: Shear strength of soil type SC obtained with triaxial test

Sample:	Sample height (cm)	Max. shear displacement (mm)	Max. shear stress (kN/m ²)
1 (SC)	8,0	13 mm	26,7
2 (SC)	8,0	12,5 mm	30,2
3 (SC)	8,0	15 mm	27,2
4 (SC)	8,0	15 mm	25,3
Mean ± s.d.	8 ± 0	13,9 ± 1,3	27,4 ± 2

Appendix D: Classification of soil type C

The soil was retrieved from a fallow land on the Thijsseweg in Delft, Holland. The location is shown in the figure below (black cross indicates the exact position).



All tests were performed according to the British soil classification system. The liquid limit was determined using the Casagrande cup (BS 1377: Part 2: 1990). Besides the liquid limit also the plastic limit (BS 1377: Part 2: 1990) was determined and a hydrometer test was performed (BS 1377: Part 2: 1990). The water content W_n of the soil is expressed as a percentage of the weight of the oven-dried soil, as follows:

$$W_n = \frac{\text{mass of water}}{\text{mass of oven-dried soil}} * 100$$

Liquid and plastic limit, plasticity index and the corresponding classification

The liquid limit W_L was found from the flow curve to be 75% at 25 blows.

The plastic limit W_p was found to be 38%.

$$\text{Plasticity index } I_p = W_L - W_p = 75 - 38 = 37\%$$

From the plasticity chart the soil is classified as MV

Hydrometer test

The results are displayed in the table and graph on the next two pages. The amount of clay is approximately 40% while the amount of silt is approximately 35%. The remaining 25% mainly consists of fine sand.

Hydrometer test

Engineering Geology Lab.

Date 22/3/2005

Calibration		
Hydrometer number	Delft	
Scale factors	-3,9286	199,71

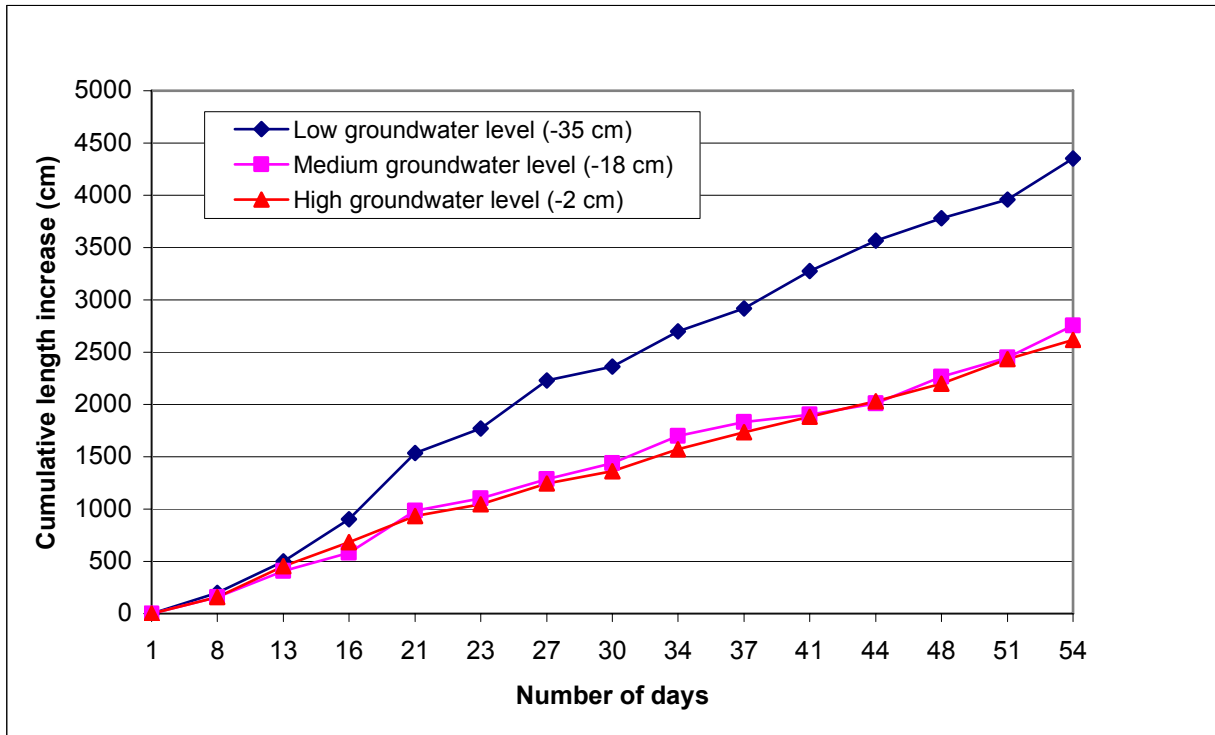
Input parameters	
Sample	s1
Temperature, T [C°]	21
Dynamic viscosity, η [mPas]	0,98969
Particle density, ρ_s [Mg/m ³]	2,65
Density reading, R_0' [-]	1,0007
Initial hydrometer reading, R_0'	0,7
Start mass of the sample, m [g]	58,37
Meniscus correction, C_m [-]	0,5

Sieving analysis			
Sieve	Retained	Passed	Passed
mm	g	g	%
37,5	0	58,37	100,00
20	0	58,37	100,00
10	0	58,37	100,00
6,3	0	58,37	100,00
3,35	0	58,37	100,00
2	0,45	57,92	99,23
1,18	0,46	57,46	98,44
0,6	1,32	56,14	96,18
0,3	3,41	52,73	90,34
0,15	4,84	47,89	82,05
0,063	4	43,89	75,19
	14,48	sum	

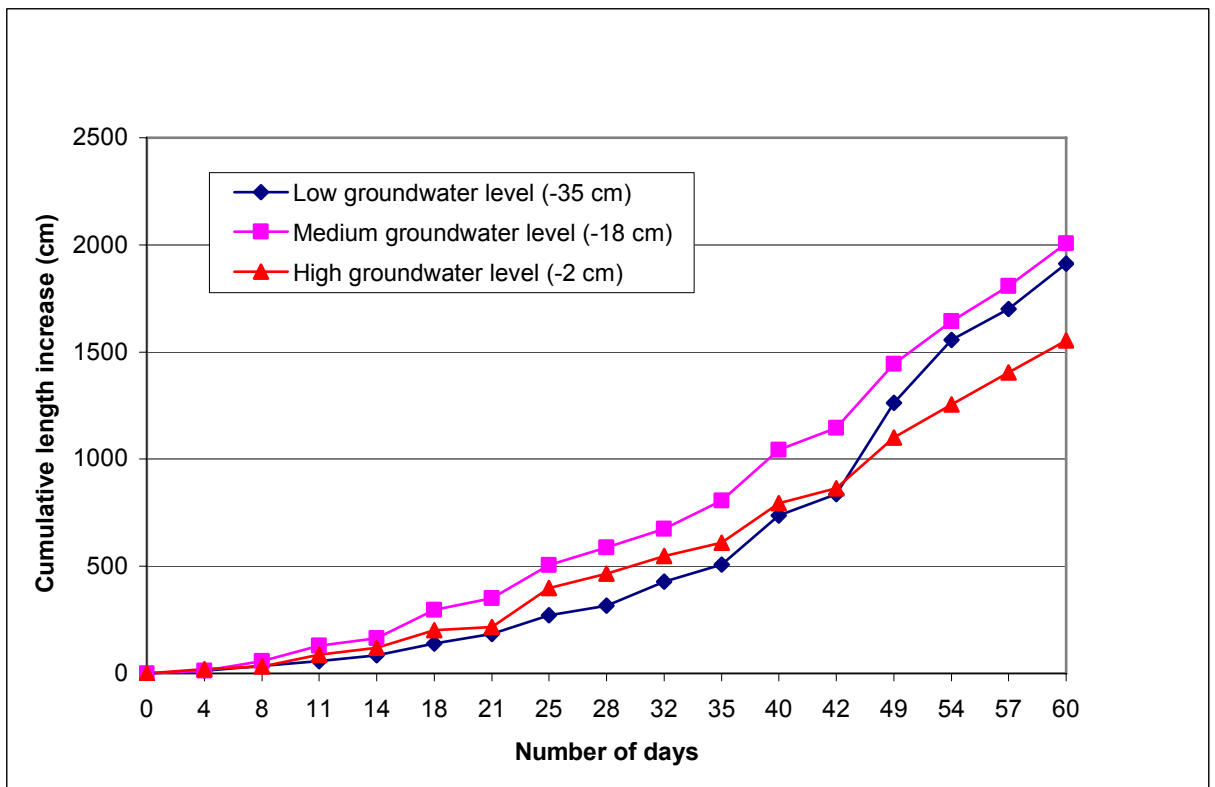
Combined test data	
Grainsize [mm]	Passing [%]
37,5	100,00
20	100,00
10,0	100,00
6,3	100,00
3,35	100,00
2,00	99,23
1,180	98,44
0,600	96,18
0,300	90,34
0,150	82,05
0,063	75,19
0,05800	72,36
0,04188	69,61
0,03022	66,86
0,02183	63,84
0,01499	59,43
0,00764	52,00
0,00458	47,05
0,00230	40,72
0,00137	36,87

Hydrometer analysis									
Time	t	Total time	Density reading	Hydrometer reading	Corrected hydrometer reading	Modified hydrometer reading	Effective depth	Particle diameter	Mass Percentage
hr	min	min	[-]	[-]	[-]	[-]	[-]	[mm]	[%]
	0,5	0,5	1,027	27	27,5	26,3	91,6735	0,058	72,36
	1	1	1,026	26	26,5	25,3	95,6021	0,042	69,61
	2	2	1,025	25	25,5	24,3	99,5307	0,030	66,86
	4	4	1,0239	23,9	24,4	23,2	103,852	0,022	63,84
	9	9	1,0223	22,3	22,8	21,6	110,138	0,015	59,43
	38	38	1,0196	19,6	20,1	18,9	120,745	0,008	52,00
1	52	112	1,0178	17,8	18,3	17,1	127,817	0,005	47,05
7	54	474	1,0155	15,5	16	14,8	136,852	0,002	40,72
23	8	1388	1,0141	14,1	14,6	13,4	142,352	0,001	36,87

Appendix E1: Cumulative length of the leaves at different groundwaterlevels (soil type MX)



Appendix E2: Cumulative length of the leaves at different groundwaterlevels (soil type C)



Appendix F: Testing of the hypotheses

Hypothesis 1: Rate of growth at a low groundwater level soil type MX

To test the hypothesis ($H_0: \mu_1 = 1$ against $H_1: \mu_1 \neq 1$) it was necessary to perform an empirical bootstrap for the studentized means for two reasons:

- It was uncertain if the rate of growth could be assumed to have a normal distribution
- There was only a small amount of data ($n=14$)

Therefore the Chi-square test and the standard t-test would not have been correct. In order to obtain a bootstrap a code was written in MATLAB and was called "bootstrap", see appendix G. MATLAB is a high-performance language for technical computing. It integrates computation, visualization, and programming in an environment where problems and solutions are expressed in familiar mathematical notation (MATLAB 7, 2004). The studentized means are given in a histogram as an end result for pot 1, see appendix H1. With the results for pot 1 (10000 simulations), it was found that:

$$\text{Value of the test statistic: } t = \frac{\bar{x}_n - 1}{\frac{s_n}{\sqrt{n}}} = \frac{1,0315 - 1}{\frac{0,1321}{\sqrt{14}}} = 0,8922$$

In which :

t = test statistic

\bar{x}_n = sample mean

s_n = sample standard deviation

n = number of data

If we test

- $H_0: \mu = 1$ against $H_1: \mu \neq 1$ then $P(T \geq 0,8922) \approx 0,1862$.

Critical values: $c_l^* = -2.0988$ and $c_u^* = 2.2562$ ($\alpha=0,05$)

The 95% bootstrap confidence interval for t : $\left(\bar{x}_n - c_u^* \frac{s_n}{\sqrt{n}}, \bar{x}_n - c_l^* \frac{s_n}{\sqrt{n}} \right) = (0.952, 1.105)$

It looks like it is not allowed to reject H_0 beyond reasonable doubt, or in other words, the probability of committing a type I error is 0,1862 if we would reject the hypothesis. The hypothesis might thus be true.

Hypothesis 2: Rate of growth comparison with different groundwater levels soil type MX

To test the second hypothesis (Rates of growth of the three pots will differ significantly from each other) the growth rates of the pots will be compared.

Again a MATLAB code was written, called "bootstrap2", as shown in appendix G. This code performed an empirical bootstrap simulation for the non-pooled studentized mean difference between two samples (non-normal, unequal variances). The histograms of the bootstraps are presented in appendix H2.

Comparison 1

The first bootstrap (10000 simulations) included the comparison between the growth rates of the low and the medium groundwater level (pot 1 and pot 2).

$$\text{Value of the test statistic: } T_d = \frac{\bar{X}_n - \bar{Y}_m}{S_d} = 1,895 \Rightarrow \left(S_d^2 = \frac{S_X^2}{n} + \frac{S_Y^2}{m} \right)$$

In which :

T_d = test statistic

\bar{X}_n and \bar{Y}_n = sample mean of respectively data set X and Y

S_d^2 = non-pooled variance

S_X^2 and S_Y^2 = variance of respectively data set 1 and 2

n and m = number of data in respectively data set 1 and 2

- $H_0: \mu_1 = \mu_2$ against $H_1: \mu_1 \neq \mu_2$

The probability of committing a type I error in this case is $P(T_d \geq 1,895) \approx 0,0375$

From this, one can conclude that it seems quite reasonable that the null hypothesis is rejected (so the growth rates differ), it is a significant result ($P < 0,05$).

Comparison 2

The bootstrap (10000 simulations) included the comparison between the growth rates of the medium and the high groundwater level (pot 2 and pot 3).

Value of the test statistic: $T_d = \frac{\bar{X}_n - \bar{Y}_m}{S_d} = 3,753$

- $H_0: \mu_2 = \mu_3$ against $H_1: \mu_2 \neq \mu_3$

The probability of committing a type I error in this case is $P(T_d \geq 3,753) \approx 0,0013$

From this, one can conclude that the null hypothesis is rejected at a very significant rate ($P < 0,01$).

Comparison 3

From the result of comparison 2 one can conclude that the null hypothesis is rejected because the differences between pot 1 and pot 3 are even larger. Thus it is a very significant result ($P < 0,01$). Still the bootstrap (10000 simulations) was performed to be sure. It included the comparison between the growth rates of the low and the high groundwater level (pot 1 and pot 3).

Value of the test statistic: $T_d = \frac{\bar{X}_n - \bar{Y}_m}{S_d} = 6,149$

- $H_0: \mu_1 = \mu_3$ against $H_1: \mu_1 \neq \mu_3$

The probability of committing a type I error in this case is $P(T_d \geq 6,149) \approx 0$

From this, one can conclude that the null hypothesis is rejected at a very significant rate ($P < 0,01$).

Hypothesis 3: Rate of growth comparison with different groundwater levels soil type C

To test the second hypothesis (Rates of growth of the three pots will not differ significantly from each other) the growth rates of the pots will be compared. However as mentioned in chapter 5, the low groundwater level data is not used.

MATLAB code "bootstrap2" was used. The histogram of the bootstrap is presented in appendix H4.

The bootstrap (10000 simulations) included the comparison between the growth rates of the high and the medium groundwater level (pot 5 and pot 6).

Value of the test statistic: $T_d = \frac{\bar{X}_n - \bar{Y}_m}{S_d} = 4,507 \Rightarrow \left(S_d^2 = \frac{S_X^2}{n} + \frac{S_Y^2}{m} \right)$

- $H_0: \mu_5 = \mu_6$ against $H_1: \mu_5 \neq \mu_6$

The probability of committing a type I error in this case is $P(T_d \geq 4.507) \approx 0,001$
From this, one can conclude that the null hypothesis is rejected at a very significant rate ($P < 0,01$). The growth rates of pot 2 and 3 do differ very significantly.

Hypothesis 4: Rate of growth comparison soil types MX and C

To test the fourth hypothesis (The rate of growth of Vetiver grass will be significantly lower than the growth rates of Vetiver grass in soil type MX under the same conditions) the growth rates of the pots will be compared.

MATLAB code "bootstrap2" was used. The histograms of the bootstraps are presented in appendix H5.

Comparison 1

The first bootstrap (10000 simulations) included the comparison between the growth rates of the medium groundwater levels of both soil types (pot 2 and pot 5).

Value of the test statistic:
$$T_d = \frac{\bar{X}_n - \bar{Y}_m}{S_d} = 11,096$$

- $H_0: \mu_3 = \mu_6$ against $H_1: \mu_3 \neq \mu_6$

The probability of committing a type I error in this case is $P(T_d \geq 11,096) \approx 0,0$
From this, one can conclude that it seems quite reasonable that the null hypothesis is rejected (so the growth rates differ), it is a very significant result ($P < 0,01$).

Comparison 2

The second bootstrap (10000 simulations) included the comparison between the growth rates of the high groundwater levels of both soil types (pot 3 and pot 6).

Value of the test statistic:
$$T_d = \frac{\bar{X}_n - \bar{Y}_m}{S_d} = 8,914 \Rightarrow \left(S_d^2 = \frac{S_x^2}{n} + \frac{S_y^2}{m} \right)$$

- $H_0: \mu_3 = \mu_6$ against $H_1: \mu_3 \neq \mu_6$

The probability of committing a type I error in this case is $P(T_d \geq 8,914) \approx 0,0001$
From this, one can conclude that it seems quite reasonable that the null hypothesis is rejected (so the growth rates differ), it is a very significant result ($P < 0,01$).

Comparison 3

Again, it is not correct to use the dataset of the low groundwater level for comparison.

Hypothesis 5: Undrained shear strength of soil type C with and without Vetiver grass roots

To test the fifth hypothesis (The shear strength of soil type C with Vetiver grass roots will be significantly higher than the shear strength of the fallow soil) the shear strength measurements are compared.

MATLAB code "bootstrap2" was used. The histograms of the bootstraps are presented in appendix K.

Comparison

The bootstrap (10000 simulations) included the comparison of the shear strength measurements.

Value of the test statistic:
$$T_d = \frac{\bar{X}_n - \bar{Y}_m}{S_d} = -1,536$$

- $H_0: \mu_1 = \mu_2$ against $H_1: \mu_1 \neq \mu_2$

The probability of committing a type I error in this case is $P(T_d \leq -1,536) = 0,0568$
It is not a significant result; therefore one cannot reject the H_0 hypothesis. With this data it is not proven that Vetiver grass increases the undrained shear strength significantly.

Hypothesis 6: Specific weight of soil type C with and without Vetiver grass roots

To test the sixth hypothesis (The specific weight of soil type C with and without Vetiver grass roots will not differ significantly from each other) the specific saturated weight measurements are compared.

MATLAB code "bootstrap2" was used. The histograms of the bootstraps are presented in appendix K.

Comparison

The bootstrap (10000 simulations) included the comparison of the specific saturated weight measurements.

Value of the test statistic: $T_d = \frac{\bar{X}_n - \bar{Y}_m}{S_d} = 1,030$

- $H_0: \mu_1 = \mu_2$ against $H_1: \mu_1 \neq \mu_2$

The probability of committing a type I error in this case is $P(T_d \geq 1,030) = 0,131$
It is not a significant result; therefore one cannot reject the H_0 hypothesis. With this data it seems quite reasonable to assume that Vetiver grass roots do not directly influence the specific saturated weight of the soil.

Appendix G: MATLAB codes

MATLAB code bootstrap

```
function bootst=bootstrap(Y,aantal);
% The function file bootstrap gives an empirical bootstrap simulation for
% the studentized means. It generates bootstraps for the
% dataset Y, which should be a vector containing data. "aantal" is
% the number of bootstrap simulations required.

b=length(Y);
% The length of the data-vector is equal to the number of measurements n

for n=1:aantal;

    for i=1:b;
        bootst(i,n)=Y(floor(rand*b+1));
    end
    bmean=mean(bootst);
    bstd=std(bootst);
end
% These 2 loops create a bootstrap for the data and calculate for each new
% dataset the mean and the standard deviation.

for p=1:aantal;
    bt(p)=(bmean(:,p)-mean(Y))/(bstd(:,p)/sqrt(b));
end
% This loop calculates the studentized means for each run

bt=sort(bt)
hist(bt,20),xlabel('Studentized means'),ylabel('Number of hits')
% The bootstrapped t values are sorted and are given as output, to check
% whether the results were good, and to determine the confidence interval.
% Besides that a histogram is drawn of the t*-values.
```

MATLAB code bootstrap2

```
function bootst=bootstrap2(X,Y,aantal);
% The function file bootstrap2 gives an empirical bootstrap simulation for
% the pooled studentized mean difference. It generates bootstraps for the
% datasets X and Y, which should be vectors containing data. "aantal" is
% the number of bootstrap simulations required.

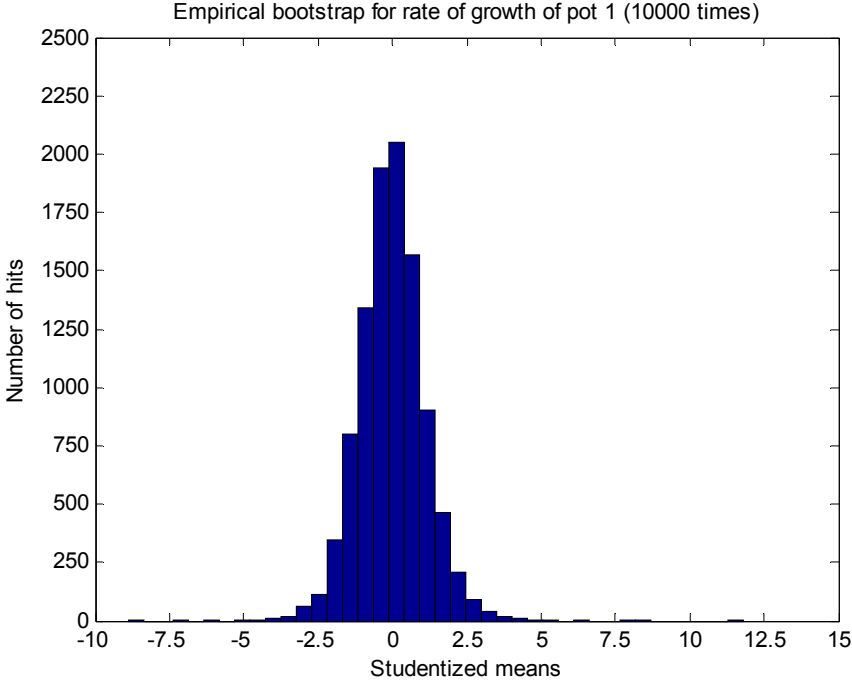
b=length(X);
c=length(Y);
% The length of the data-vector is equal to the number of measurements n

for n=1:aantal;
    for i=1:b;
        bootst(i,n)=X(floor(rand*b+1));
        bootst2(i,n)=Y(floor(rand*c+1));
    end
end
```

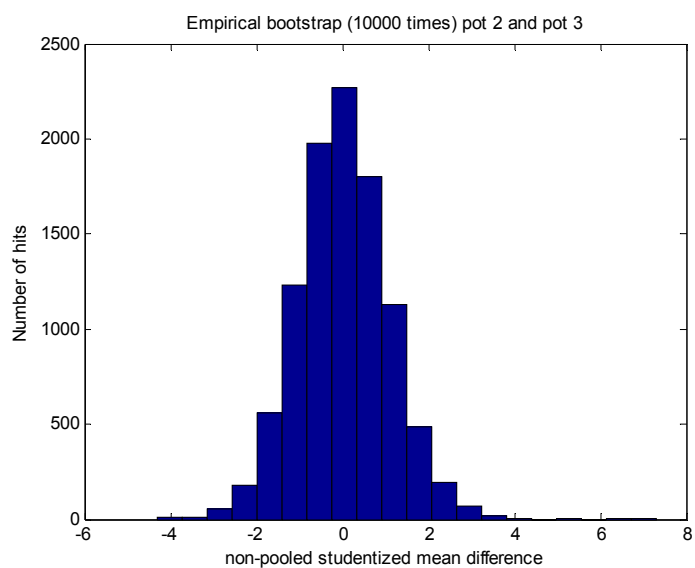
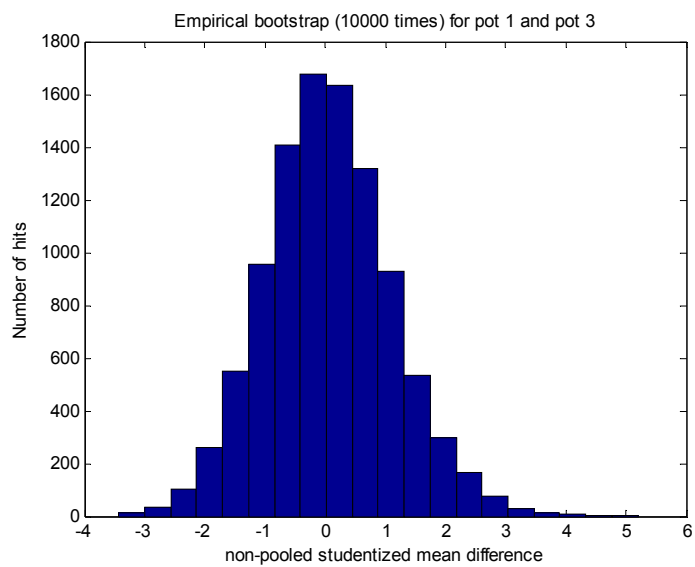
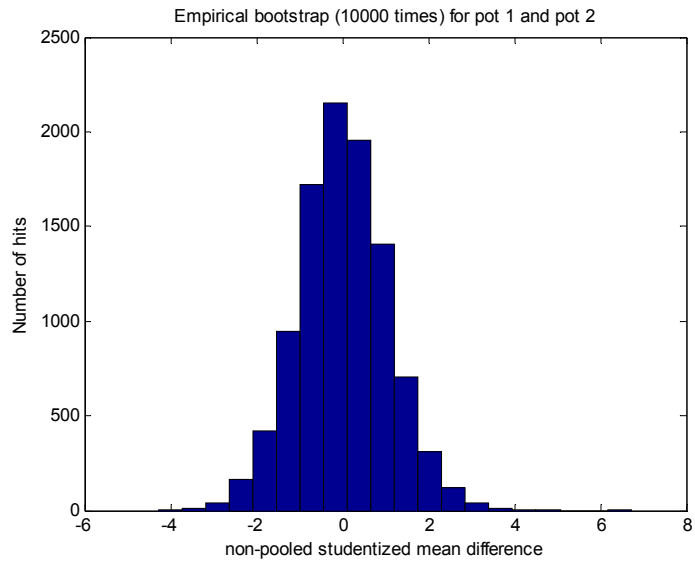
```
bmean=mean(bootst);
bvar=var(bootst);
bmean2=mean(bootst2);
bvar2=var(bootst2);
varp(n)=(bvar(:,n)/b)+(bvar2(:,n)/c);
btp(n)=((bmean(:,n)-bmean2(:,n))-(mean(X)-mean(Y)))/sqrt(varp(:,n));
end
% This loop creates a bootstrap for the data and calculates for each new
% dataset the mean and the variance. Also the pooled variance and with
% that the pooled studentized means for each run are calculated.

btp=sort(btp)
hist(btp,20),xlabel('non-pooled studentized mean difference'),ylabel('Number of hits')
% The bootstrapped t values are sorted and are given as output, to check
% whether the results were good, and also to determine the confidence interval.
% Besides that a histogram is drawn of the t*-values.
```

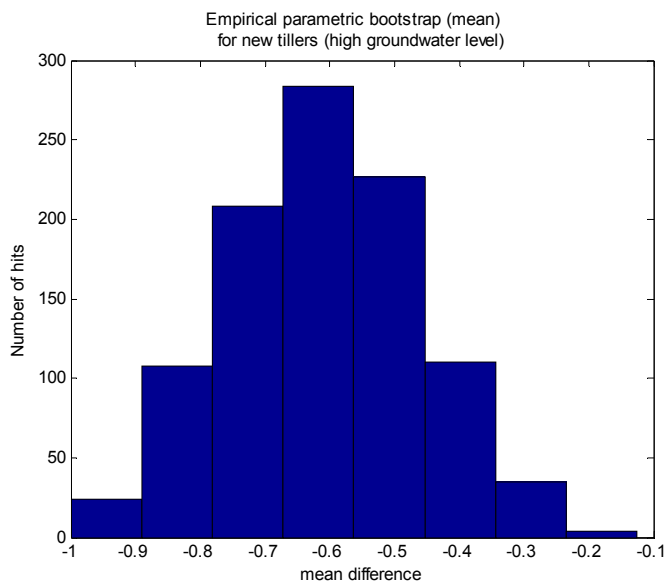
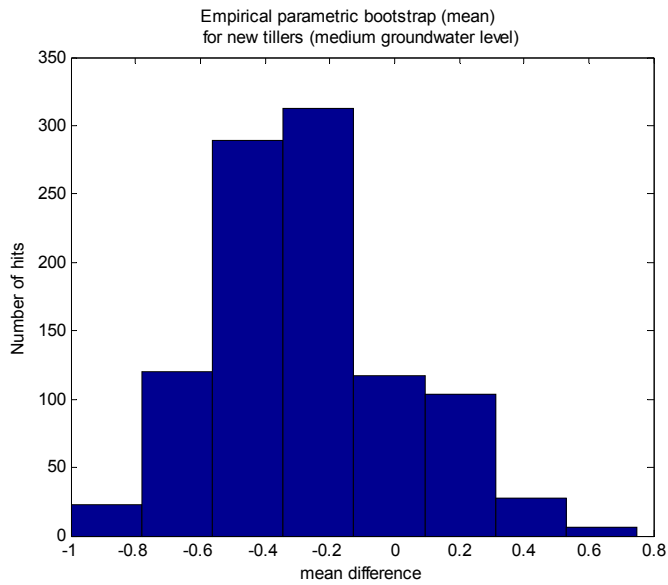
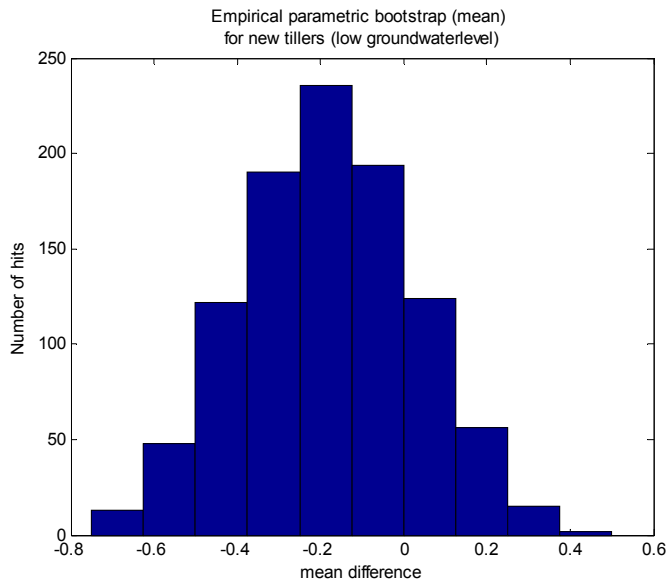
Appendix H1: Bootstrap comparison ($\mu=1$) MX



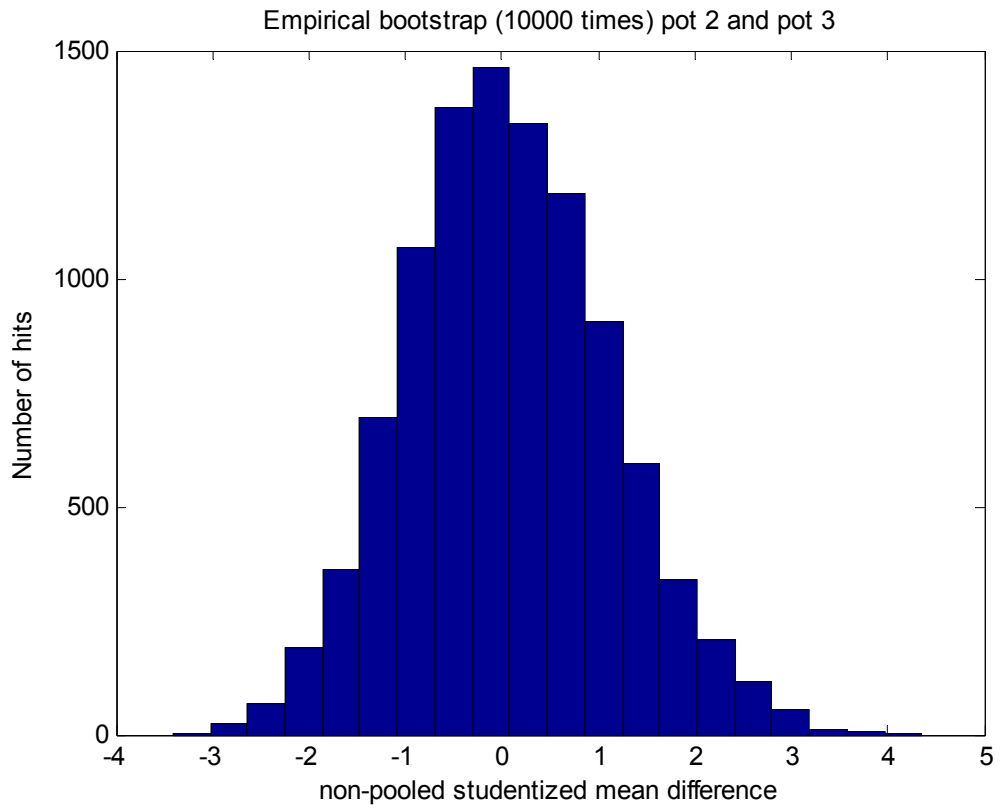
Appendix H2: Bootstrap comparison growth rates MX



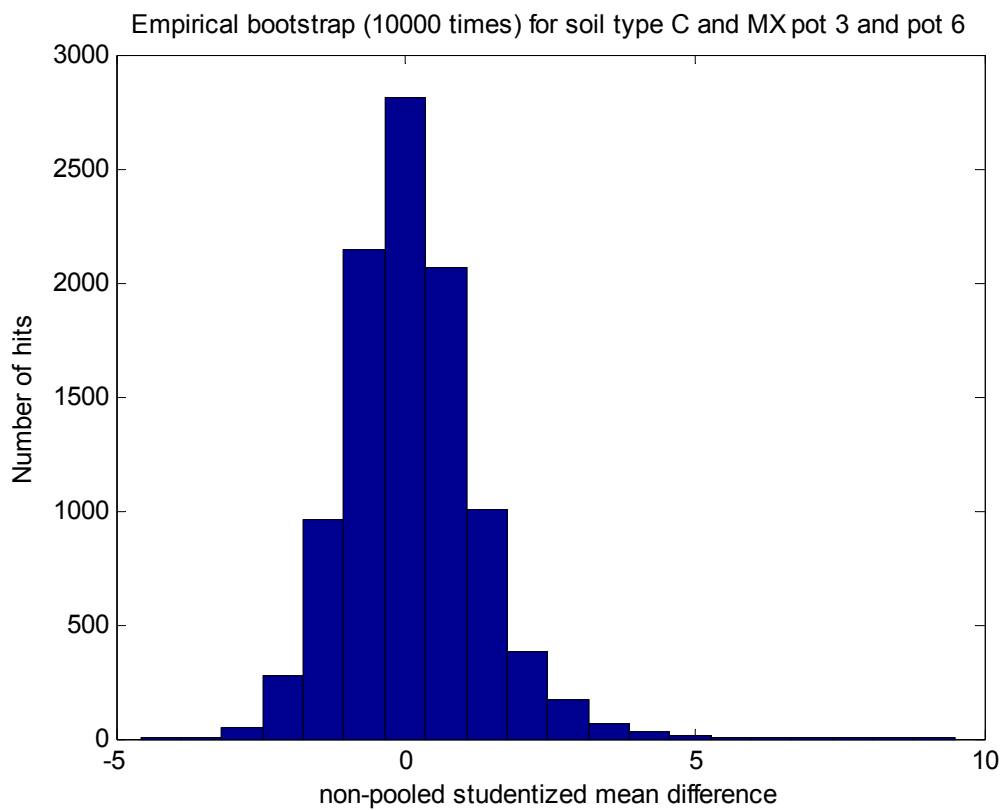
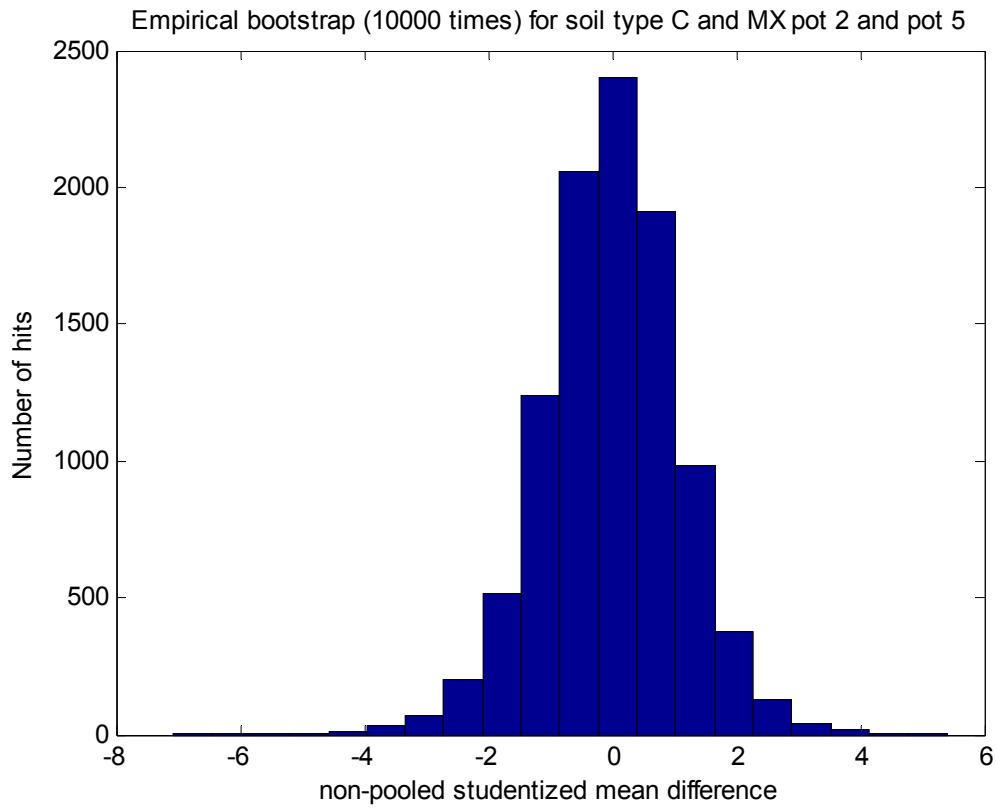
Appendix H3: Bootstrap new tillers MX



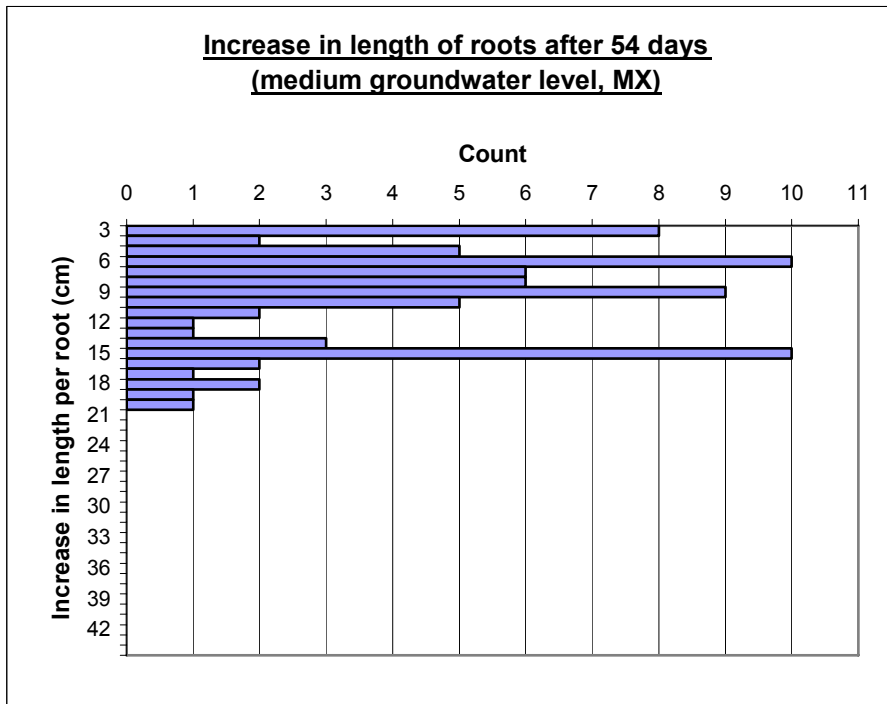
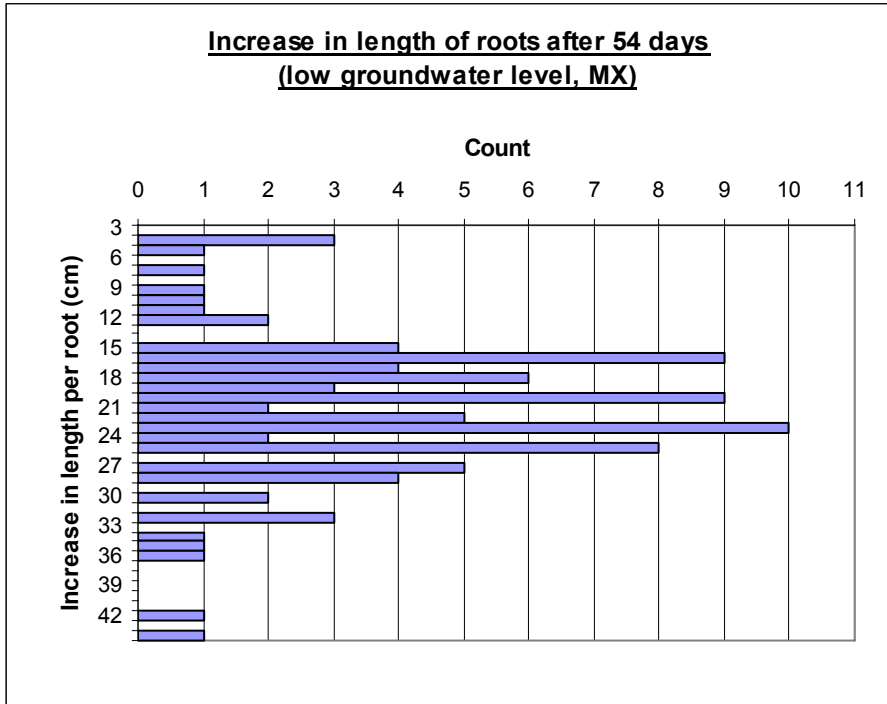
Appendix H4: Bootstrap comparison growth rates C



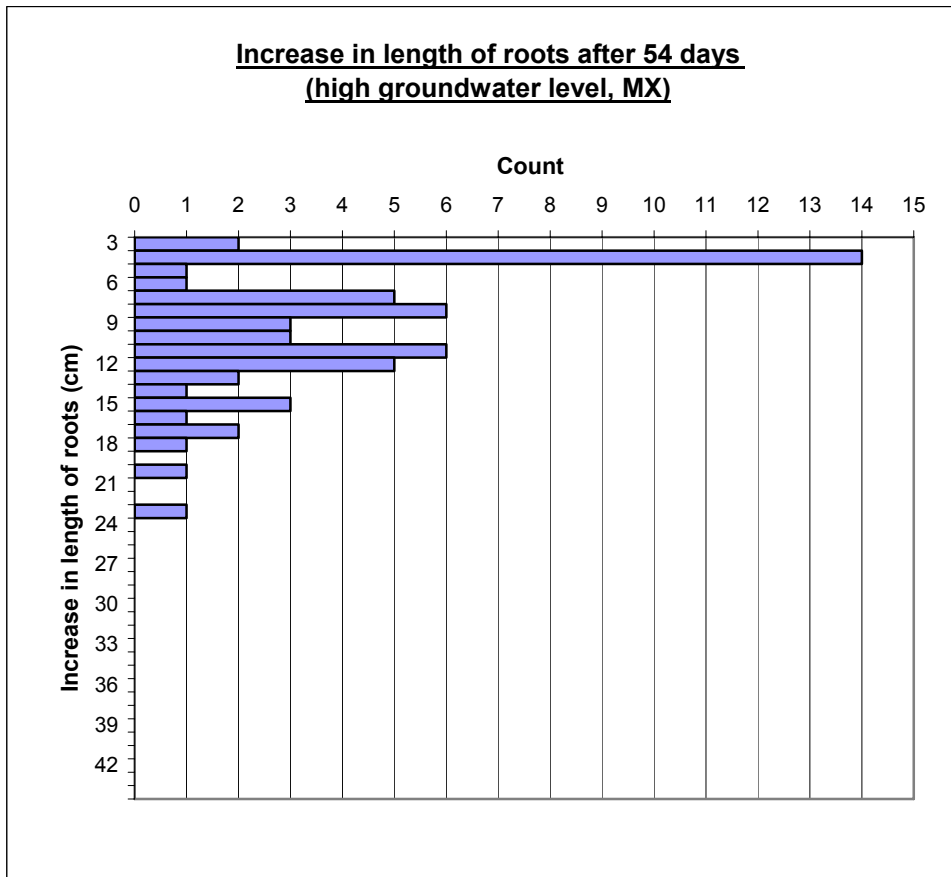
Appendix H5: Bootstrap comparison growth rates C and MX



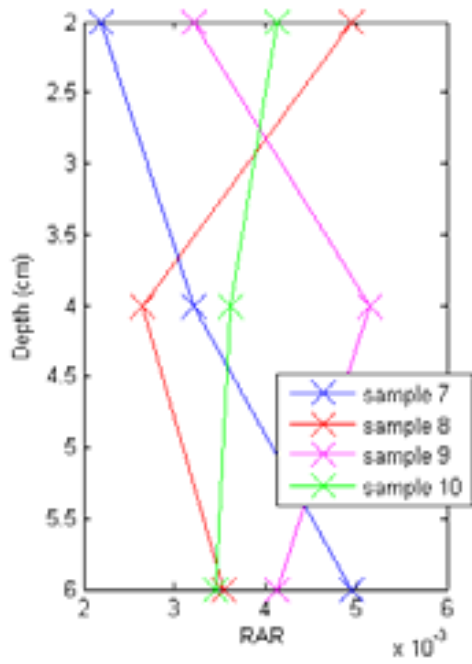
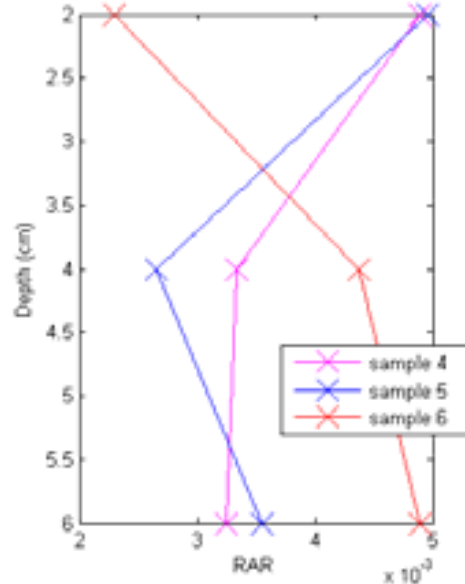
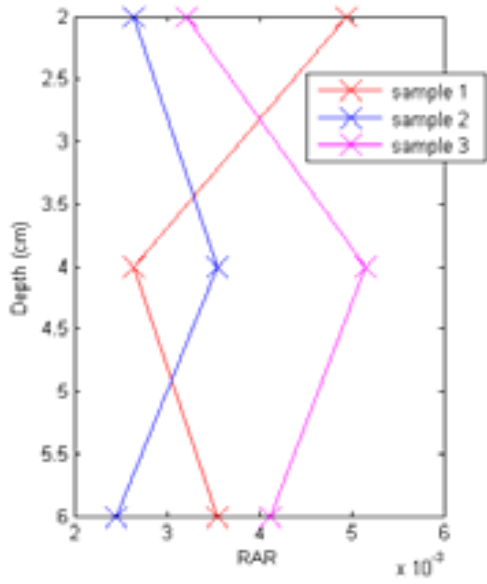
Appendix I: Graphs rate of growth below-ground biomass



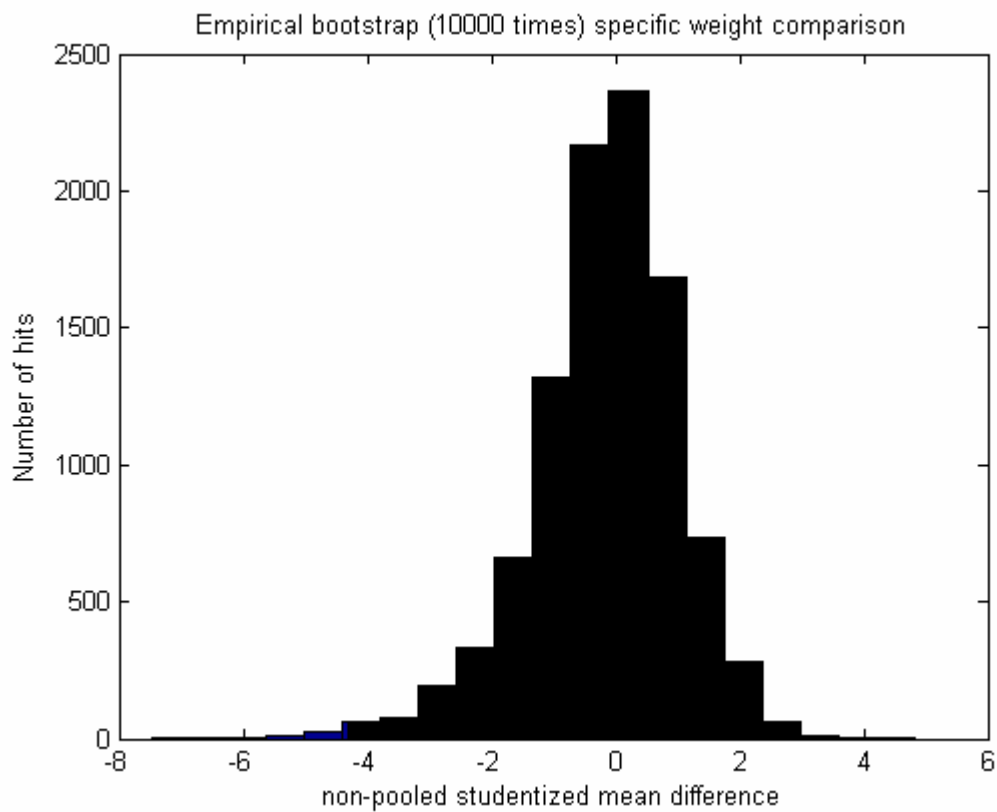
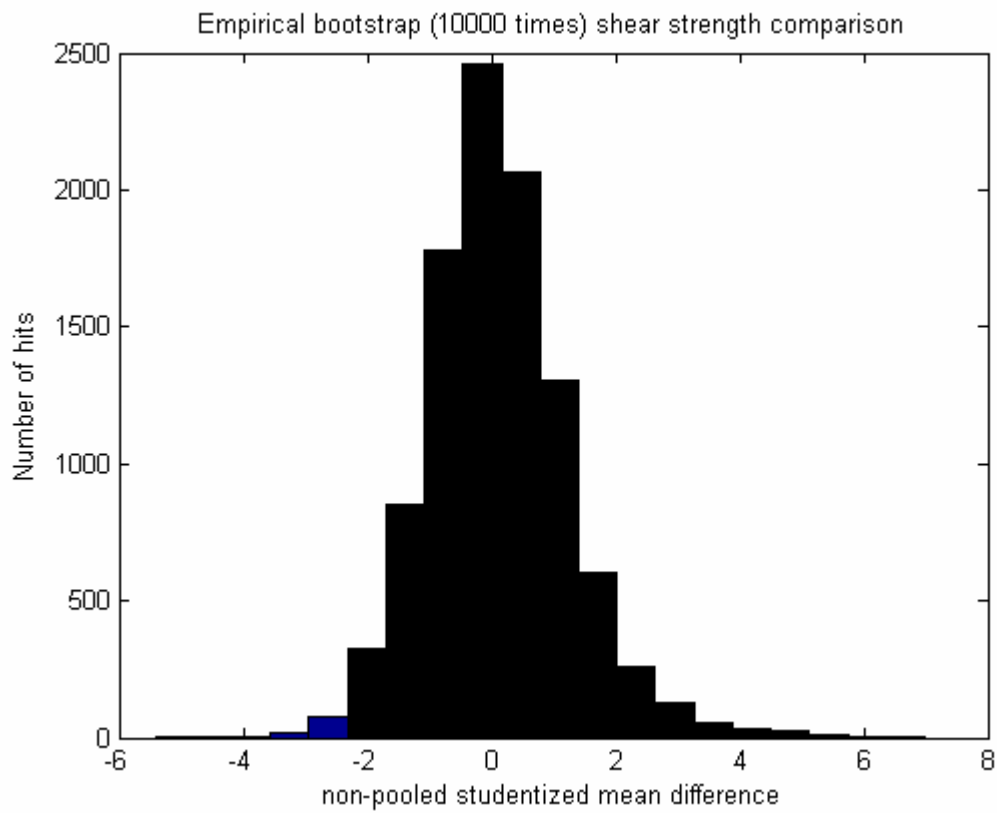
Appendix I (cont.): Graphs rate of growth below-ground biomass



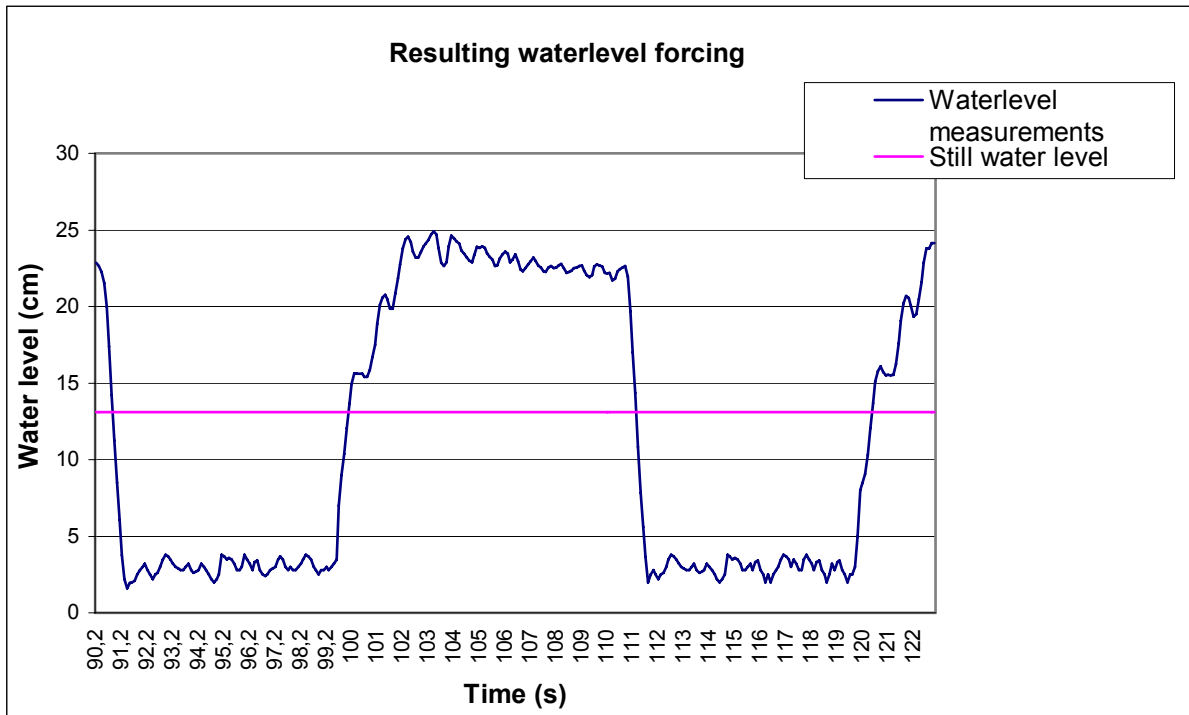
Appendix J: Root area ratios at 3 different heights of triaxial test samples (2, 4 and 6 cm)



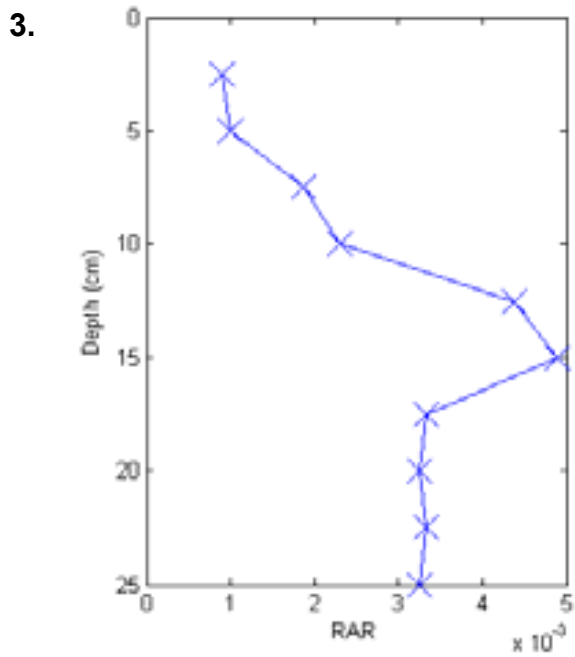
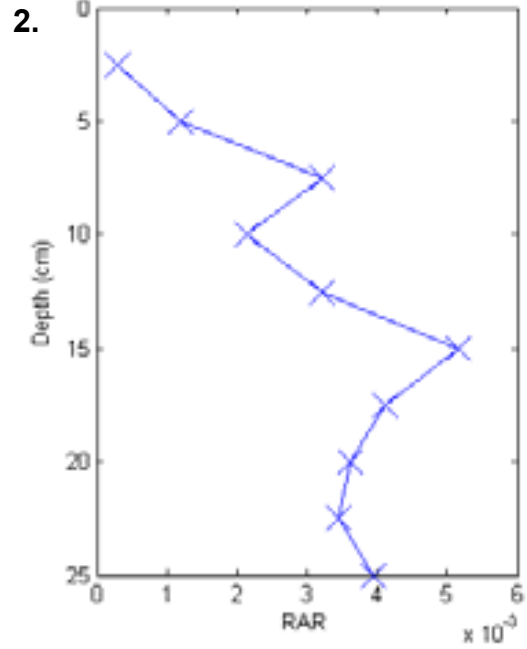
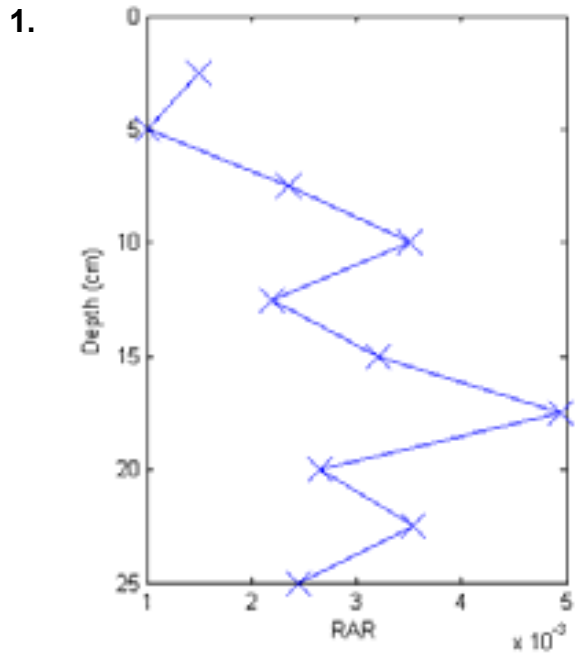
Appendix K: Bootstrap comparison undrained shear strength and specific weight



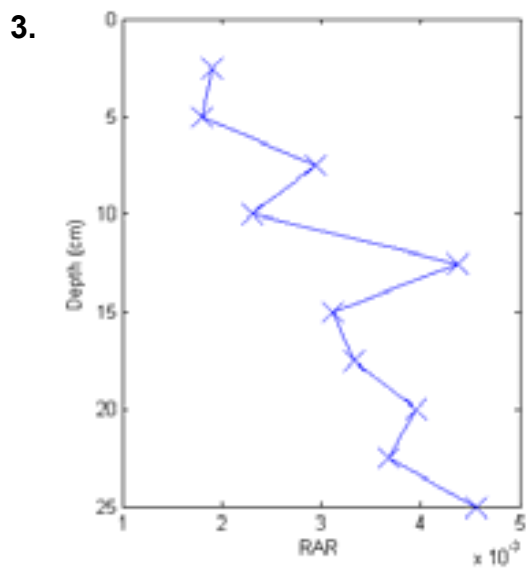
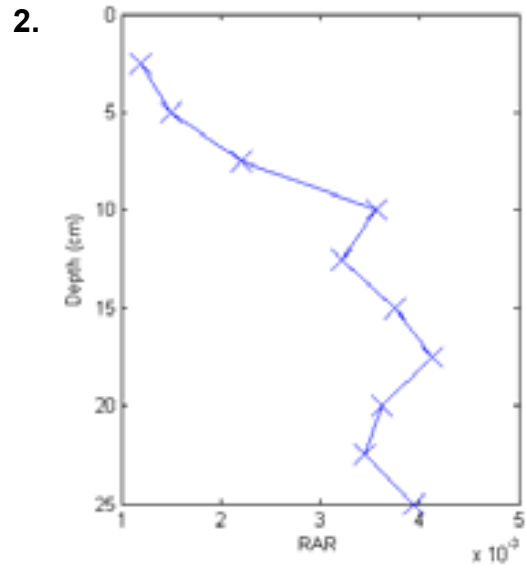
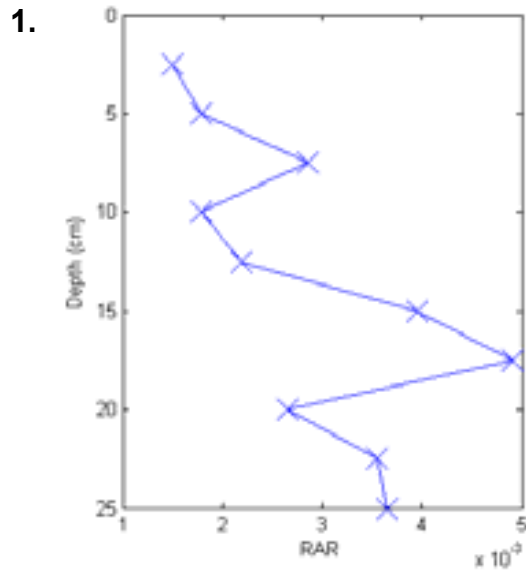
Appendix M: Forcing signal provided by the wave generator, measured by the wave height meter



Appendix N: Root area ratio (RAR) by depth for run 1 to 3 of soil type MX with Vetiver grass



Appendix O: Root area ratio (RAR) by depth for run 1 to 3 of soil type C with Vetiver grass



Appendix P: Small scale mass failure test results of soil type SC

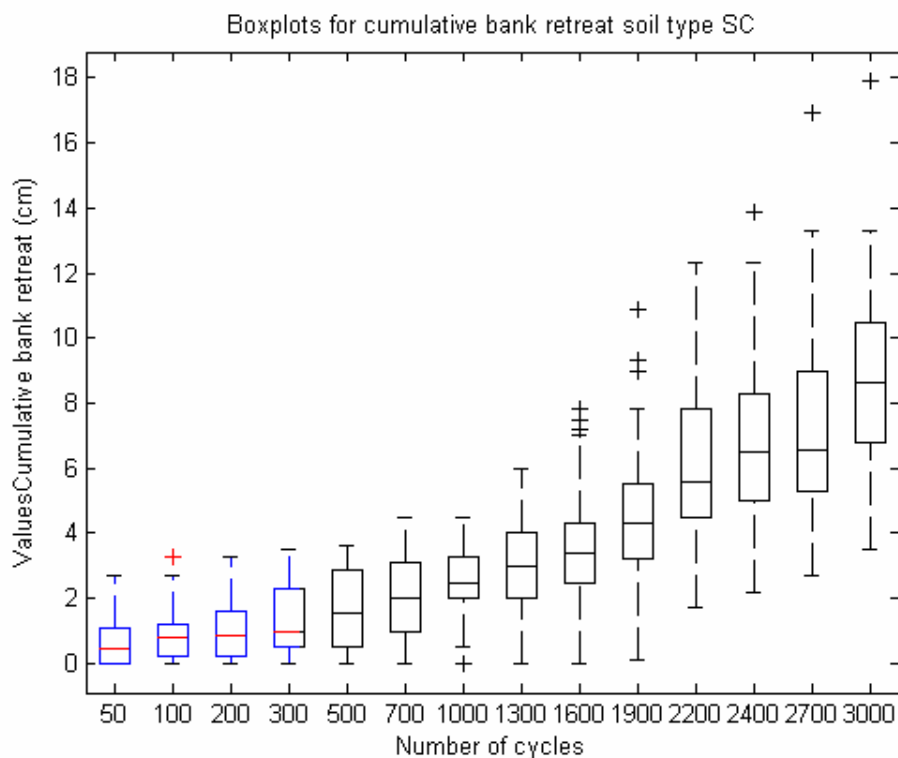
A qualitative description of the observations during the test is given, after which the quantitative results are shown. The temperature of the water during the experiment was approximately 18 °C.

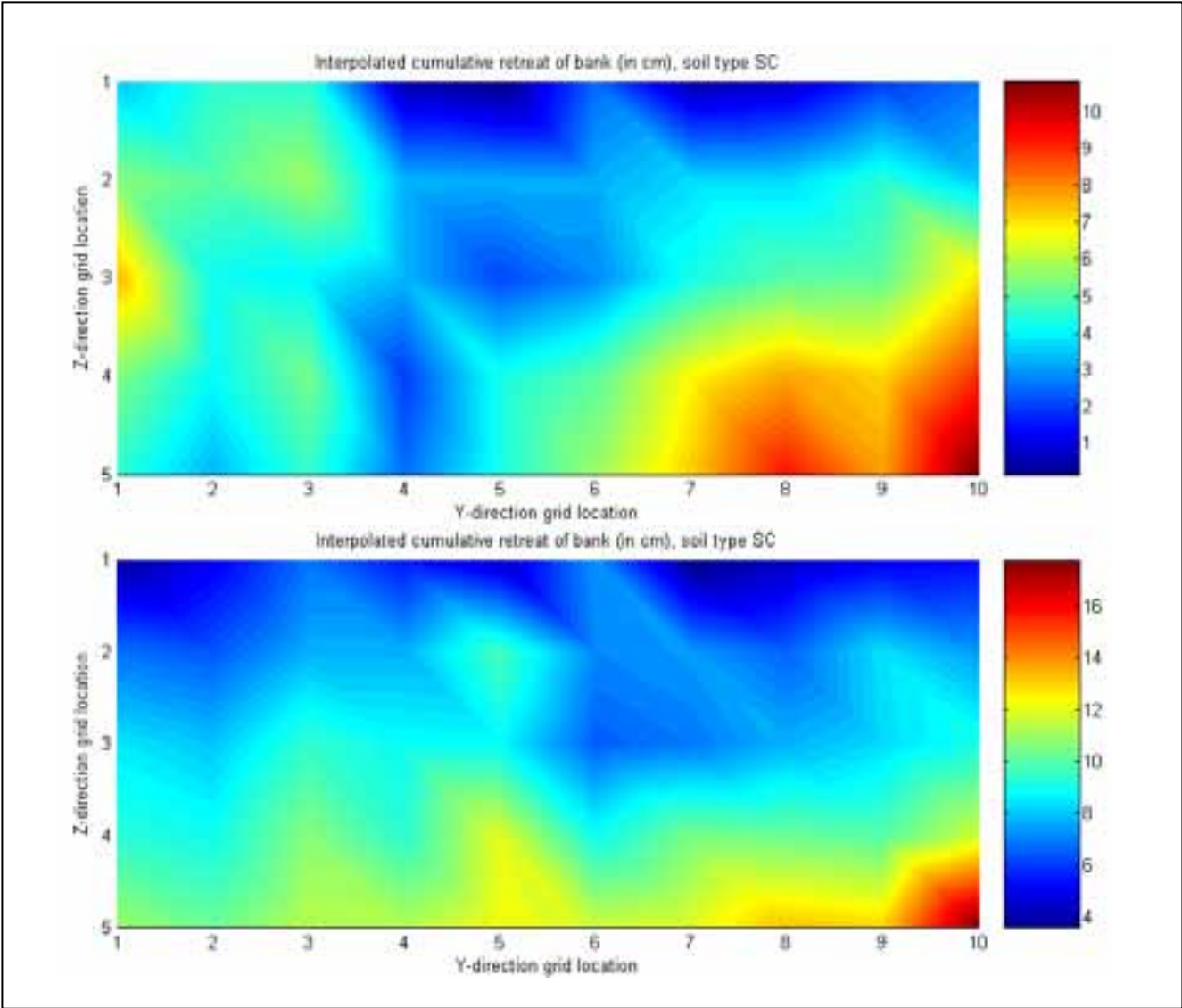
Qualitative description erosion soil SC

The groundwater level was equal to the surface water level in about 7 hours. The erosion of the sandy clay was a lot more steady and uniform. The slope steepened and after a while it almost became vertical (90°). At the beginning mainly erosion of small parts, about 0,5 cm down to the size of individual grains occurred. Later on also bigger parts of soil were eroded (up to about 3 cm). This lead to a less straight and uniform bank. Whenever a part of the bank did not erode right away though, it became more exposed and therefore more susceptible for erosion, due to the decrease in binding with surrounding soil.

Quantitative description erosion soil SC

The graphical output is presented in boxplots and two contourplots, as shown in the figures below and on the next page. There are no indications that the erosion would come to a stop after same time. The contourplots provide us with strong indications that no holes were formed, in contrary with soil type C. As described in the qualitative description, the bank retreat was much more uniform.





Bank retreat of soil type SC, after 1900 cycles (above) and after 3000 cycles (below)

Appendix Q: Proposal location further research, Delft, Schiekade

